MESSAGE FROM Dr. G.P.Vadodaria

Dr. G. P. Vadodaria
Principal, L.D College of Engineering
Member Secretary – ACPC

Ex-Registrar, Gujarat Technological University

Technology Education without research and development becomes meaningless in the era of skill development. On the occasion of publishing third issue of SARJAN, I feel more encouraged and appreciate the step taken by 'SOCET' in providing a platform for publishing findings of the young researcher. I am confident that this journal will help in providing forums for academician and researcher who are interested in the discussion of current and future issues and challenges impacting the Globe as well as promoting and disseminating relevant, high quality research in the field of engineering.

I congratulate to those who contributed through research papers, editors, reviewers and especially to whole team of SOCET for bringing the third issue of SARJAN.

I look forward for grand success of similar issues and with a hope that this platform will be continuously provided in the future also to expand the engineering horizon.

Dr. G. P. Vadodaria

EDITORIAL

Welcome to the III volume of SARJAN journal.
This journal 'SARJAN' is based on a multidisciplinary efforts of SOCET and ASOIT. It attempts to examine the innovative initiatives and research coordination to shape up the surrounding for committed and dedicated researchers. This journal offers the inclusive exploration of the complex, advance as well as contemporary and dynamic changes in technology.

Over the years Silver Oak College of Engineering and Technology has mapped out the innovatory modifications in the field of research. But this year one more feather has been adding to this journal as it is a combine effort of SOCET and ASOIT. I hope this third edition will serve the purpose to bring out an efficient research work and fulfill the expectations of our readers, who have immense faith in our excellence. This belief on us motivates us to come out with new and effective creation.

'SARJAN' is a mirror to judge and review our own work in a better way. I acknowledge all those who have put their efforts to bring out this issue to the higher potency of publication and wish it will grow with the help of our reader's healthy feedback.

I hope you will find current journal relevant and novel.

Dr. Poonam Darbar
Editor

Co-ordinators,
Prof. Ankita Mandowara
Prof. Rikkin Thakkar
Prof. Harsha Gupta
Prog. Anant Patel
Prof. Hardik Shukla

INDEX

Simulation of AODV Routing Protocol

Ashwin R Rathod * Lipi Kothari
ashwinrathod.it@socet.edu.in
Information Technology Department, Silver Oak College of Engineering & Technological Gujarat Technological University, India

Abstract—

A Mobile Ad hoc Network is a kind of wireless ad-hoc network, and is a self configuring network of mobile routers connected by wireless links. Mobile Ad-Hoc Network (MANET) is a wireless network without infrastructure. Self configurability and easy deployment feature of the MANET resulted in numerous applications in this modern era. Efficient routing protocols will make MANETs reliable. In this paper, an attempt has been made to know protocols AODV. The simulation of AODV has been done by using simulation tool NS2 which is the main simulator, NAM (Network Animator) and excel graph which is used for preparing the graphs from the trace files.

1. INTRODUCTION

An ad-hoc network is a collection of wireless mobile hosts forming a temporary network without the aid of any stand-alone infrastructure or centralized administration. Mobile Ad-hoc networks are self- organizing and self-configuring multihop wireless networks where, the structure of the network changes dynamically. This is mainly due to the mobility of the nodes. Nodes in these networks utilize the same Random access wireless channel, cooperating in a friendly manner to engaging themselves in multihop forwarding. The node in the network not only acts as hosts but also as routers that route data to/from other nodes in network. Each device in a MANET is free to move independently in any direction, and will therefore change its links to other devices frequently. Each device must forward traffic that is unrelated to its own use, and therefore be a router will be there. Routing in ad-networks has been a challenging task ever since the wire-less networks came into existence. The major reason for this is the constant change in network topology because of high degree of node mobility. A number of protocols have been developed for accomplish this task. Routing is the process of selecting paths in a network along which to send network traffic. In packet switching networks, routing is process of directing the forwarded packets, the transit of logically addressed packets from their source toward their ultimate destination through intermediate nodes. An ad hoc routing protocol is a convention, or standard, that controls how nodes decide which way to route packets between computing devices in a mobile ad-hoc network. In ad hoc networks, nodes do not start up with familiar the topology of their networks; instead, they have to discover it. The basic idea is that a new node may announce its presence and should listen for announcements broadcast by its neighbours. Each node learns about nodes nearby and how to reach them, and may announce that it, too, can reach them. Wireless ad-hoc networks have gained a lot of importance in wireless communications. Wireless communication is established by nodes acting as routers and transferring packets from one to another in ad-hoc networks. Routing in these networks is highly complex due to moving nodes and hence many protocols have been developed. In this paper we have selected AODV routing protocols for analysis of their performance. Figure1 below represents the scenario of MANET.

One of the main difficulties in MANET (Mobile Ad hoc Network) is the routing problem, which is aggravated by frequent topology changes due to node movement, radio interference and network partitions. Many Routing protocols have been proposed in past and reported in the literature [1]. The proactive approaches attempts to maintain routing information for each node in the network at all times [2, 3], where as the reactive approaches only find new routes when required [5, 6, 7, 8] and other approaches make use of geographical location information for routing [8]. Traditional routing protocols used for wired networks cannot be directly applied to most wireless networks [10] because some common assumptions are not valid in this kind of dynamic network, like a node can receive any broadcast message sent by others in the same subnet. The bandwidth in this kind of network is usually limited. Although the researchers have suggested other techniques to enhance the overall network bandwidth by integrating wireless network with Optical network [11]. Thus, this network model introduces great challenges for routing protocols.

2. APPLICATION OF MANET

- With the increase of portable devices as well as progress in wireless communication, ad hoc networking is gaining importance with the increasing number of widespread applications [4].
- Military battlefield. Military equipment now routinely contains some sort of computer equipment. Ad hoc networking would allow the military to take advantage of commonplace network technology to maintain an information network between the soldiers, vehicles, and military information head quarters. The basic techniques of ad hoc network came from this field.
- Commercial sector. Ad hoc can be used in emergency/rescue operations for disaster relief efforts, e.g. in fire, flood, or earthquake. Emergency rescue operations must take place where non-existing or damaged communications infrastructure and rapid deployment of a communication network is needed. Information is relayed from one rescue team member to another over a small handheld. Other commercial scenarios include e.g. ship-to-ship ad hoc mobile communication, law enforcement, etc.
- Local level. Ad hoc networks can autonomously link an instant and temporary multimedia network using notebook computers or palmtop computers to spread and share information among participants at a e.g. conference or classroom. Another appropriate local level application might be in home networks where devices can communicate directly to exchange information. Similarly in other civilian environments like taxicab, sports stadium, boat and small aircraft, mobile ad hoc communications will have many applications.

3. CLASSIFICATION OF ADHOC ROUTING PROTOCOL

Routing protocol in MANET can be classified into several ways depending upon their network structure, communication model, routing strategy, and state information and so on but most of these are done depending on routing strategy and network structure Based on the routing strategy the routing protocols can be classified into two parts: 1.Table driven and 2. Source initiated (on demand) while depending on the network structure these are classified as flat routing, hierarchical routing and geographic position assisted routing. Flat routing covers both routing protocols based on routing strategy.

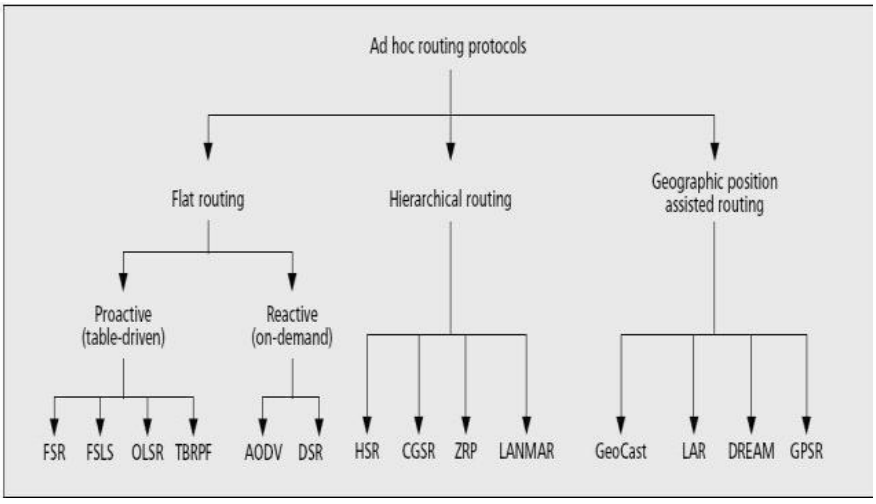

Fig 1 Classification of Adhoc Routing Protocol.

4. AODV (ADHOC ON DEMAND DISTANCE VECTOR)

AODV is a variation of Destination-Sequenced Distance-Vector (DSDV) routing protocol which is collectively based on DSDV and DSR. It aims to minimize the requirement of system-wide broadcasts to its extreme. It does not maintain routes from every node to every other node in the network rather they are discovered as and when needed & are maintained only as long as they are required.

The key steps of algorithm used by AODV for establishment of Uni-cast routes are explained below.

When a node wants to send a data packet to a destination node, the entries in route table are checked to ensure whether there is a current route to that destination node or not. If it is there, the data packet is forwarded to the appropriate next hop toward the destination. If it is not there, the route discovery process is initiated. AODV initiates a route discovery process using Route Request (RREQ) and Route Reply (RREP). The source node will create a RREQ packet containing its IP address, its current sequence number, the destination's IP address, the destination's last sequence number and broadcast ID. The broadcast ID is incremented each time the source node initiates RREQ.

Basically, the sequence numbers are used to determine the timeliness of each data packet and the broadcast ID & the IP address together form a unique identifier for RREQ so as to uniquely identify each request. The requests are sent using RREQ message and the information in connection with creation of a route is sent back in RREP message. The source node broadcasts the RREQ packet to its neighbors and then sets a timer to wait for a reply. To process the RREQ, the node sets up a reverse route entry for the source node in its route table. This helps to know how to forward a RREP to the source. Basically a lifetime is associated with the reverse route entry and if this entry is not used within this lifetime, the route information is deleted. If the RREQ is lost during transmission, the source node is allowed to broadcast again using route discovery mechanism.

The source node broadcasts the RREQ packet to its neighbors which in turn forwards the same to their neighbors and so forth. Especially, in case of large network, there is a need to control network-wide broadcasts of RREQ and to control the same; the source node uses an expanding ring search technique. In this technique, the source node sets the Time to Live (TTL) value of the RREQ to an initial start value. If there is no reply within the discovery period, the next RREQ is broadcasted with a TTL value increased by an increment value. The process of incrementing TTL value continues until a threshold value is reached, after which the RREQ is broadcasted across the entire network.

When the destination node or an intermediate node with a route to the destination receives the RREQ, it creates the RREP and Unicast the same towards the source node using the node from which it received the RREQ as the next hop. When RREP is routed back along the reverse path and received by an intermediate node, it sets up a forward path entry to the destination in its routing table. When the RREP reaches the source node, it means a route from source to the destination has been established and the source node can begin the data transmission.

A route discovered between a source node and destination node is maintained as long as needed by the source node. Since there is movement of nodes in mobile ad hoc network and if the source node moves during an active session, it can reinitiate route discovery mechanism to establish a new route to destination. Conversely, if the destination node or some intermediate node moves, the node upstream of the break initiates Route Error (RERR) message to the affected active upstream neighbors/nodes. Consequently, these nodes propagate the RERR to their predecessor nodes. This process continues until the source node is reached. When RERR is Received by the source node, it can either stop sending the data or reinitiate the route discovery mechanism by sending a new RREQ message if the route is still required.

A. Benefits and Limitation of AODV

The benefits of AODV protocol are that it favors the least congested route instead of the shortest route and it also supports both Unicast and multicast packet transmissions even for nodes in constant movement. It also responds very quickly to the topological changes that affects the active routes. AODV does not put any additional overheads on data packets as it does not make use of source routing.

The limitation of AODV protocol is that it expects/requires that the nodes in the broadcast medium can detect each others' broadcasts. It is also possible that a valid route is expired and the determination of a reasonable expiry time is difficult. The reason behind this is that the nodes are mobile and their sending rates may differ widely and can change dynamically from node to node. In addition, as the size of network grows, various performance metrics begin decreasing. AODV is vulnerable to various kinds of attacks as it based on the assumption that all nodes must cooperate and without their cooperation no route can be established.

5. SIMULATION AND RESULT

The following metrics are used in this paper for the analysis of AODV routing protocols.

A. Packet Delivery Ratio

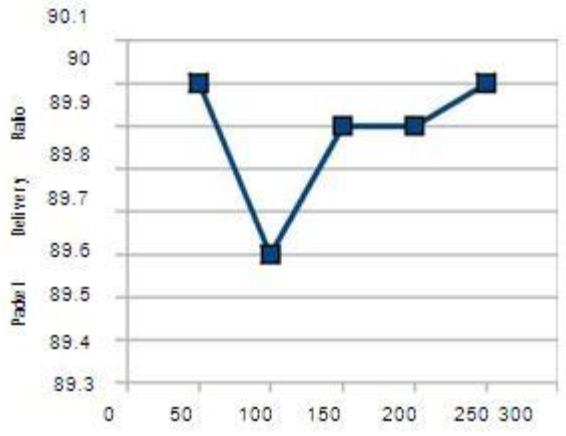

Nuber of nodes
Fig. 1 Packet Delivery Ratio

The packet delivery ratio in this simulation is defined as the ratio between the number of packets sent by constant bit rate sources and the number of received packets by the CBR sink at destination. It describes percentage of the packets which reach the destination. AODV shows high packet delivery ratio.

B. Average End to End Data packet Delay

The average end to end delay include all possible delay caused by route discovery propagation, transfer times etc. While the nodes are less than 400 nodes, the delay of AODV is a little more because of cluster forming. With the higher node density, overall end-to-end delay for AODV increases as number of hopes increases and the packet needs to cover long distance to reach the destination.

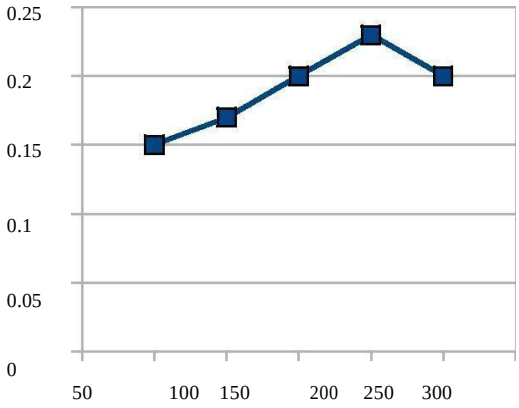

Fig 3 Average End to End Packet Delay

C. Throughput Analysis

When number of nodes increases, initially throughput increases as large number of routes are available but after a certain limit throughput becomes stable due to increase in end-to-end delay. Throughput increasing from node 50 to node 250.

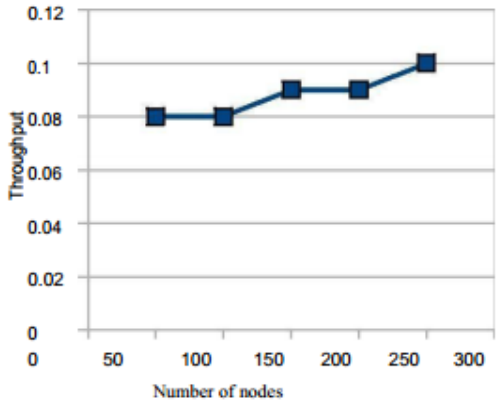

Fig 3 Average End to End Packet Delay

D. Average Control Packet

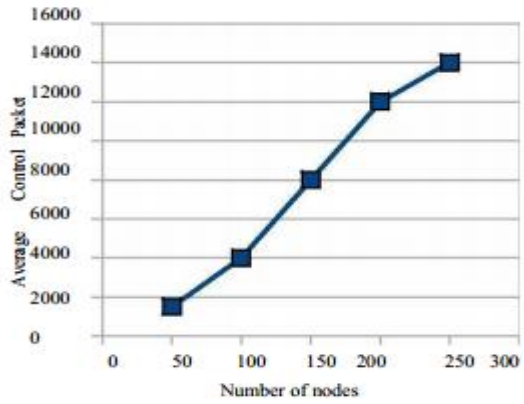

Fig. 4 Throughput Analysis

Figure 5. Show the route overhead of the comparing route protocol. after the nodes are more than 200, overhead of AODV increase rapidly. In the case of high-density as all routing over heads increases.

6. CONCLUSION

In this paper routing model which maintain node hierarchical based on AODV.our routing scheme hybrid in nature as it uses both flat and hierarchical approach for finding the route to destination. The Simulation result show that AODV provide better packet delivery rate with less route latency and overhead. The results confirm to achieve better scalability.

REFERENCES

[1] R.Asokan, A.M.Natragan, C.Venketesh, "Ant Based Dynamic Source Routing Protocol to Support Multiple Quality of Service (QoS) Metrics in Mobile Ad Hoc Networks" International Journal of Computer Science and Security, volume (2) issue (3)

[2] C. E. Perkins and P. Bhagwat, "Highly dynamic destination sequenced distance-vector routing (dsdv) for mobile computers" ACM SIGCOMM: Computer Communications Review, vol. 24, no. 4, pp. 234–244, 1994.

[3] P.Jacquet, P.Muhlethaler, and A.Qayyum, "Optimised link state routing protocol" IETF MANET, Internet Draft,
1998.

[4] C.Perkins, E.Belding-Royer, S.Das "Ad hoc On-Demand Distance Vector (AODV) Routing" feb .2003 http://www.ietf.org/internet-drafts/draftietf-manet-aodv-13.txt

[5] D.Johnson and D. Maltz, "Dynamic source routing in ad hoc wireless networks," Mobile Computing, 1996.

[6] C. E. Perkins and E. Royer, "Ad-hoc on-demand distance vector routing," in the Second IEEE Workshop o Mobile Computing systems and Applications, 1999.

[7] V.D.Park and M. S. Corson, "A highly adaptive distributed routing algorithm for mobile wireless networks," *in Proceedings of the IEEE Conference on Computer Communications (INFOCOM), 1997.*

[8] Y.B.Ko and N. H. Vaidya, "Location-aided routing (lar) in mobile ad
hoc networks," in Proceedings of the IEEE/ACM International Conference on Mobile Computing and Networking (MOBICOM' 98), 1998.

[9] ns-2 http://www.isi.edu/nsnam/ns

[10] Aditya Goel, Ravi Shankar Mishra, "Remote Data Acquisition Using Wireless – Scada System" International Journal of Engineering (IJE), Volume (3): Issue (1)

[11] Aditya Goel, Er.R.K.Sethi, "Integrated Optical wireless Network for
Next Generation Wireless Systems" Signal Processing: An International Journal (SPIJ), Volume (3): Issue (1)

Application of Graphics Processing Unit on Finite Element Method

Konark P. Patel

konarkpatel.cl@socet.edu.in

Civil Engineering Department, Silver Oak College of Engineering & Technological, Gujarat Technological University, India

Abstract:-

Today's computing environments are becoming more multifaceted, exploiting the capabilities of a range of multi-core microprocessors, central processing units (CPUs), digital signal processors, and graphic processing units (GPUs). Presented with so much heterogeneity, the process of developing efficient software for such a wide array of architectures poses a number of challenges to the programming community. One of such case is application of Finite Element Method on Graphics Processing Unit with help of OpenCL programming and it is a step in the direction of heterogeneous computing for smarter, faster and better analysis of FEM problem. In this paper matrix multiplication process is performed on Graphic processing unit (GPU) to compare the computing efficiency of normal sequential computing and parallel computing using graphics card. The main purpose of using this parallel computation is to minimize the time of analysis of Finite Element problem having large number of matrix computations.

KEYWORDS: *Parallel computing, GPU, CPU, OpenCL, FEM*

1. Parallel Computing

Parallel computing is a form of computation in which many calculations are carried out simultaneously, operating on the principle that large problems can often be divided into smaller ones, which are then solved concurrently ("in parallel"). There are several different forms of parallel computing: bit-level, instruction level, data, and task parallelism. Parallelism has been employed for many years, mainly in high-performance computing, but interest in it has grown lately due to the physical constraints preventing frequency scaling. As power consumption (and consequently heat generation) by computers has become a concern in recent years, parallel computing has become the dominant paradigm in computer architecture having multicore processors.

Parallel computers can be roughly classified according to the level at which the hardware supports parallelism. For example, with multi-core and multi-processor computers having multiple processing elements within a single machine; clusters, MPPs, and grids use multiple computers to work on the same task. Specialized parallel computer architectures are sometimes used alongside traditional processors for accelerating specific tasks.

Parallel computer programs are more difficult to write than sequential ones because concurrency introduces several new classes of potential software bugs, of which race conditions are the most common. Communication and synchronization between different subtasks are typically some of the greatest obstacles to getting good parallel program performance.

The current trend supports parallel computing hardware:

- Right now it is difficult to buy a computer that has only a single processor - even laptops have multiple cores.
- GPUs having multiple processing elements imbedded on chip have become basic necessity of the day to support graphic loads.
- This increasing processor core count trend is going to continue in the future trend.
- Parallel Software race behind as compared to parallel processors:
- Software parallelism is lagging behind the hardware.
- Some specialized parallel libraries for multicore systems are required.
- Some APIs for harnessing multiple cores (OpenMP) and multiple machines (MPI).

2. Flynn's taxonomy

Michael J. Flynn created one of the earliest classification systems for parallel (and sequential) computers and programs, now known as Flynn's taxonomy.

A. SISD-Single Instruction, Single Data
- Sequential (non-parallel) instruction flow
- Predictable and deterministic

B. SIMD-Single Instruction, Multiple Data
- Single (typically assembly) instruction operates on different data in a given clock tick.
- Requires predictable data access patterns - "vectors" that are contiguous in memory.

C. MISD-Multiple Instruction, Single Data
- Multiple instructions applied independently on same data.
- "Theoretical" rather than practical architecture - few implementations

D. MIMD-Multiple Instruction, Multiple Data
- Multiple instructions applied independently on different data.
- Very flexible-can be asynchronous, non-deterministic
- Most modern supercomputers follow MIMD design, albeit with SIMD components/sub-systems

3. General-purpose computing on graphics processing units (GPGPU)

General-purpose computing on graphics processing units (GPGPU) is a recent trend in computer engineering research. GPUs are co-processors that have been heavily optimized for computer graphics processing. Computer graphics processing is a field dominated by data parallel operations—particularly linear algebra matrix operations.

In the early days, GPGPU programs used normal graphics APIs for executing programs. However, several new programming languages and platforms have been built to do general purpose computation on GPUs with both Nvidia and AMD (Advanced Micro Devices) releasing programming environments like CUDA (Computer Unified Device Architecture) and Stream SDK respectively. Other GPU programming languages include BrookGPU, PeakStream, and RapidMind. Nvidia has also released specific products for computation in their Tesla series of GPU. The technology consortium Khronos Group has released the OpenCL (Open Computing Language) specification, which is a framework for writing programs that execute across platforms consisting of CPUs and GPUs. AMD, Intel, and Nvidia processors supports OpenCL.[Ref.2]

4. Introduction to OpenCL Programming

The Open Computing Language (OpenCL) is an open and royalty-free parallel computing API designed to enable GPUs and other coprocessors to work in tandem with the CPU by providing additional raw parallel computing power. As a standard, OpenCL 1.0 was released on December 8, 2008, by The Khronos Group, an independent standards consortium.

Developers have long sought to divide computing problems into a mix of concurrent subsets, making it feasible for a GPU to be used as a math coprocessor working with the CPU to better handle general problems. The potential of this heterogeneous computing model was encumbered by the fact that programmers could only choose proprietary programming languages, limiting their ability to write vendor-neutral, cross-platform applications. Proprietary implementations such as NVIDIA's CUDA limited the hardware choices of developers wishing to run their application on another system without having to retool it. [Ref.3]

Benefits of OpenCL

A primary benefit of OpenCL is substantial acceleration in parallel processing. OpenCL takes all computational resources such as multi-core CPUs and GPUs, as peer computational units and correspondingly allocates different levels of memory and tasks, taking advantage of the resources available in the system. OpenCL also complements the existing OpenGL® visualization API by sharing data structures and memory locations without any copy or conversion overhead.

A second benefit of OpenCL is cross-vendor software portability. This low-level layer draws an explicit line between hardware and the upper software layer. All the hardware implementation specifics, such as drivers and

runtime, are invisible to the upper-level software programmers through the use of high-level abstractions, allowing the developer to take advantage of the best hardware without having to reshuffle the upper software infrastructure. The change from proprietary programming to open standard also contributes to the acceleration of general computation in a cross-vendor fashion. [Ref.4]

Anatomy of OpenCL

- **Language Specification:** The language specification describes the syntax and programming interface for writing kernel programs that run on the supported accelerator (GPU, multi-core CPU, or DSP). Kernels can be precompiled or the developer can allow the OpenCL runtime to compile the kernel program at runtime.
- **Platform API:** The platform-layer API gives the developer access to software application routines that can query the system for the existence of OpenCL-supported devices. This layer also lets the developer use the concepts of device context and work-queues to select and initialize OpenCL devices, submit work to the devices, and enable data transfer to and from the devices.
- **Runtime API:** The OpenCL framework uses contexts to manage one or more OpenCL devices. The runtime API uses contexts for managing objects such as command queues, memory objects, and kernel objects, as well as for executing kernels on one or more devices specified in the context. [Ref.5]

Executing an OpenCL Program

1. Query the host system for OpenCL devices.
2. Create a context to associate the OpenCL devices.
3. Create programs that will run on one or more associated devices.
4. From the programs, select kernels to execute.
5. Create memory objects on the host or on the device.
6. Copy memory data to the device as needed.
7. Provide arguments for the kernels.
8. Submit the kernels to the command queue for execution.
9. Copy the results from the device to the host.

5. Multiplication of Large Square Matrices: From Serial CPU Code to Parallel GPU Code

The task at hand is standard, i.e. to multiply two matrices. It is chosen primarily due to the fact that quite a lot of information on the subject can be found in different sources. Most of them, one way or another, offer more or less coordinated solutions. This is the road that we are going to go down, giving step-by-step clarifications of the meaning of model structures while keeping in mind that we are working on real hardware. [Ref.6]

Below is a matrix multiplication formula well-known in linear algebra, modified for computer calculations. The first index is the matrix row number; the second index is the column number. Every output matrix element is calculated by sequentially adding each successive product of elements in the first and second matrices to the accumulated sum. Eventually, this accumulated sum is the calculated output matrix element:

$$C_{i,j} = C_{i,j} + \sum_{k=0}^{P} A_{i,k} * B_{k,j}$$
$$0 \le i \le N$$
$$0 \le j \le M$$

[Formula for matrix multiplication]

It can schematically be represented as follows:

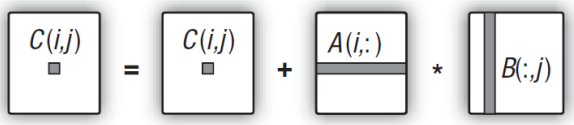

Figure-1 Graphical representation of matrix multiplication

Since we will have to create three linear buffers for the OpenCL kernel, it would be reasonable to rework the initial algorithm so that it is as similar to the kernel algorithm as possible. The optimality of the code with two-dimensional arrays does not mean that its analog will also be optimal for linear buffers: all tests will have to be repeated.

The OpenCL kernel for matrix multiplication looks as follows:

```
__kernel void matrixMultiplication(__global float* A, __global float* B, __global float* C,  int widthA, int widthB )
{
	int i = get_global_id(0);
	int j = get_global_id(1);
	float value=0;
	for ( int k = 0; k < widthA; k++)
	{
		value = value + A[k + j * widthA] * B[k*widthB + i];
	}
	C[i + widthA * j] = value;
}
```

5.1 Comparison of time between CPU and GPU calculation

I. TIME DIFFERENCE BETWEEN CPU AND GPU CALCILATION

MATRIX	GPU TIME(ms)	CPU TIME(ms)
8	171	0
72	140	0
136	172	31
200	171	62
264	203	156
328	187	280
392	202	484
456	249	795
520	312	1295
584	345	2059
648	447	2933
712	546	4150

776	668	6209
840	781	7940
904	921	9969

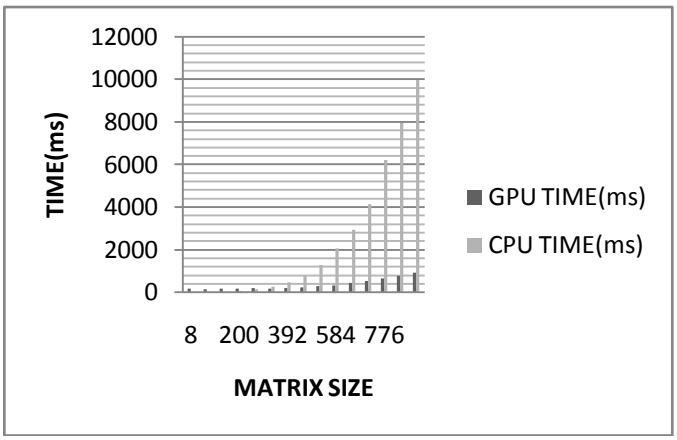

Figure-2 GPU vs CPU matrix multiplication time for various size of matrix of NxN order

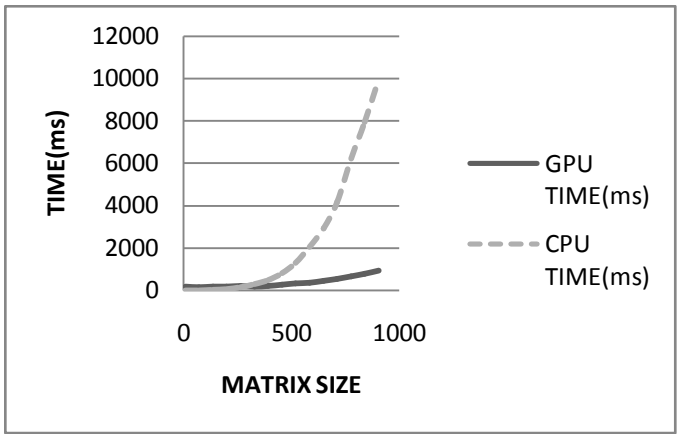

Figure-3 Line-Chart for GPU vs CPU matrix multiplication time for various size of matrix of NxN order

6. CONCLUSION

- It can be concluded that use of GPU for general Purpose Computing can open new horizons in field of FEM analysis GPU's computing speed is far more better than that of existing CPU.
- Nowadays, parallel computation is unavoidable in most of the finite element analysis (FEA) problems. If problem size increased, a high computing power should be required to get efficient analysis results. Most of the large scale FE simulations codes are preferred to incorporate with parallel computing technique. Long term continuous development of parallel sparse linear equation solvers makes available of various parallel solvers which reduces computing time significantly. Parallelization of complete FEM problem rather than only concentrating equation solvers will lead to greater performance.
- Discretization of FE domain and assembly of system global matrix always lead to bottleneck
- Parallel computing using GPUs for a complete FEM problem is still a primitive state. Current researches in GPU parallelization FEM area in intensively focused on efficient sparse matrix solvers also how to

incorporate with discretization and assembly. One can think of completely solving a FEM problem using GPU.

References

[1] Graphics processing unit - Wikipedia.
[2] Introduction to OpenCL Programming-Training Guide – AMD
[3] General-purpose computing on graphics processing units - Wikipedia.
[4] OpenCL Specifications by http://www.khronos.org
[5] Benedict Gaster, Lee Howes, David R. Kaeli, Perhaad Mistry, Dana Schaa "Heterogeneous Computing with OpenCL".
[6] OpenCL™ Zone - AMD Developer Central

\

Comparative Study of Ground Water Recharge Methods and Its Sustainability through Parametric Evaluations

Sejal D. Desai

sej_c2@rediffmail.com

Civil Engineering Department, Silver Oak College of Engineering & Technological, Gujarat Technological University, India

Abstract:-

Artificial recharge project was carried out at tyre manufacturing industry in Vadodara, Gujarat State of India. Ground water was the only source for various industrial processes. Hence due to continuous pumping of ground water depleted and lowered by 1m to 1.5m every year. Owing to the conditions prevailing in the vicinity a need was felt to introduce artificial recharge to meet the water requirements. In this paper two recharging methods i.e. Percolation Tank (PT) and Roof Top Rain Water Harvesting (RWH) are studied. A PT was excavated between two tubewells namely, T-5 & T-6, which were recharged through percolation. As a result Total Dissolved Solids (TDS) in T-5, T-6 reduced 32%. Annual recharge quantity was found out to be 2040 m^3. Another two tube wells T-7 & T-16, were taken under RWH and the amount of recharge was found as 9466m^3.Also TDS of the water in the tube well reduced by 58%. Thus compared to PT the amount of recharge through RWH was found to be three times more effective. The average rise of water level in T-5 and T-6 was 4.13m, for T-7 and T-16 1.805m.Hence the rise in water level through the PT was almost twice compared to RWH. Subsequently permeability (K) parameter of soil was calculated using Theim and Dupuit's equation (Todd, 1980) for all the tubewells in the industrial premises to verify their recharging capacity. The Soil Conservation System (SCS) was used to calculate runoff for PT & RWH which was found as 34.3% & 89.9% respectively.

Keywords: *Artificial recharge (AR), Percolation Tank (PT), Roof Top Rain Water Harvesting (RWH)*

1. INTRODUCTION

Basic source of all recharge, natural or artificial is rainfall on land surface. The distribution of the same comes in the form of surface runoff, subsurface infiltration, and returns back to atmosphere as evaporation or evapotranspiration losses from land surface or from root zone. Water reaching root zone supplements soil moisture and surplus if, any goes as deep percolation or recharge. In general recharge is that portion of infiltration that reaches ground water level. Athavale et al. (1994) have studied borehole injection recharging technique in Deccan Trap Basalts near Nagpur, India. Athavale (2003) have given the detailed information regarding water harvesting and sustainable supply in India. The summary of artificial recharge is given in subsequent sections.

1.1 Benefits of Artificial Recharge

Artificial ground water recharge techniques have been used throughout the world for more than 200 years for a variety of purposes. Some of the uses are as under:(1) Seasonal Storage (2) Agricultural water supply (3) Long-term storage or water banking (4) Nutrient reduction in agricultural runoff (5) Diurnal Storage (6) Reclaimed water storage for reuse (7) Restore ground-water levels (8) Soil aquifer treatment (9) Maintain distribution system

pressure (10) Store fresh water, derived from rain and snow melt (11) Maintain water temperature for fish hatcheries (12) Improve water quality (13) Reduce environmental effects of stream flow diversions (14) Prevent salt water intrusion into aquifers (15) Compensate for surface salinity barrier leakage losses etc.(16) Reduction of land subsidence. (17) Renovation of waste water (18) Improvement of ground water quality (19) Storage of stream waters during periods of high or excessive flow and thereby reduction of flood flows (20) Increase well yield (21) Decrease the size of areas needed for water supply systems.

1.2 Rain water harvesting techniques

Water Harvesting means deliberate collection and storage of rain water from a catchments and its storage including the methods or innovations which are adopted for its beneficial use like ground water recharge, drinking, irrigation, agriculture etc and thereby efficient utilization of limited water. The ultimate intention of water harvesting is to provide supply of water at the most wanted period to its users. Conservation of rainwater by artificial means can be identified as water harvesting and the structures constructed or developed for collection of rainwater can be termed as Water Harvesting Structures. [Ref.1]

The common method for rain water harvesting and structures related to artificial recharge of ground water can be widely classified as: (1) Recharge through induced infiltration. (2)Recharge through water spreading (i) Flooding (ii) Basins (iii) Ditches (iv) Natural channel modification (v) Irrigation(3)Recharge pits and shafts (4)Hydrofracturing of bore wells(5)Farm ponds(6)Storage tanks, M.I. tanks, M.I. schemes, village tanks(7)Percolation tanks(8)Recharge wells or Injection wells(9)Check dams(10)Sub surface dykes or dams(11) Gully plugging (12) Contour bunding (13)Contour trenching (14)Roof top rain water harvesting - (i)Recharge through abandoned dug well (ii) Recharge through open well method (iii) Rain water harvesting through bore well (iv)Recharge through abandoned hand pump (v) Recharge pit (vi) Recharge trench (vii) Gravity head recharge tube wells (viii) Recharge shaft. While in this study percolation tank technique along with recharge in tube well has been studied.

2. STUDY AREA

The artificial recharging project included five tube wells in the factory premises of Apollo Tyres Industries, Vadodara, and Gujarat State of India. The factory layout plan and location of tube wells is shown in Fig. 1.

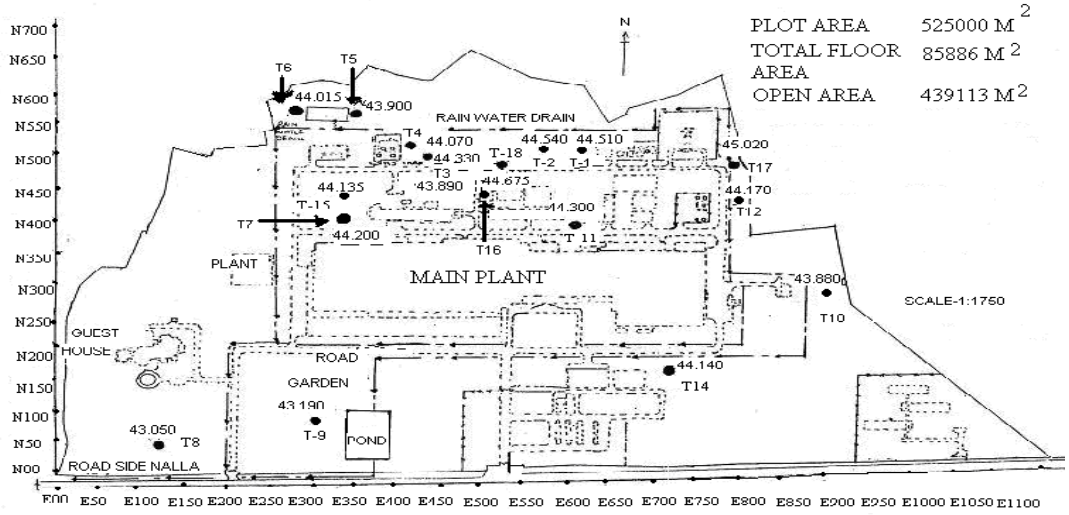

Fig. 1 Layout of the study area and position of tube wells

The area falls under arid to semi arid climatic conditions and temperature varies from 10^0C in winter to 45^0C in summer. Geologically this area falls under recent alluvial formation over lains the Deccan trap formation. The geological strata consists of the over burden of 30m to 40m in thickness and is composed of soil, silt and gravels. The lower portion belongs to the rocky stratum of basalt, a formation of igneous and metamorphic rocks, with poor porosity and permeability. This formation contains negligible water circulation in it. Only in case of fractured rocks it gives higher yield of water during pumping. [Ref.2]

Hydrological, aquifers of this area are recharged by two rivers, which are semi perennial namely Vishwamitri and Dev. However recharge capacity of these rivers is much less and there are no such efforts to store the surplus water in any form during non-monsoon period. Particularly in this area ground water occurs in two phases in alluvial formation as unconfined aquifer and in rock formation. In fine grained unconfined aquifer, gravity drainage of the pores is often not instantaneous; consequently the water is released only, some time after lowering of water table. So it is also called as unconfined aquifers with delayed yield. Such type of phenomenon is observed in this area, along with decreasing water level by 1m to 1.5 m every year. Hence it was decided to suggest suitable method for recharge by considering a pilot study at Apollo Tyres.

The factory area contains 17 tube wells out of which some of them are abandoned. The requirement of water during non-monsoon season particularly February to May every year increases. In this pilot study, tube wells T-5 and T-6 were considered for analysis purpose and further recommendations for use. Especially when the depth of these tube wells T-5 & T-6 below ground level reached to 81m & 76.2m respectively.

3. METHODOLOGY

3.1Artificial recharge through Percolation tank

In the recharge through percolation tank a trapezoidal tank of top width 45m x 20m and bottom width 35m x 14m with side slopes 1:1.67 along lengthwise and 1:1 slope along width in section and depth 3m including 0.5m free board was excavated as shown in Fig. 2.2(in section). Water from nearby storm water drain was conveyed to the tank, through PVC pipe of 15cm diameter and 50m length. Change in water level of the tank was daily monitored by measuring staff fitted in tank. Water percolates through bottom and sides of tank into the ground. Holes of 2 to 3mm diameter and of 70 numbers were made in the casing pipe of tube well which were covered by steel wire mesh to allow the water injection from the percolation tank in to the wells T5 and T6 from ground level up to 1.5m depth as seen in section of the tank . A trench was excavated and the filter material like gravel & sand was placed in it. Gravel layer with grain size of 10 to 15mm underlies sand layer of grain size 2 to 3mm. Water from the percolation tank before entering the holes of casing pipe of tube wells, was filtered through sand and gravel layer placed around the well.

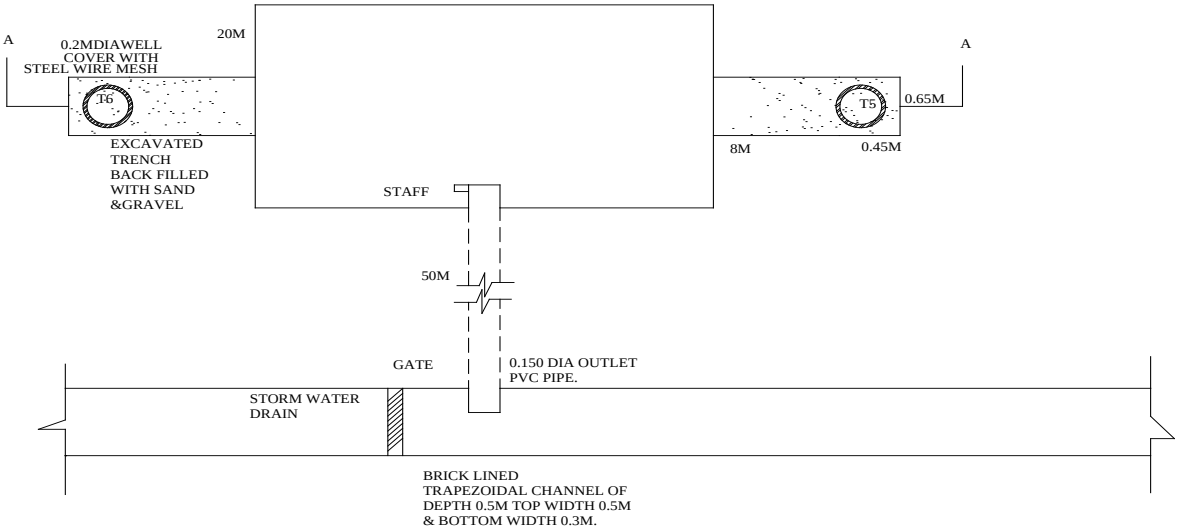

PLAN

Fig. 2.1 Recharge through Percolation Tank in plan and section

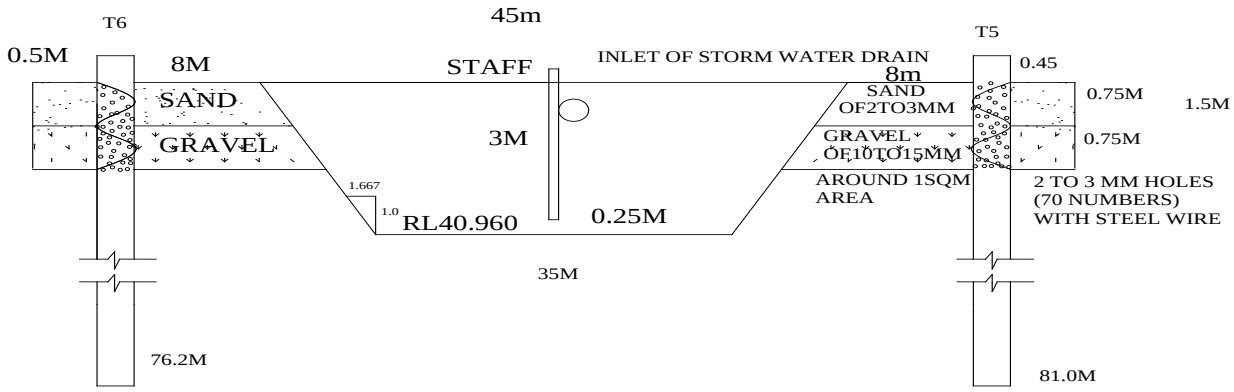

SECTION

Fig. 2.2 Recharge through Percolation Tank in plan and section

3.2 Artificial recharge through RWH

As shown in Fig. 3 (in elevation), rain water is collected from the roof of the main building through mild steel drain pipe of diameter 0.3 m. [Ref.4]

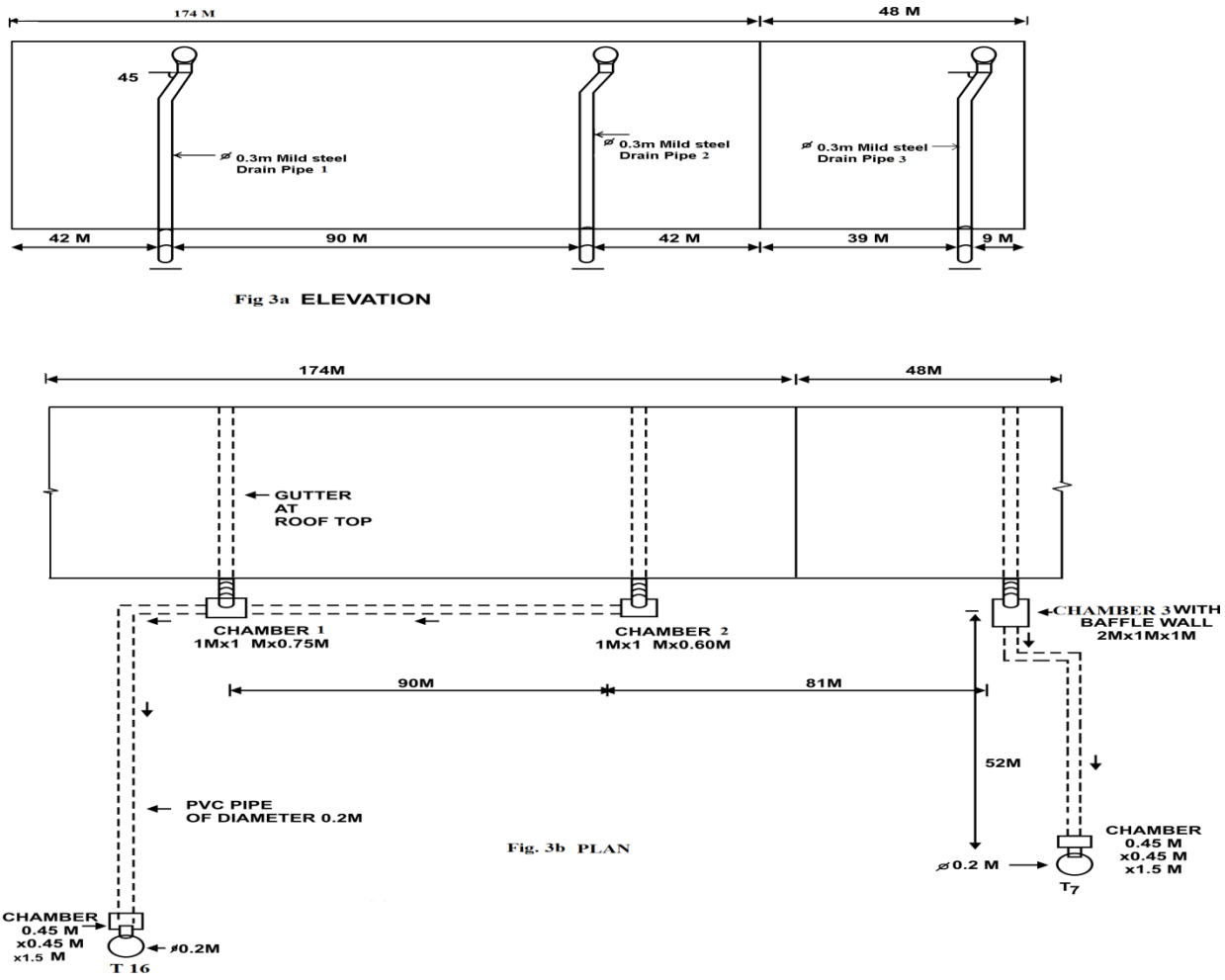

Fig. 3 Roof top harvesting system for recharge

These pipes have an inclination of 45° to the vertical for the purpose of maintenance and replacement. Height of the building was 11 m and height of the drain pipe was 10 m. Total length of the building was 222 m. The complete arrangement of such drain pipes is shown in Fig. 3(in elevation).The tube wells T-7 and T-16 under RWH were having the depth of 85m and78m below ground level respectively.

Roof top rain water harvesting system works in the following manner. Roof water is collected into the steel gutter as shown in Fig. 3(in plan), from which it is transferred to the storm water drain pipe, and then it is collected into the chamber. Rain water is collected in to drain-2 and collected to chamber-2 of size 1 m x 1 m x 0.6 m (LxBxD) as shown in Fig. 3(Plan).While storm water drain-1 transfers rain water in chamber-1 of size 1 m x 1 m x 0.75 m. Since the chamber-1 has depth greater than chamber-2, water from the chamber-2 flows to chamber-1 under slope 1: 600, through the underground PVC pipe of 20cm diameter. [**Ref.5]**

From chamber-1 PVC pipe conveys water to the chamber of size 0.45 m x 0.45 m x 1.5 m near T-16. A hole of diameter 20cm was drilled into the tube well casing to introduce a PVC pipe of diameter 20cm from chamber to tube well in order to convey the rain water into tube well and thereby recharging T-16. [Ref.1]

Drain pipe-3 collects the roof top rain water through roof gutter and transfer the water to chamber-3 as shown in Fig. 3(plan). This chamber of size 2 m x 1 m x 1 m is provided with baffle wall, so that silt and other suspended particles are arrested and clean water is available for recharging. Water from chamber-3 is conveyed to

chamber constructed near T-7 of size 0.45 m x 0.45 m x 1.5 m through under ground PVC pipe of diameter 0.2 m with slope 1: 104. Similar to T-16, after drilling hole in tube well another inlet PVC pipe is introduced to transfer the water collected in the chamber to T-7 in order to recharge it. The detailed arrangement of the roof top harvesting components for T-7 and T-16 are shown in Fig. 4.

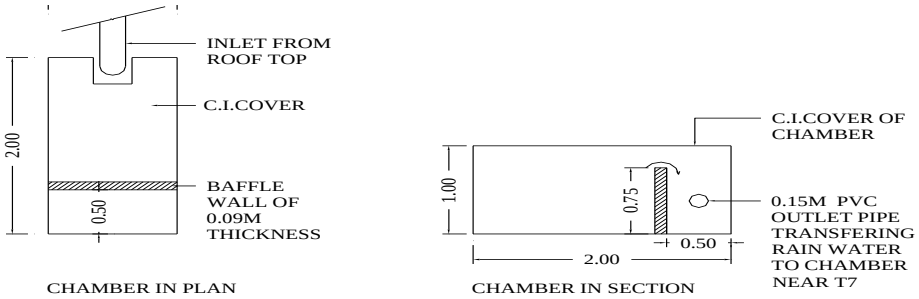

FIG:4.9(a) CHAMBER AT T7 WITH DRAIN PIPE

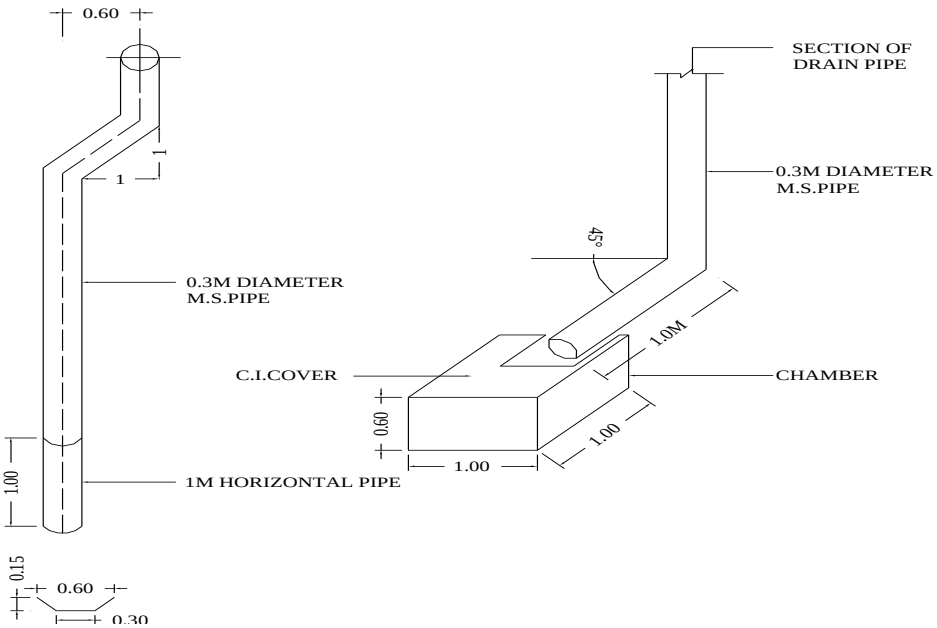

Fig. 4 Details of chamber and gutter of roof top harvesting system

3.3 Runoff Calculations by Soil Conservation Services Method (SCS)

The average rainfall in the study area ranges between 900mm to 1000mm, as per the data collected from Jilla Panchayat of Vadodara, Gujarat. The study was carried out based on the rainfall data available in 2001 i.e. 937mm. SCS method, as used by Mishra & Singh, 1999 has been used in the present study.

For the pasture, Curve no. (CN) = 84, $S = (1000 / CN) - 10$, $R = (P - 0.2S)^2 / (P + 0.8 S)$.Total runoff for the pasture was calculated as 338.66 mm. SCS method for roof top, Curve no. (CN)=98, $S = (1000 / CN) - 10$, $R = (P - 0.2S)^2 / (P + 0.8 S)$.Total runoff for the roof top was calculated as 843.30 mm.

3.4 Lithological and resistivity study

Resistivity and lithological survey of site was carried out and its data were analysed to get an idea of average lithological strata of the site. The summary is shown in Table 1

Strata no.	Thickness of each stratum in m	Formations
1.	2.6 - 4.1	Top soil
2.	6.2 - 9.4	Silt, clay, kankar, sand, etc.
3.	8.2 - 16.6	Sandy strata
4.	4.0– 6.0	Weathered basalt
5.	30 - 100	Massive trap

Table 1 Lithological Strata Chart of Site

3.5 Permeability Calculations for the tube wells

From difference of Static Water Level (SWL) and Pumping Water Level (PWL), Drawdown (DD) was obtained; also the discharge was measured for various tube wells. Using Theim and Dupuit's equation (Todd, 1980), permeability for various tube wells was calculated. For tube well T-5 and T-6 its average permeability was found as 0.03m/hr.While for tube well T-7 and T-16 it was 0.08m/hr on an average.

3.6 Water level calculations

Periodic water level was monitored in various tube wells (Trivedi S., 2002). Before installing the recharge system, R.L. of the water level was measured as 21.600m, 22.055m, 24.750m, and 23.940m for tube wells T-5, T-6, T-7, and T-16 respectively. While the maximum water level after the recharge was observed as 26.650m, 25.265m, 26.200m, 26.100m.

Rise in water level in tube wells T-5, T-6 and T-7, T-16 is calculated by the difference between maximum water level and initial water level, which was obtained as 5.050m, 3.210m and 1.450m, 2.160m respectively. Hence the average water level rise for T-5, T-6 was obtained as 4.130m, while for T-7, T-16 it was 1.805m.

3.7 Total dissolved solids calculations

TDS was monthly monitored for various tube wells (Trivedi S., 2002). Before caring out the recharging process, initial TDS values for tube wells T- 5 & T-6 were measured as 1000ppm and 1100 ppm respectively, on averaging it came to 1050 ppm. While for T- 7 & T-16 tube wells TDS was 1500ppm & 1800ppm which was averaged to 1650 ppm.

After implementing recharging, TDS values for tube wells T- 5 & T-6 was found to be 730ppm and 715 ppm respectively, which averaged to 722ppm. While for T-7 & T-16 tube wells it was 715ppm & 700ppm respectively, which averaged to 707.5ppm.

3.8 Recharge calculations

For percolation tank, total volume of water recharged can be calculated by measuring daily water level fluctuation in the tank, amount of evaporation and the area of the tank for recharging (Trivedi S., 2002). It was found out as 2040m^3. For roof top rain water harvesting system recharging was found by multiplying the area of

the roof with 90% (Mishra & Singh, 1999) of runoff from the roof surfaces. It was found as 9466 m^3. Secondly, recharging capacity of tube wells through RWH was 601.43m^3/day for T-7 and T-16 was 2268m^3/day (Driscoll, 1987) which was higher than the actual water injected in to the tube wells i.e. 57 m^3/day, 206m^3/day for T-7, T-16respectively.

4. RESULTS AND ANALYSIS

4.1 Aquifer strata

From the Table 1 aquifer characterization using lithological information was analyzed. The analysis shows that aquifer was divided into five strata. First stratum was top soil consisting of thickness from ground level to 4.1m maximum. While second strata was of variable thickness from 6.2to 9.4m which consists of different soil layers like silt clay kankar, sand, etc. Third stratum was sandy, which extends from thickness 8.2m to 16.6 m. Due to high porosity, this strata holds good amount of water. Weathered basalt of 4m to 3m thickness contributing 20 to 25% of ground water. Last stratum was massive basalt or trap of thickness 38m to 69m, which is highly compacted and contributing negligible amount of groundwater during pumping. The details of lithological formations are shown in the fence diagram (Fig. 5).

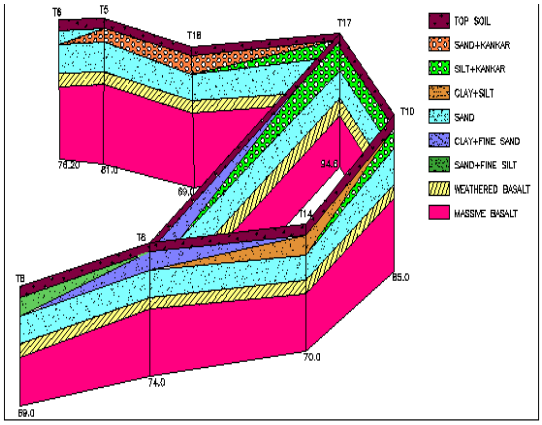

Fig. 5 Fence diagram

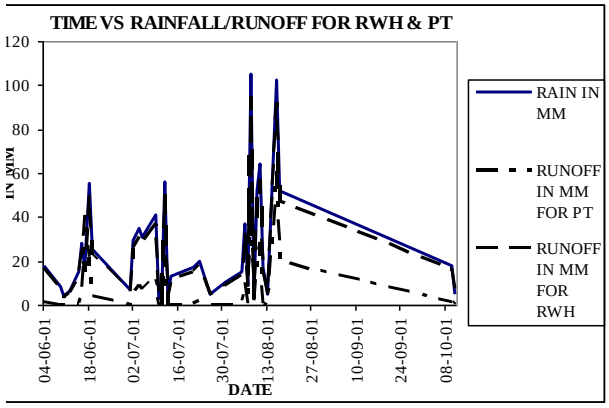

Fig. 6 Time Vs Rainfall /Runoff for RWH & PT

4.2 Runoff for RWH and PT

Total rainfall total rainfall recorded in the year 2001 was 937 mm. For pasture, runoff was 338.66 mm i.e. 34.3%, runoff of the total rainfall. This can be observed graphically as shown in the Fig. 6. It matches with SCS condition for the pasture (Mishra and Singh, 1999).Total runoff for the roof top was calculated as 843.30 mm i.e. 89.9%, runoff of the total rainfall (Fig. 6). This matches with SCS condition for the pasture of 90% runoff for paved surfaces (Mishra and Singh, 1999)

4.3 Permeability of tube wells

Permeability graph (Fig. 7) was plotted for various tube wells and it was observed that T-5, T-6, T-7 & T-16 had the permeability of 0.006 m/hr, 0.053 m/hr, 0.148 m/hr & 0.023 m/hr respectively. Whereas T-4 and T-8 tube

wells had permeability of 1.27m/hr and 0.45 m/hr respectively, highest permeability compared to any other tube wells and so for the next phase of recharging these two tube wells should be included in the system.

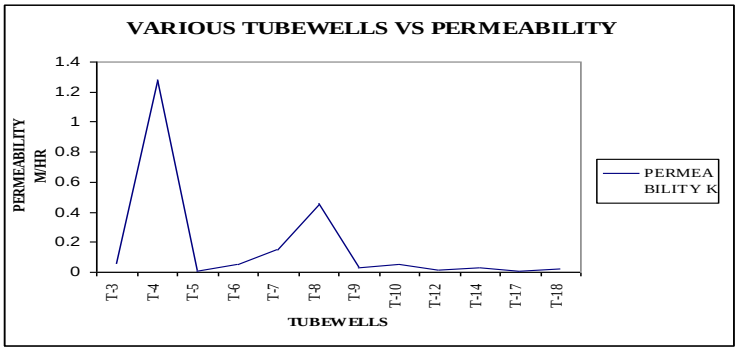

Fig. 7 Permeability Vs Tube wells

4.4 Water level rise in tube wells

The average water level rise for T-5, T-6 under percolation tank recharge was obtained as 4.13m, while for T-7, T-16 which was under RWH recharge it was 1.805m. Hence from the above results it can be analysed that water level raised in T-5, T-6 was twice than that of observed in T-7, T-16. The comparison in this case was also made with tube well T-1 which was none operating. The rise in the water level of the same is shown in Fig. 8 and Fig. 9.

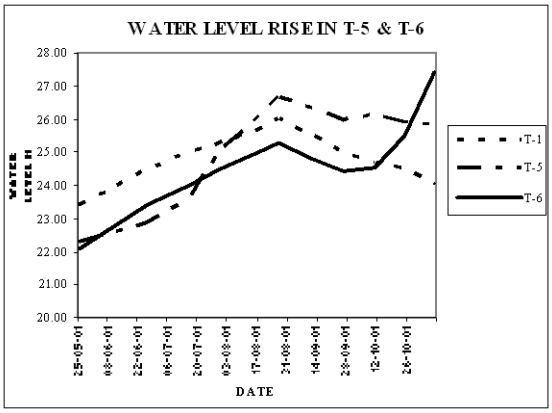

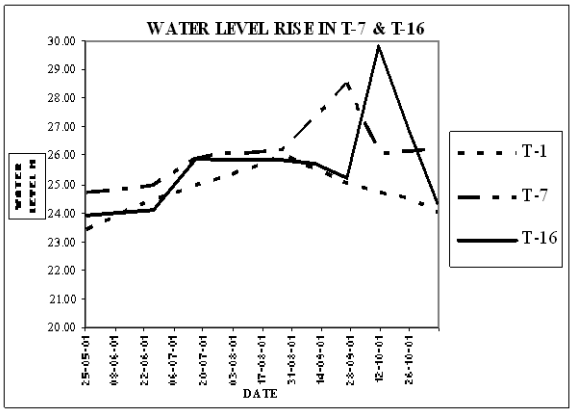

Fig. 8 Water level rise inT-5, T-6

Fig. 9 Water level rise in T-7, T-16

4.5 Total dissolved solids

For T- 5 & T-6 as the TDS level fall from 1050ppm to 722ppm, percentage of reduction in TDS value was more than 32% after artificial recharging, while for T- 7 & T-16 TDS reduced from 1650 ppm to 707.5ppm, which gave the reduction value of more than 58%. The comparative reduction is shown in Fig. 10 & 11. It was analyzed that TDS reduction in RWH was more by 26% as compared to percolation tank recharge. [Ref.6]

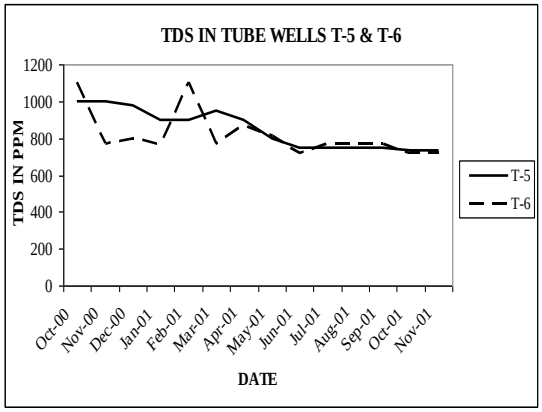

Fig. 10 TDS level inT-5, T-6

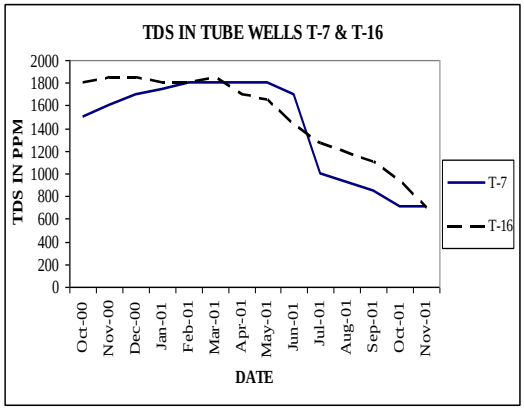

Fig. 11 TDS level in T-7, T-16

4.6 Recharge volume

Total volume of water recharged by PT was found as 2040m^3, while by RWH it was 9466 m^3. Hence the amount of recharge through RWH measured 4 times more than PT.

From the above results it was found that for T-7 and T-16 the recharging capacity was 601.43m^3/day and 2268m^3/day respectively. This was higher than the water injected in to the wells i.e. 57 m^3/day, and 206m^3/day for both the tube wells respectively. Thus it can be concluded that T- 7 & T-16 tube wells has much more recharging capacity than the volume of water injected. This shows that the designed capacity of T7, T16 found to be 10 times more than the actual recharging practiced. Hence it will work much efficiently in the heavy rains. [Ref.6]

5. CONCLUSIONS

- Rise in water level in the tube wells indicates that the tube well recharging technique was successful in increasing ground water level. From the results it can be analysed that water level raised in T-5, T-6 was twice than that of T-7, and T-16.Hence for quick raising of the water level in tube wells PT is much more effective. In percolation tank due to buffer storage continuous percolation takes place throughout the monsoon (even in between two successive rainfall interval) and after monsoon. Thus to recharge through the bed of percolation tank, higher rise in water level has been found in nearby tube wells. The results of combined recharge system i.e. injection of water in tube well through filter and from bed of percolation tank gives good results as compared to individual system.
- Permeability calculations and analytical results suggest that tube wells T-4 and T-8 should be taken in recharging whenever next recharging system is implemented.
- Analytically and graphically verification of site conditions like amount of runoff of the site was in agreement with the conditions as recommended by SCS curve method.
- The decrease in TDS values shows an effective artificial recharge in improving the water quality. Percentage reduction in TDS, in the RWH system in tube wells T-7, T-16, was 26% higher as compared to tube wells T-5, T-6 in PT. Which suggest RWH is more effective than PT for reducing TDS level in tube wells.
- Least amount of evaporation loses takes place in RWH. Secondly, maximum recharge capacity was much more than the volume of water injected in to the tube well. Thus it can be concluded that the system would work effectively during the heavy rains.
- Volume of water recharge through RWH is much more than PT .Hence whole roof top area of industry should be taken under RWH in the next phase of recharging.
- Both the recharging systems i.e. RWH & PT are compatible to the site conditions and further recharging of the entire site can be done, which will be very beneficial to the industry.

ACKNOWLEDGEMENT

Authors are thankful to M/S Apollo Tyres Industry for providing various site information and data for the research work.

REFERENCES

[1] Athavale R. N., Muralidharan D. and Rangarajan R., (1994) Borehole Injection studies in Deccan Trap Basalts near Nagpur- Proceedings of the Second International Symposium on 'Artificial Recharge of Ground Water', Ed. A. Ivan Johnson and R. David G. Pyne, pp.775-788.

[2] Athavale R. N water harvesting and sustainable supply in India (2003).

[3] Driscoll F. G., 1987. Ground Water Wells, 2nd edition Scientific Publisher

[4] Mishra S.K., Singh V. P., 1999. Soil Conservation Service Curve Number (SCS-CN) Methodology, Water Science and Technology Library, Vol. 42

[5] Todd D. K., Ground Water Hydrology, 1980, 2nd ed. John Wiley, New York.

[6] Trivedi Sejal H. 2002. Artificial recharge by tube wells and percolation tank: A case study Apollo Tyres Industry at Waghodia taluka, Vadodara.A dissertation submitted to M. S. Univ. Baroda, 2002 for ME (Hydraulic Structure).

Measuring the Effect of Variable Input Parameters in Fuzzy Back Propagation Network

Manan Bhavsar[1],Snehi Patel[2],,Drashti Patel[3],

mananbhavsar132@gmail.com[1], snehi_1910@yahoo.co.in[2], drashti.0104@gmail.com[3]

Computer Engineering Department, Silver Oak college of Engineering & Technological Gujarat Technological University, India, Ahmedabad,India

Abstract:-

Organizing data into sensible groupings is one of the most fundamental modes of understanding and learning. Classification & Cluster analysis is the formal study of methods and algorithms for grouping. Most of the real life classification problems have ill defined, imprecise or fuzzy class boundaries. We provide a brief overview of Fuzzy logic methods, summarize well known Fuzzy logic[1] classification methods, discuss the major challenges and key issues in designing combination of Fuzzy & neural network algorithms[3]. Hence, in this paper , Feed Forward neural networks, use back propagation learning algorithm[4] with fuzzy objective functions, are investigated. A learning algorithm is proposed that minimizes an error term, which reflects the fuzzy classification from the point of view of possibility approach. Since the proposed algorithm has possibility classification ability, it can encompass different back propagation learning algorithms based on crisp and constrained fuzzy classification[4][18]. A methodology has been presented for adequate classification of fuzzy information. First hidden layer generates the degree of membership for all the input-output pattern pairs. This vector of degree of membership is now being trained into the neural networks for generating the final classification rules using the Back propagation algorithm of neural networks[4]. Thus, neural networks as a whole performs two tasks. First, it generates the degree of membership and later it classifies the rules in different classes on the basis of membership function and measures the effect of input variables.

Keywords: Fuzzy K-Mean, Fuzzy KNN, FBP,KNN

1. Introduction

Aspects of knowledge representation and reasoning have dominated research in fuzzy set theory (FST)[1] for a long time, atleast in that part of the theory which lends itself to intelligent system's design and applications in artificial intelligence (AI). Yet, plenty of problems related to automated learning and knowledge acquisition have come in front during the recent years.

1.1. How Fuzzy Logic works?

In Fuzzy Logic, unlike standard conditional logic, the truth of any statement is a matter of degree. (e.g. How cold is it? How high shall we set the heat?) The degree to which any Fuzzy statement is true is denoted by a value between 0 and 1. Fuzzy Logic should be able to manipulate degrees of "may be" in addition to true and false. Eg:

tall(x) = {

0, = if height(x) < 5 ft.,

height(x), if 5 ft. <= height (x) <= 7 ft., (1)

1,= if height(x) > 7 ft.

}

where,

U: universe of discourse (i.e. set of people)

TALL: Fuzzy Subset

~TALL: Membership value

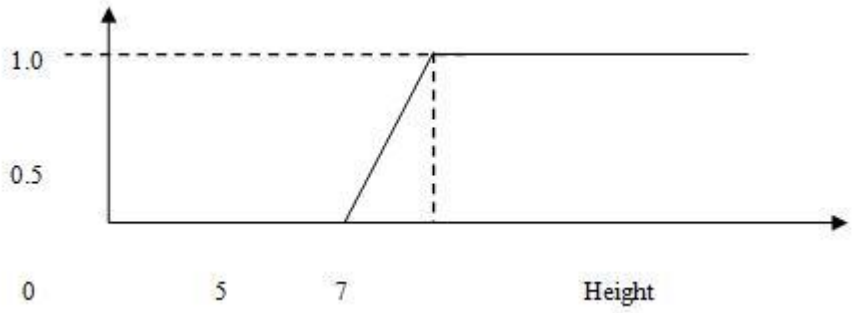

Fig.1. Membership function based on height of persons

Table 1.1 enholds , height details of certain students in feet and inches, along with which, membership of corresponding student has been calculated using eq(1).

Name	Height	Membership/Degree
Ravi	3'2"	0.00
Raj	5'5"	0.21
Dev	5'9"	0.38
Eshan	5'10"	0.42
Manan	6'1"	0.54
Karim	7'2"	1.00

Table 1:- Relation between height and membership/degree

From this definition: we can say that, the degree of truth of the statement "Dev is TALL" is 0.38. More often than not, it does not even lead to fully satisfying results. An alternative is to proceed from a fixed fuzzy partition for each attribute, i.e., a regular "fuzzy grid" of the input space, and to consider each cell of this grid as a potential antecedent part of a rule. This approach is advantageous from an interpretability point of view. On the other hand, it is less flexible and may produce inaccurate models when the one-dimensional partitions define a multi-dimensional grid that does not reflect the structure of the data. Especially important in the field of fuzzy rule learning are hybrid methods that combine FST with other methodologies, notably evolutionary algorithms and neural networks[20]. For example, evolutionary algorithms are often used in order to optimize ("tune") a fuzzy rule base or for searching the space of potential rule bases in a (more or less) systematic way [2].

Quite interesting are also neuro-fuzzy methods [2]. For example, one idea is to encode a fuzzy system as a neural network and to apply standard methods (like back propagation) in order to train such a network. This way, neuro-fuzzy systems combine the representational advantages of fuzzy systems with the flexibility and adaptively of neural networks[4][20].

The following sections will hopefully serve to elucidate the classification problem. Section-2 Fuzzy classification provides details of classification and prediction task of data analysis. It gives brief idea of different classification techniques. Section-3 explains the concept of Fuzzy classification techniques in depth. It explains the rule-based classification algorithm based on NEURO-FUZZY[12][22] concept, which is called LR-Type Back propagation. It also gives brief overview of difference between classification methods . Section-4 explains the structure of LR-TYPE Back propagation with suitable example. It gives overview of algorithm of LR-TYPE Back propagation method. Section-5 provides the implementation details of LR-TYPE Back propagation and it shows the output of different runs of program. It also shows the comparison of accuracy of different runs of program by using momentum factor & learning coefficient training dataset[4].

.2. Classification Techniques

This section gives basic knowledge of Fuzzy classification and the two forms of data analysis: Classification and Prediction. There are various techniques available for classification, which fall into two broad categories: Rule-based Classification and Mathematical Classifiers. Rule-based classifiers are easy to understand and easy to interpret for users than mathematical classifiers which are very difficult to understand for users[4]. The section gives the overview of Fuzzy K-mean & Fuzzy KNN and FBP.

2.1 Data Mining and Classification

Databases are rich with hidden information that can be used for intelligent decision making. Classification and prediction are two forms of data analysis that can be used to extract models describing important data classes or to predict future data trends. Such analysis can help provide us with a better understanding of the data at large. Whereas, classification predicts categorical (discrete, unordered) labels, prediction models continuous valued functions. Data classification is a two-step process. In the first step, a classifier is built describing a predetermined set of data classes or concepts. This is the learning step (or training phase), where a classification algorithm builds the classifier by analyzing or "learning from" a training set made up of database tools and their associated class labels[4][18].

When the class label of each training tool is provided, this step is also known as supervised learning (i.e., the learning of the classifier is "supervised" in that it is told to which class each training tool belongs). It contrasts with unsupervised learning (or clustering)[11], in which the class label of each training tool is not known, and the number or set of classes to be learned may not be known in advance. While testing, the predictive accuracy of the classifier is estimated. If we were to use the training set to measure the accuracy of the classifier, this estimate would likely be optimistic, because the classifier tends to over fit the data (i.e., during learning it may incorporate some particular anomalies of the training data that are not present in the general data set overall).[5][6]

Data prediction is a two-step process, similar to that of data classification. However, for prediction, we lose the terminology of "class label attribute" because the attribute for which values are being predicted is continuous-valued (ordered) rather than categorical (discrete-valued and unordered). The attribute can be referred simply as the predicted attribute. Classification methods can be compared based on various criteria such as predictive accuracy, speed, robustness, scalability and interpretability. The complete process of classification has been picturised in figure 2.

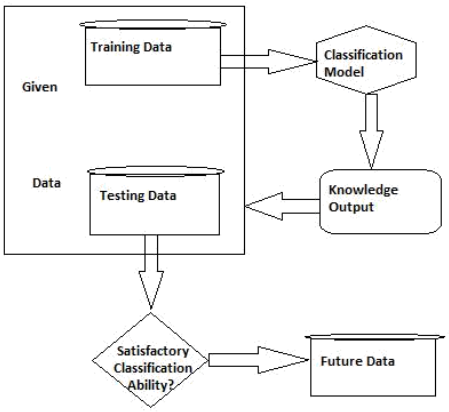

Fig.2. Classification Process[10]

2.2. Classification Methods in Fuzzy logic

Fuzzy logic was first developed by Zadeh [1] in the mid-1960s for representing uncertain and imprecise knowledge. It provides an approximate but effective means of describing the behavior of systems that are too complex, ill-defined, or not easily analyzed mathematically. Fuzzy variables are processed using a system called a fuzzy logic controller. It involves fuzzification, fuzzy inference, and defuzzification. The fuzzification process converts a crisp input value to a fuzzy value. The fuzzy inference is responsible for drawing conclusions from the knowledge base. The defuzzification process converts the fuzzy control actions into a crisp control action[19].

Fuzzy logic techniques have been successfully applied in a number of applications: computer vision, decision making, and system design including ANN training. The most extensive use of fuzzy logic is in the area of control, where examples include controllers for cement kilns, breaking systems, elevators, washing machines, hot water heaters, air-conditioners, video cameras, rice cookers, and photocopiers[17].

2.2.1. Types of learning

Often, a clear distinction is made between learning problems that are (i) supervised (classification) or (ii) unsupervised (clustering)[13], the first involving only labeled data (training patterns with known category labels) while the latter involving only unlabeled data [5]. There is a growing interest in a hybrid setting, called semi-supervised learning [6]. In semi-supervised classification, the labels of only a small portion of the training data set are available. The unlabeled data, instead of being discarded, are also used in the learning process[19].

2.3 Classification by Back propagation

Back propagation is a neural network learning algorithm[20]. Roughly speaking, a neural network is a set of connected input/output units in which each connection has a weight associated with it. During the learning phase, the network learns by adjusting the weights so as to be able to predict the correct class label of the input tools[8]. For example, it is difficult for humans to interpret the symbolic meaning behind the learned weights and of “hidden units” in the network. These features initially make neural networks less desirable for data mining. The back propagation algorithm performs learning on a multilayer feed-forward neural network. It iteratively learns a set of weights for prediction of the class label of tuples. A multilayer feed-forward neural network consists of an input layer, one or more hidden layers, and an output layer[4][19][20].

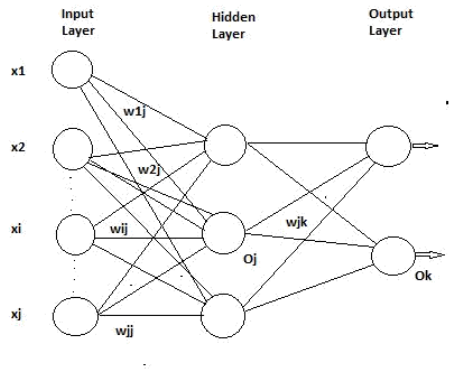

Fig.3. A multilayer feed-forward neural network[20]

Each layer is made up of certain input units. The inputs to the network correspond to the attributes measured for each training tuple. The inputs are fed simultaneously into the units making up the input layer. These inputs pass through the input layer and are then weighted and fed simultaneously to a second layer of "neuronlike" units, known as a hidden layer[20][22]. The outputs of the hidden layer units can be input to another hidden layer, and so on. The number of hidden layers is arbitrary, although in practice, usually only one is used. The weighted outputs of the last hidden layer are input to units making up the output layer, which emits the network's prediction for given tuples[19]. The units in the input layer are called input units. The units in the hidden layers and output layer are sometimes referred to as neurodes, due to their symbolic biological basis, or as output units[20][22]. A multilayer neural network has been shown in figure 3.

Back propagation learns by iteratively processing a data set of training tools, comparing the network's prediction for each tool with the actual known target value. The target value may be the known class label of the training tuple (for classification problems) or a continuous value (for prediction). For each training tuple, the weights are modified so as to minimize the mean squared error between the network's prediction and the actual target value[14]. These modifications are made in the "backward" direction, that is, from the output layer, through each hidden layer down to the first hidden layer (hence the name backpropagation). Although it is not guaranteed, in general the weights will eventually converge, and the learning process stops[4][18].

2.3.1 Fuzzy Back Propagation (FBP)

This section presents an extension of the standard back propagation algorithm (SBP). The proposed learning algorithm is based on the fuzzy integral of Sugeno and thus called Fuzzy Back Propagation (FBP) algorithm. Necessary and sufficient conditions for convergence of FBP algorithm for single-output networks in case of single- and multiple-training patterns are proved. A computer simulation illustrates and conforms the theoretical results. FBP algorithm shows considerably greater convergence rate compared to SBP algorithm[4]. Other advantages of FBP algorithm are that it reaches forward to the target value without oscillations, requires no assumptions about probability distribution and independence of input data. The convergence conditions enable training by automation of weight's tuning process (quasi-unsupervised learning) pointing out the interval where the target value belongs to[17]. This supports acquisition of implicit knowledge and ensures wide application, e.g. for creation of adaptable user interfaces, assessment of products, intelligent data analysis, etc. Neural networks[21], fuzzy logic and evolutionary computing have shown capability on many problems, but have not yet been able to solve the really complex problems that their biological counterparts can (e.g., vision). It is useful to fuse neural networks, fuzzy systems and evolutionary computing techniques for offsetting the demerits of one technique by the merits of another techniques. Some of these techniques are fused as[19][21]:

[9]Neural networks for designing fuzzy systems
[10] Fuzzy systems for designing neural networks
[11] Evolutionary computing for the design of fuzzy systems

(iv)Evolutionary computing in automatically training and generating neural network architectures.

3. Implementation

This section explains the implementation strategy of the LR-type (proposed) FBP algorithm. It provides guidance about how to improve performance and efficiency of LR- BP algorithm with modifications. In simple words, both neural nets and fuzzy logic are powerful design techniques that have its strengths and weaknesses. Neural network can learn from data sets while fuzzy logic solutions are easy to verify and optimize. If you look at these properties in a portfolio, the idea becomes obvious, that a clever combination of the two technologies delivers best of both worlds. Combine the explicit knowledge representation of fuzzy logic with the learning power of neural networks, and you get NeuroFuzzy. This implementation has been motivated by membership concept of fuzzy logic and training manner of neural networks(back propagation technique). Current research focuses on the design of optimal algorithm which implements faster and reduces the number of scans of a dataset..The proposed algorithm is as follows:-

Proposed Algorithm:-

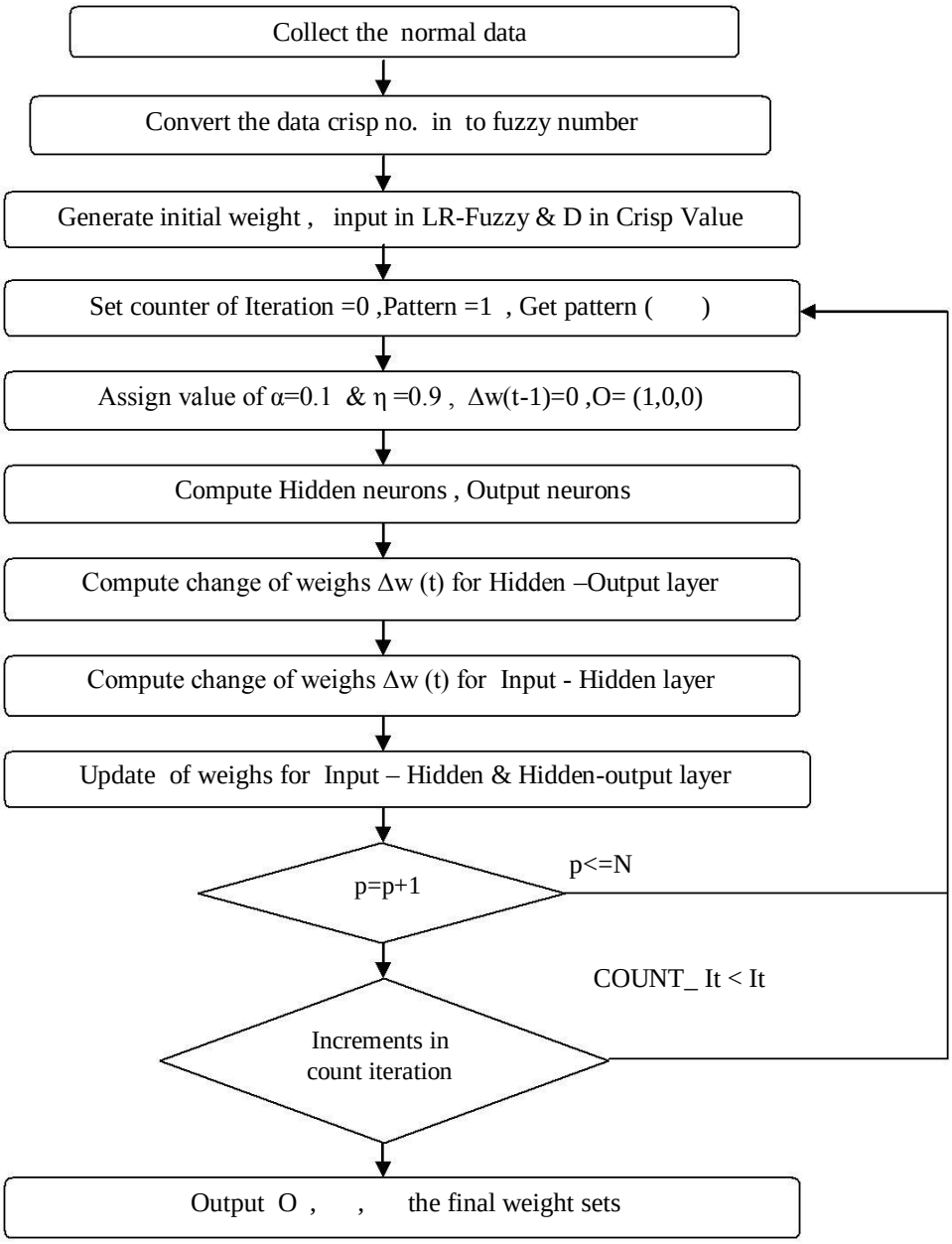

3.1. Data Collection:-

This implementation uses data set of employees[17] to judge ability of an employee. In this data set there are six input variables :

1.Worth value

2.Employee acceptance

3. Salutation availability

4. Teach ability. Easier

solution 6.Risk.

All the inputs have more than one part , which is converted to Fuzzy set likewise:

1.Worth value : 1. Negative 2.Low

3. Moderate 4. High

Instances	Worth value	Employee Acceptance	Salutation Availability	Teach ability	Easier solution	risk	output
1	High	Positive	None	Frequent	None	Low	Good

Table 2:- Employee data set used for implementation[17]

3.2. Membership allocation to data using fuzzy logic(LR Concept):-

A fuzzy number means if there exists reference function L(left) &R(right) and scalars, $\alpha>0$, $\beta>0$ with

$$\mu(x) = \qquad (2)$$

Symmetric triangle LR type Fuzzy number : This diagram defines the value of Membership Degree and related data and assigns the value of α & β.

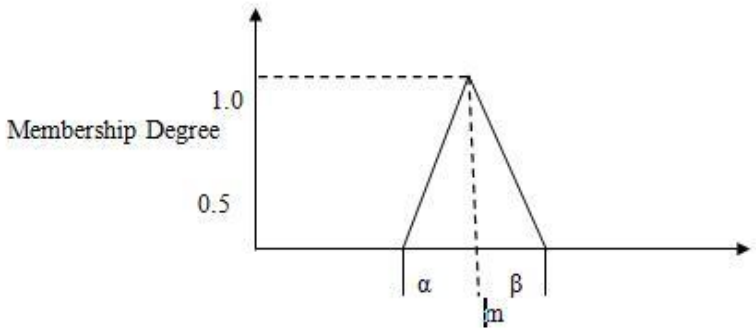

Fig.5. Symmetric triangle LR type Fuzzy number

3.3. Generating initial weight:-

Initially, weight is assumed to be zero[17]. This if for first tuple I_1 of first input layer. After that, random weights between -1 to 1 may be assigned to the rest of the tuples of first input layer. These tuple weights are forwarded to hidden layer tuples using eq(3). This has been represented in table 3.

$$H_i = I * w \quad (3)$$

Pattern				Output
1	(1,0,0)	(1,0.2,0.3)	(0,0.1,0.4)	0.8
2	(1,0,0)	(0.5,0.2,0.1)	(0.4,0.5,0.4)	0.2

Table 3:- Initial inputs of input layer

After assigning random weights to input tuples, now, we are finding actual weight of input-hidden layer as follows:-

Input pattern 1( )

= (1,0,0) , (1,0.2,0.3) ,(0,0..1,0.4)

= 0.8

The output of input neurons :

= = (1,0,0) , (1,0.2,0.3) ,(0,0..1,0.4)

The input of the hidden neurons :

= 0

= (1,0,0)(0.62,0.505,0.405)+ (1,0.2,0.3) (0.89,0.634,0.101) + (0,0..1,0.4) (0.66,0.567,0.64)

= (1.514,1.3838,1.0382)

Input-hidden	Layer		Hidden_ op lay
			(0.154,0.033,0.498)
(0.62,0.505,0.405)	(0.89,0.634,0.101)	(0.66,0.567,0.64)	(0.092,0.277,0.223)
(-0.23,0.32,0.498)	(-0.72,0.71,0.855)	(0.134,0.719,0.153)	(0.972,0.137,0.72)

Table 3:-Updated weights of input-hidden layer

3.4. Generating weights from hidden-output layer:-

The Fuzzy neuron is the element of FBP. In fig. given vector I=(i_1, i_2,.. i_n) &weight vector W=(w1,w2,..wl).compute the crisp output O is:

$$O = f(NET) = f(CE$$

Here i0= (1,0,0) is bias. Fuzzy weighted summation :

$$\textbf{Net=} \sum W_i I_i$$

Is first computed & NET= CE(net).The function CE is centriod of triangle Fuzzy no & treated as Deffuzification operation .if net(, α') then:

CE (net) = +1/3(-)= NET

After that first define :

f (NET)=1/exp(-NET)

That is the final computation to obtain the crisp output value O.

Finding the = 0 ;

= CE (1.514,1.3838,1.0382)

= 1.514 + 1/3 (1.0382-1.3838)

= 1.3988

The output of the hidden neurons :

= 1

= f (1.3899) = 1/ 1+ = 0.8020

= f (-1.0254) = 1/ 1+ e^(-1.0254) = 0.2640

. The output of the output neurons :

=

Assign the value for η= 0.9 & α =0.1 set ΔW(t-1) = 0.

ΔE (t) = { ∂E/∂ , ∂E/∂ , ∂E/∂ } gives

∂E/∂ = - (0.8-0.6629) (0.6629) (1-0.6629)(1)(1)

= - 0.0306

∂E/∂ =0.0102 **& ∂E/∂** =-0.0102

Compute changes in weights :

Δ (t) = - η Δ E (t) + α Δ (t-1)

= (0.0276,-0.0092,0.0092)

Update weights for the hidden-output layer are

(t) = (t - 1) + Δ (t)

= (0.1816,0.0238,0.5072)

Update weights for the Input-hidden layer are

= - (-) ( ) (1 -)

= -(0.8-0.6629) (0.6629)(1-0.6629)

= -0.036

This procedure is repeated upto its optimal solution. i.e. , a time will come when, there will be no change in output of output layer.

4. Results and discussion

The algorithm has been applied to Employee data set, to get the crisp value which is related with the data set. The algorithm has been run several times using different size, proper value of η .

Comparative Analysis of Results

The comparative accuracy of all runs of the program with respect to different size of training dataset and different value of η has been shown in figure 6, where X-axis represents size of training dataset and Y-axis represents accuracy rate. As we can see from the graph, that accuracy rate increases as the size of training dataset is increased. The reason is very clear that as training size of dataset get increased, the classifier is trained properly and so it can classify the future data properly.

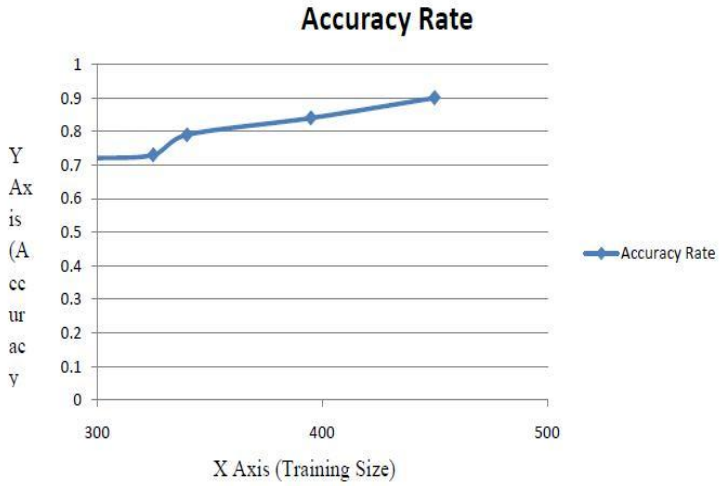

Fig.6. Graph of Accuracy of Classifier

Now , the Value of Learning co-efficient (η) is available between 0 to 1. Figure 8 represent relation between the Error-rate & Learning co-efficient (η)[7].

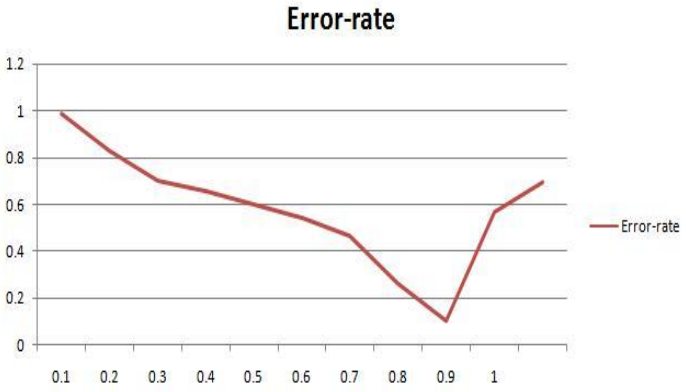

Fig.8. Graph of different value of Learning co-efficient (η).

5. Conclusion

Fuzzy logic have ability to convert the data from Real world to mathematical form so, we are using classification methods of Fuzzy set theory. After classifying this method, we conclude that Fuzzy Logic has no power of Generalization. Using the concept of Neural Network : It have more ability to train the data and power of Generalization. Finally, we worked on Hybrid System[9] and so combined both the technologies. So, we collected the data from the real world and converted into Fuzzy number, then using concept of Back propagation Method using neural networks , we found the optimal solution .When compared with another classification methods, we get more accuracy .But every time we have to change the value of input variables like Learning co-efficient (η)[7] .

FUTURE WORK : We are working on the Real data using LR-Type Back propagation. This algorithm can be implemented on various other data sets. Apply the concept of Genetic algorithm on it and which are the factors affecting it.

6. REFERENCES

1. L. A. Zadeh, " Fuzzy Sets", *Info. Control*,vol. 8, pp.338–353 ,1965.
2. L.A. Zadeh,"Fuzzy logic, neural networks and soft computing", One-page course announcement of CS 294-4, Spring 1993, University of California at Berkeley, 1992.
3. S. Jakubek and T. Strasser. " Artificial neural networks for fault detection in large-scale data acquisition systems". *Engineering Applications of Artificial Intelligence*, vol17,pp:233–248, May 2004.
4. Fahlman, S.E., "An Empricial Study of Learning Speed on BP Networks",*Carnegie Mellon Report* , No CMU-Cs,pp 88.162,(1988b)
5. K. Asakawa and H. Takagi, "Neural networks in Japan*," Commun.* ACM, vol. 37, no. 3, pp. 106–112, Mar. 1994.
6. J. C. Bezdek, E. C.-K. Tsao, and N. R. Pal, "Fuzzy Kohonen clustering networks," *in IEEE Int. Conf. Fuzzy Syst.*, pp. 1035–1043,1992.
7. J. J. Buckley, P. Krishnamraju, K. Reilly, and Y. Hayashi, "Genetic learning algorithms for fuzzy neural nets," *in Proc. 3rd IEEE Int. Conf. Fuzzy Syst.*, vol. 3, pp. 1969–1974,1994.
8. Bei, C.-D., & Gray, R. M. "An improvement of the minimum distortion encoding algorithm for vector quantization*". IEEE Transactions on Communications*, vol33, pp.1132–1133,1985.
9. A. Kandel, Y.-Q. Zhang, and T. Miller, "Hybrid fuzzy neural system for fuzzy moves," *in Proc. 3rd World Congr. Expert Syst*,pp. 718–725,1996.
10. Neural network ,Fuzzy logic, Genetic Algorithms, Synthesis & Applications : S.Rajasekaran & G.A Vijayalakshmi Pai.
11. http://en.wikipedia.org/wiki/Data_clustering#Fuzzy_c-means_clustering.
12. M. M. Gupta and D. H. Rao, "On the principles of fuzzy neural networks," *Fuzzy Sets Syst.*, vol.61, pp. 1–18, 1994.
13. C. Elkan, "Using the triangle inequality to accelerate k-means," *International Conference on Machine Learning* , pp. 147-153, 2003.
14. A. Yajnik, S. Rama Mohan, "Identification of Gujarati Characters Using Wavelets and Neural Network", *Proc.Of 10th IASTED International Conference on Artificial Intelligence and Soft Computing,* Acta press , pp. 150-155 ,2006.
15. H. Ishigami et al., "Structure optimization of fuzzy neural network by genetic algorithm," *Fuzzy Sets Syst*., vol. 71, pp. 257–264, 1995.
16. J. Yen and Wang L. "Application of statistical information criteria for optimal fuzzy model construction". *IEEE Transactions on Fuzzy Systems,* 6(3):362 – 372, August 1998.
17. J. B. Kiszka and M. M. Gupta, "Fuzzy logic neural network," *BUSEFAL*, vol. 4, pp. 104–109, 1990.
18. D Nauck and R Kruse, " A fuzzy neural network learning fuzzy control rules and membership functions by fuzzy error back propagation ". *In Pro. IEEE Int. Conf. on Neural Networks*, 1993.
19. Y. Wang and G. Rong, "A self-organizing neural network- based fuzzy system ", *Fuzzy Sets and Systems*,

1999.

20. Y. Yang, X. Xu and W. Zang ,"Design neural networks based fuzzy logic", *Fuzzy Sets and Systems*, 2000.

21. C. Yao and Y. Kuo, "A fuzzy neural network model with three layered structure," *in Proc. of FUZZ-IEEE/IFES*, vol. III, pp.1503-1511,1995.

22. Y. Shi, and M. Mizumoto, "A new approach of neuro-fuzzy learning algorithm for tuning fuzzy rule s", *Fuzzy Sets and Systems*, 2000.

Voltage and Frequency Control of Parallel Operated Synchronous and Induction Generators in Micro Hydro scheme

Pochana Janardhan Reddy

janardhan505@gmail.com

Electrical Engineering Department, Silver oak college of Engineering & Technological Gujarat Technological University, India

Abstract:-

The conventional control system for a standalone generator or more than one generator feeding the local load is not cost effective. This is because of the control system cost remains almost the same for the wide variations in the mini or micro hydro plant power rating. It is therefore envisaged that while using the combination of synchronous and induction generators can cut down the cost of electro-mechanical equipment. The synchronous generator may provide reactive requirements of the load. The frequency sensitive load controllers is proposed to provide a variable load in the system in order to make the load seen by two generators, due variation in the consumer load remains constant. This shall ensure the constant voltage and frequency operation of the system.

Keywords: *Electronic Load Controller, Excitation control system, Dump load.*

1. Introduction

In sparsely populated areas which are located far away from the common grid, installation of micro hydro plant(MHP) is a common practice.[1] The use of induction generators is becoming more common in MHP application because of its simpler excitation system, lower fault level, lower capital cost, less maintenance requirement. However, one of its major drawback is that it cannot generate the reactive power as demanded by the load. Most of the early stage MHP are equipped by the synchronous generators. In future many of the existing MHP plants with synchronous generator may have to install an add on plants and connect in parallel with the existing MHP plants to full fill the increasing load demand. In such a situation the plant cost can be reduced further if induction generator could be used as add on plant to the MHP with synchronous generator.[2-3]

2. Proposed Scheme

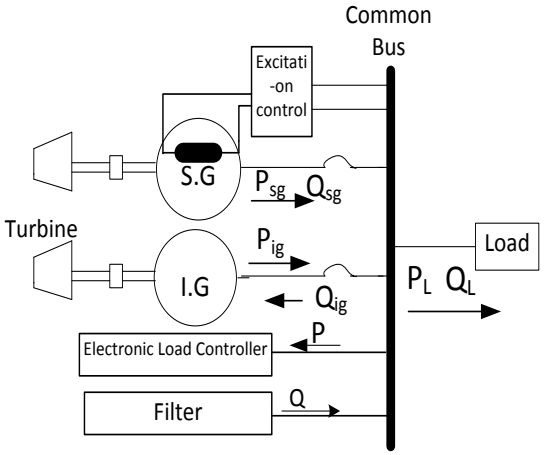

Fig.1: Block diagram of Proposed Scheme.

Fig.1 shows the schematic diagram of the proposed scheme. The synchronous generator has the exciter which provides variable excitation under different load conditions. Further the synchronous generators are connected to governor less turbine. i.e there is no input control to regulate speed or frequency. On the other hand induction generator does not have either excitation control or speed control and it can provide constant power subjected to available head and flow[4]. The synchronous generator has to generate the reactive power required by the load as well as induction generator. In addition capacitor bank is connected to provide constant VAR of load. However, the variable VAR shall met by synchronous generator. Since induction generator does not have speed controller it is bound to follow the synchronous generator and runs with a constant speed.

3. Modelling of the Proposed Scheme

The synchronous and induction machine models available in the MatLab-Simulink are used to performing the dynamic behaviour of the proposed scheme. The d–q equivalent circuit models of the synchronous and induction machines are used in the simulation model, which takes care of dynamics of stator, field and damper windings. Both the models have considered the effect of magnetic saturation. Stator windings of synchronous and induction generators are assumed to be connected in star with grounded neutral. The system consists of two controllers. One is the load controller to maintain constant speed and the other is excitation controller to stabilize the voltage.

3.1 Reactive Power Control

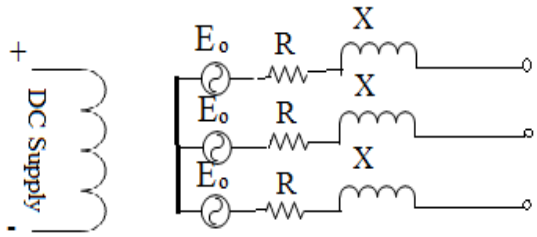

Fig.2. phase equivalent ckt of synchronous generator.

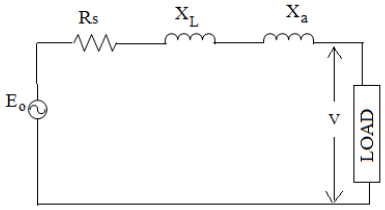

Fig.3. The equvalent ckt of one phase

If the excitation of an alternator is adjusted to give rated voltage at no load and then the load is thrown on, the terminal voltage falls (considering lagging loads) even though the speed of synchronous generator is constant. The change in terminal voltage is due to armature resistance, armature reactance and armature reaction. When the alternator is operating at no load its circuit diagram is as shown in the figure. Each phase generates an emf E_o per phase. The equivalent circuit for one phase is as shown in the figure. While the excitation current and the speed remains constant, the terminal voltage of the alternator changes with the change in load or armature current as mentioned above. The relation between terminal voltage V and load current I of an alternator is known as its load characteristics. Normally the terminal voltage falls with the increase in load current, but when the power factor is leading one the curve may raise.

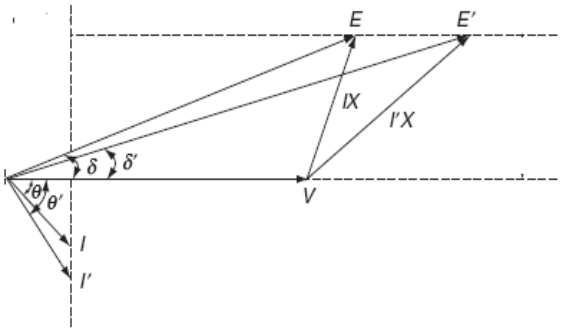

Fig.4. Effect of varying excitation on terminal voltage of Isolated synchronous generator

Total voltage drop on load = $IR_e+j(IX_L+IX_a) = IZ$

If $R_e= 0$; then Total voltage drop = IX_s

And voltage on no load => $E_o=V_o+IZ_s$

From the figure 3, phasor diagram it is clear that excitation should be increased inorder for the constant voltage under varying load conditions. The figure shows the dynamic excitation control of synchronous generator. It consists of one power circuit and control circuit. Power circuit consists of one single phase uncontrolled diode rectifier, filter capacitor to remove the ripple content in DC side and MOSFET/IGBT which acts as switch to control the average current in excitation winding. The circuit also consists of freewheeling diode to ensure the continuity of current.

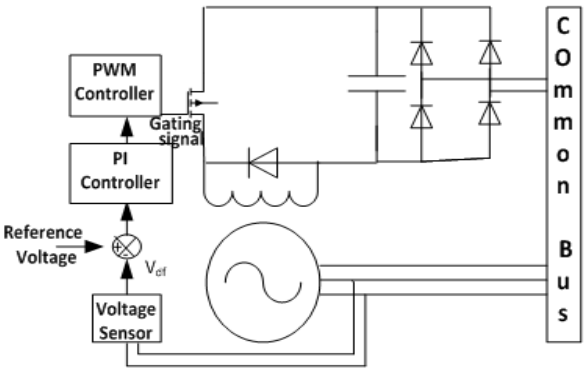

Fig.5. Block diagram of the dynamic excitation control of system synchronous generator.

Control circuit consists of voltage sensor which senses the terminal voltage of the generator and gives feedback signal. This is compared with the reference input and error is processed through the PI controller. After sensing the processed error the PWM controller gives the corresponding pulses (duty ratio of which varies according to the error). That is how the excitation is varied dynamically with change in load.

3.2 Active Power Control:

This system is to be installed in micro-hydro projects where the input power through the turbines is uncontrolled and constant. Since the input power is constant, the output power also should be constant. Otherwise the system may go to unstability, i.e speed and there by frequency may increase change beyond the limits. However it is not possible to maintain the load power constant as it changes with time. So there should be the control circuit where exactly the remaining power can be dumped. For this reason the dump load is shunted with the consumer load.[6-12]

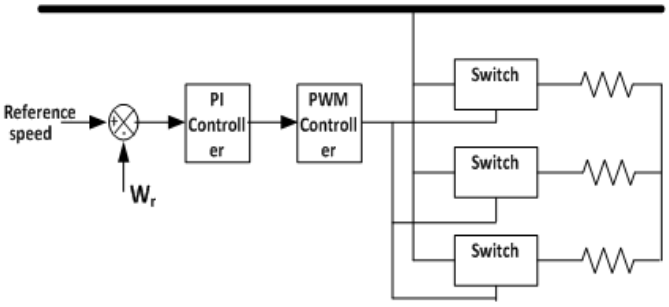

Fig.6. Block diagram of the Electronic Load Controller and its control Scheme.

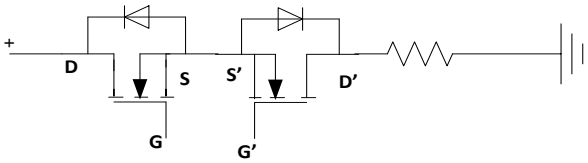

Fig.7. Per phase switch configuration.

4. Results and discussion

Initially steady state is achieved by operating synchronous and induction generators in parallel with 13kVA connected to it. Loads connected to the system at different instants of time are as follows

From time 0 to 2 seconds P=10.5 and Q=4.4kVAR.

From time 2 to 3 seconds load is increased to P=17kW and Q=5.95kVAR as shown below.

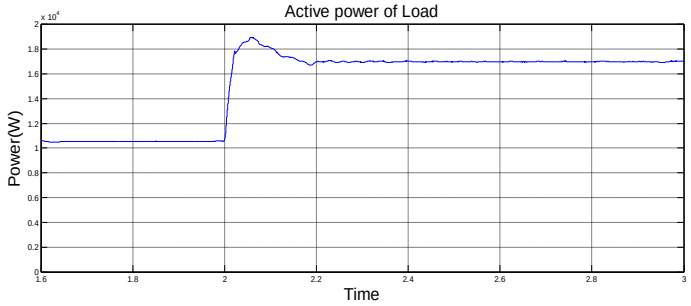

Fig.8 Active power consumption of the load.

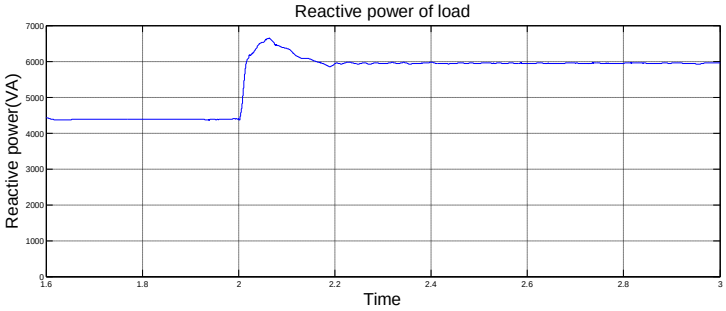

Fig.9. Reactive power consumption of the load.

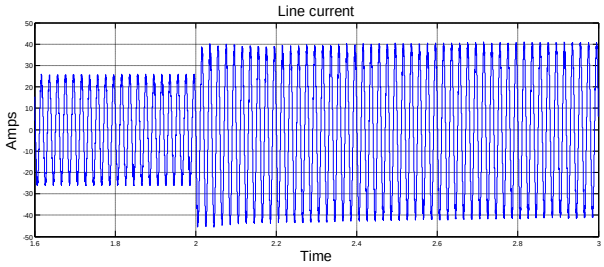

Fig.10. Line Current

The steady state current for initial load 17A and for increase in load at time instant 2 s, current increases to 28A.

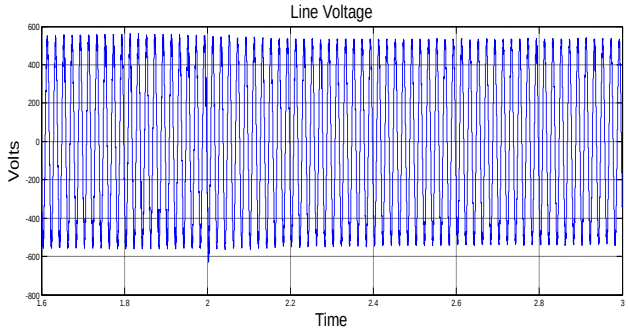

Fig.11 Load voltage

Terminal voltage of the load remain constant at V_{rms}=400V(V_{p-p}=560V) even with the increase in load. This is due to excitation control system of the synchronous generator.

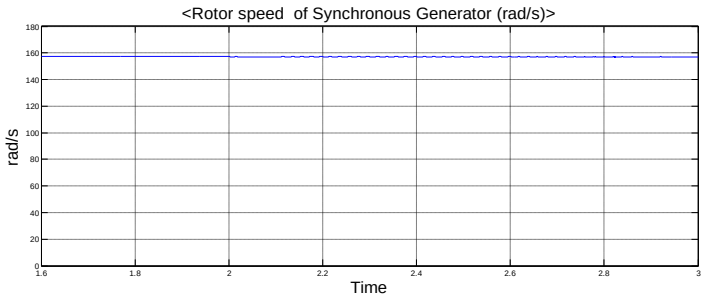

Fig.12 Rotor speed of synchronous generators.

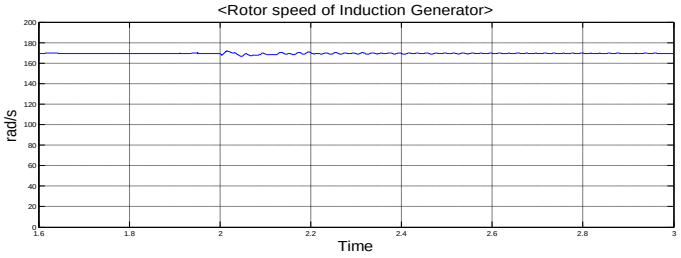

Fig.13 Rotor speed of Induction generators respectively.

From the simulation it is observed that speed of the synchronous generator is 157 rad/s (1500 r.p.m) and remain constant even under load changes. The speed of the induction generator is bound to follow the synchronous generator with the negative slip of 0.082.

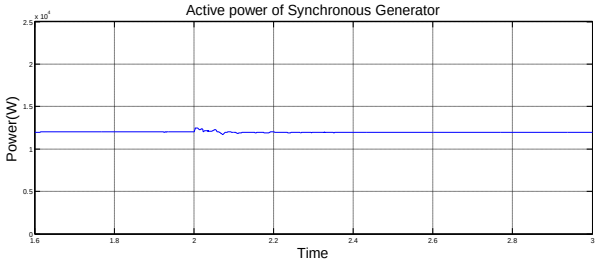

Fig.14 Active power generation of synchronous generator

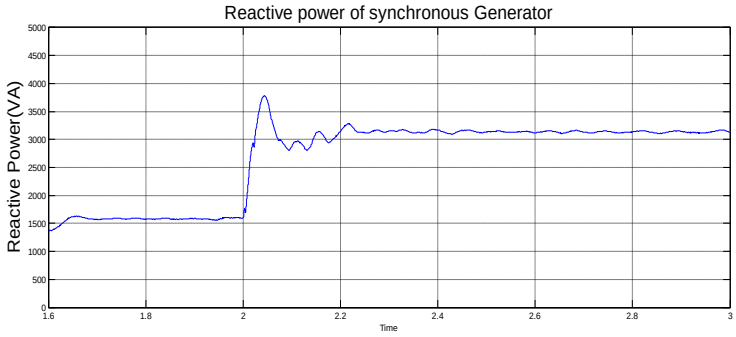

Fig.15 Reactive power generation of synchronous generator

Active power of the synchronous generator remain constant (12kW) because the generator is driven by governor less turbine. Reactive power changes(1.6kVAR upto2 seconds and 3.1kVAR) as demanded by the load.

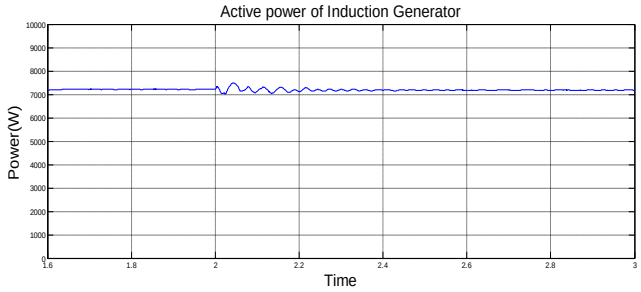

Fig.16 Active power of the Induction motor.

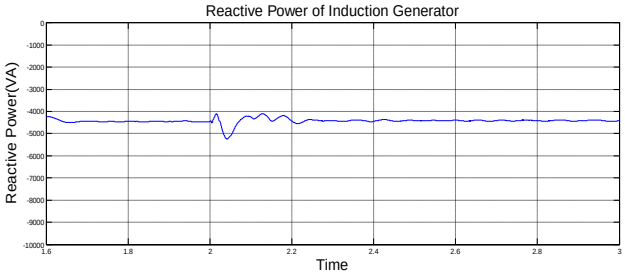

Fig.17 Reactive power of the Induction motor.

Induction generator has neither excitation control nor speed controller. It is driven by the governor less turbine. So active power generated is constant(P=7.2kW). The amount of reactive power consumed by the Induction generator is also constant(Q=-4.4kVAR).

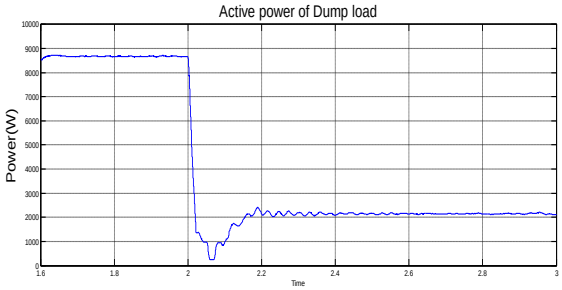

Fig.18 Active power consumed by the dump load

Here electronic load controller is placed and its power consumption is modified so as the total active power on the system remains constant. (8.7kW upto 2s and 2.2kW from 2 to 3 s).

Upto 2 s: P_L=10.5kW and P_D=8.7kW. total power on system P=19.2kW

From 2 to 3 seconds:P_L=17kW and P_D=2.2. Total power on system P=19.2kW.

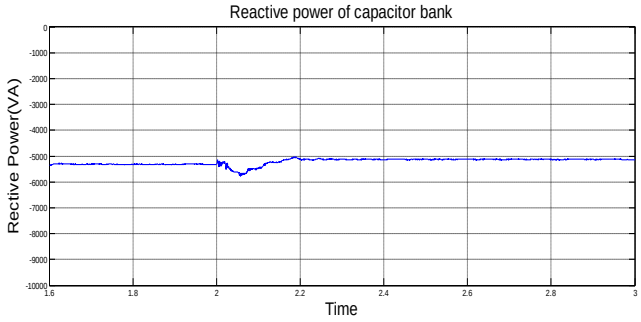

Fig.19 Reactive power generated by the capacitor

A capacitor is connected to the common bus to decrease the rating of the synchronous machine.

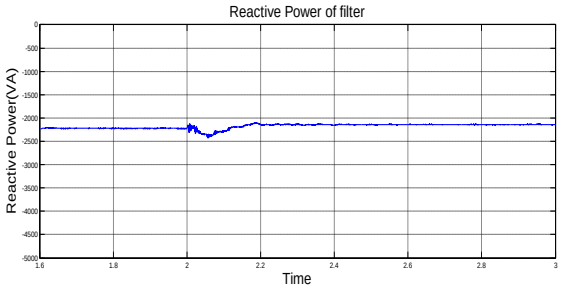

Fig.20. A filter is connected to reduce the harmonic content in the line voltage waveform.

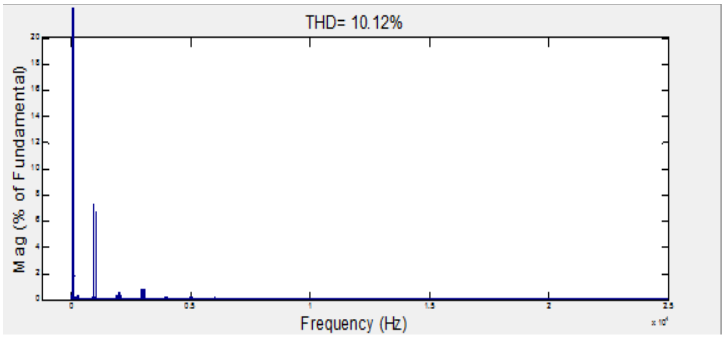

Fig.21 THD analysis of Load voltage waveform before adding filter(THD=10.12%)

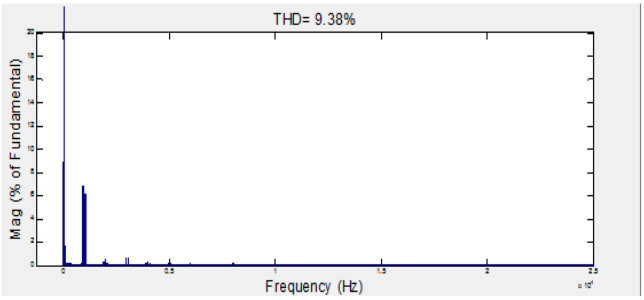

Fig.22 THD analysis of Load current waveform before adding filter(THD=9.38%)

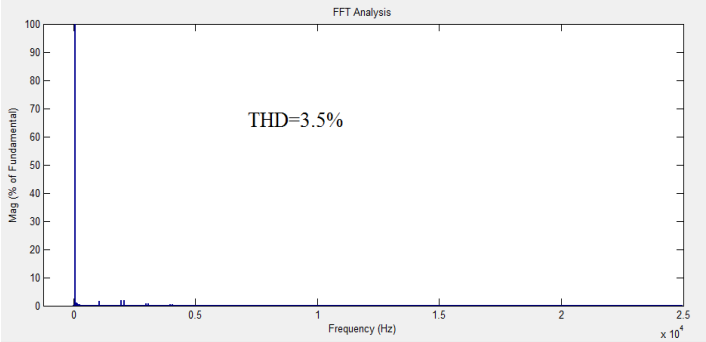

Fig.23 THD analysis of Load voltage waveform after adding filter (THD=3.5%)

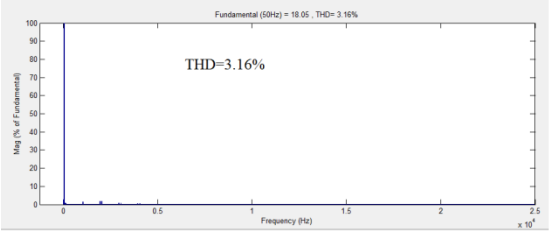

Fig.24 THD analysis of Line current waveform after adding filter (THD=3.16%)

BALANCE OF ACTIVE POWER BETWEEN GENERATION AND CONSUMPTION

Sources/ Sinks	**Time duration in seconds**	
	1.6-2	***2-3***
P_{sg}	+12kW	+12kW
P_{ig}	+7.2kW	+7.2kW
P_L	-10.5kW	-17kW
P_D	+8.7kW	-2.2kW
P Unbal-anced	0kW	0kW

TABLE II. BALANCE OF REACTIVE POWER BETWEEN GENERATION AND CONSUMPTION

Sources / Sinks	Time duration in seconds	
	1.6-2	*2-3*
Q_{sg}	+1.58kVAR	+3.15kVAR
Q_{ig}	-4.4kVAR	-4.4kVAR
Q_L	-4.4kVAR	-5.9kVAR
Q_c	+5.3kVAR	+5.12kVAR
Q_f	+2.22kVAR	+2.14kVAR
Q Unbal-anced	0kVAR	0kVAR

5. Conclusion

The simulation results show that when an induction generator driven by constant mechanical power input is connected in parallel with the synchronous generator, the induction generator is bound to follow the synchronous generator with a speed little above the speed of synchronous generator. The speed deviation because of increase in load is very small and is found to settle down to steady state value. The results also show that connecting an induction generator in parallel with the synchronous is much simpler than connecting two synchronous generators in parallel. It does not require synchronizing panel hardware and a simple commercially available induction motor can be used as generator without governor. Any change in consumers reactive load is responded by the synchronous generator to keep the voltage nearly constant to 1 pu. The induction generator does not respond to the change in consumer's load and it always operates at its full rating.

6. REFERENCES

[1]I.Tamrakar,L.B.Shilparkar,B.G.Fernandes and R.Nelsen.'Voltage and frequency control of parallel operated synchronous generator and induction generator withSTATCOM in micro hydro scheme':,*IET, Gener.,Transm, Distrib, Vol 1,no.5,* September 2005.

[2] Bhim Singh, Gaurav Kumar Kasal.: 'Voltage and Frequency Controller for parallel operated Isolated Asynchronous Generators"., *IEEE, Transaction , 2007, 1,(5).*

[3]Henderson D.S.:'Synchronous or induction generator?-The choice for small scale generation".Opportunities and advances in Int.power generation, *IEE Conf.* March 1996, (publication no.419) PP. 146-149.

[4]Singh b.,Shilparkar, L.B.: 'Analysis of a novel Solid state Voltage regulator for self excited Induction generator', *IEEProc. ,Gener.,Transm, Distrib,* 1998, 145, (6), PP. 647-655.

[5]Chakraborti C.,Das, S.P.and Bhadra ,S.N.: 'Some studies on parallel operation of Self excited Induction generators'., Proc. Of *Int.Conf.on energy Conversion*, 1994, 14, (3) , PP.497-485..

[6]Singh B., Murthy , S.S., and Gupta , S.:Analysis and desing of Electronic load controller for self excited Induction generator', *IEEE Transaction .Energy Conversion*, 2006, 21,(1), PP.285-293.

[7]Bhim Singh, S. S. Murthy, Shushma Gupta, “Analysis and design of electronic load controller for self-excited induction generators,” *IEEE Trans. on Energy Conversion*, Vol. 21, No. 1, pp. 285-293, March 2006.

[8]Bhim Singh, S. S. Murthy, Shushma Gupta, “Transient analysis of selfexcited induction generator with electronic load controller(ELC) supplying static and dynamic loads,” *IEEE Trans. on Industry Applications*, Vol. 41, No. 5, pp. 1194-1204, Sept. 2005.

[9]S.P.Singh, B. Singh, M.P. Jain, “Comparative study on the performance of a commercially designed induction generator with induction motors operating as self excited induction generators,” *IEE Proceedings-C*, Vol. 140, No. 5, pp. 374 – 380, Sept. 1993.

[10]Al-Bahrani, A.H., and Malik, N.H.: ‘Steady state analysis and performance characteristics of a three phase induction generator self excited with a single capacitor’, IEEE Trans. Energy Conversion, 1990, 5, (4), pp 725–732

[11] Wang, L., Yang, Y.-F., and Kuo, S.-C.: ‘Analysis of grid-connected induction generators under three-phase balanced conditions’. Proc.of the Int. Conf. on Energy Conversion 2002, 2002, pp. 413–416

[12] Singh, B., and Shilpakar, L.B.: ‘Analysis of a novel solid state voltage regulator for self-exited induction generator’, IEE Proc. Gener. Transm. Distrib., 1998, 145, (6), pp. 647–655.

[13] Wang, L., and Lee, C.H.: ‘Dynamic analyses of parallel operated self-excited induction generators feeding an induction motor load’, IEEE Trans. Energy Conversion, 1999, 14, (3), pp. 479–485.

[14]Bhim Singh, S. S. Murthy, Shushma Gupta, “Transient analysis of selfexcited induction generator with electronic load controller(ELC) supplying static and dynamic loads,” *IEEE Trans. on Industry Applications*, Vol. 41, No. 5, pp. 1194-1204, Sept. 2005.

[15]Douglas Henderson, “An advanced electronic load governor for control of micro hydroelectric generation”, *IEEE Trans. on Energy Conversion*, Vol. 13, No. 3, pp. 300-304, Sept. 1998.

WaveletbasedSpecal Reduction Technice Using Unisotropic Diffusion Filter

Mr. Minkal B. Patel

patelminkal88@gmail.com

Electronics & Communication Engineering Department, Silver oak college of Engineering & Technological Gujarat Technological University, India

Abstract:-

In diagnosis of diseases Ultrasonic devices are frequently used by healthcare professionals. The main problem during diagnosis is the distortion of visual signals obtained which is due to the consequence of the coherent of nature of the wave transmitted. These distortions are termed as 'Speckle Noise'. The present study focuses on proposing a technique to reduce speckle noise from ultrasonic devices. This technique uses a SRAD filter with wavelet based BayesShrink technique. The proposed filter is compared with traditional filters and existing filters using anisotropic diffusion. Experimental results prove that the proposed method is efficient in reaching convergence quickly and producing quality denoised images.

Keywords: *Anisotropic Diffusion, BayesShrink, Speckle denoising, SRAD Filter, Wavelet Based.*

1. INTRODUCTION

Medical digital images have become an essential part in the healthcare industry for diagnosis of diseases. These images are produced by various medical imaging devices like x-ray, CT / MRI scanners and electron microscope all of which produce high resolution images. Medical images are usually corrupted by Noise during their acquisition and transmission. Noisy images often lead to incorrect diagnosis. The main objective of Image Denoising techniques is to remove such noises while retaining as much as possible the important signal features. Ultrasonic imaging is a widely used medical-imaging procedure because it is economical, comparatively safe, transferable and adaptable [1].

One of the major problems of ultrasound images is that they suffer from a special kind of noise called 'speckle'. Speckle is a complex phenomenon and it significantly degrades image quality. Speckle appears interference of back-scattered wave from many microscopic diffused reflection which passing through internal organs and makes it more difficult for the observer to discriminate fine detail of the images in diagnostic examinations.

This paper is an effort made to produce a speckle noise removal using various filtering technique. This paper is organized as below. The second section gives an overview to the noise under discussion, while Section 3 discusses the wavelet based denoising uses for ultrasound. Section 4 presents results of experimented images and comparison of parameters. Section 5 presents a conclusion.

2. SPECAL NOISE

The most critical part of developing a method for -recovering a signal from its noisy environment seems to be choosing a reasonable statistical (or analytic) description of the physical phenomena underlying the data-formation process. The availability of an accurate and reliable model of speckle noise formation is a prerequisite for development of a valuable de-speckling algorithm. In ultrasound imaging, however, the unified definition of such a model still remains arguable. Yet, there exist a number of possible formulae whose probability was verified via their practical use. A possible generalized model of the speckle imaging is

$$g(n, m) = f(n, m)u(n, m) + \xi(n, m) \qquad (2.1)$$

Where g, f, u and ξstand for the observed image, original image, multiplicative component and additive component of the speckle noise basically. Here **(***n, m*) denotes the axial and lateral indices of the image samples or, alternatively, the angular and range indices for images. When it applied to ultrasound images, only the multiplicative component of the noise is to be considered and thus, the model can be considerably simplified by disregarding the additive term, so that the simplified version of (2.1) becomes

$$g(n, m) = f(n, m)u(n, m) \quad (2.2)$$

Speckle has a negative impact on ultrasound imaging. Presence of speckle noise prevents Automatic Target Recognition (ATR) and texture analysis algorithm to perform efficiently and gives the image a grainy appearance. Several adaptive filters have been implemented for speckle noise removal and some examples include Lee filter, Frost filter, Kaun Filter and SRAD Filter. Most of these proposed local adaptive speckle filters are able to reduce speckle while preserving the data. However, all these uses a lossy approach, as all these filters rely on local statistical data related to the filtered pixel. This data depends on the occurrence of the filter window over an area. The achievement of both speckle reduction and preservation of edge data is only possible when the filter window is uniform. If the filter window happens to cover an edge, the value of the filtered pixel will be replaced by the statistical data from both sides of the edge that is from two different intensity distributions. An alternative approach is to use wavelet transform Page Layout

3. WAVELET BASED THRESHOLDING

we show several adaptive filters for speckle noise removal and some examples include Lee filter [09], Frost filter [13], Kaun Filter [12] and SRAD [15] Filter. Most of these proposed local adaptive speckle filters are able to reduce speckle while preserving the data. However, all these uses a lossy approach, as all these filters rely on local statistical data related to the filtered pixel. This data depends on the occurrence of the filter window over an area. The achievement of both speckle reduction and preservation of edge data is only possible when the filter window is uniform. If the filter window happens to cover an edge, the value of the filtered pixel will be replaced by the statistical data from both sides of the edge that is from two different intensity distributions.

Wavelet filtering exploits the decomposition of the image into the wavelet basis and zeroes out the wavelet coefficients to despeckle the image. Wavelet analysis is particularly useful for the analysis of transient, nonstationary, or time-varying signals. Wavelets can be used to analyze signals in different spatial resolutions. Their advantage is in their ability to analyze a signal with accuracy in both the time and frequency domains. This is not the case when applying traditional Fourier analysis, where there is significant accuracy in the frequency domain, but less accuracy in the temporal domain. In other words, increasing accuracy in one domain implies a decrease in precision in the other domain. Wavelets are also known for their capacity to identify singularities associated with fine variations of the signal to be evaluated [08]. For denoising, we need to identify the specific image scales where most of the image energy lies ([07],[08]).

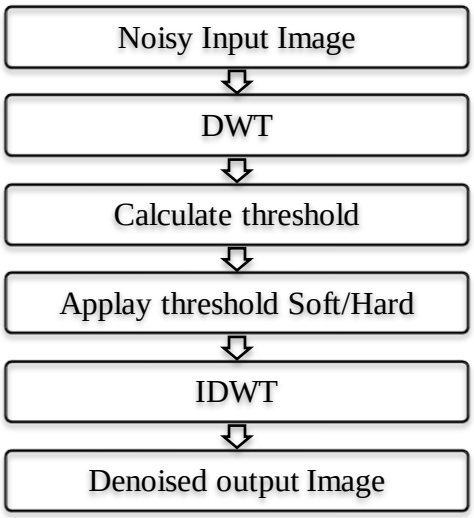

Figure 3.1 Flow of Wavelet based Denoising Process

The Figure 3.1 shows wavelet based denoising method for speckle reduction implemented in this study is described as follows.

Compute the discrete wavelet transform (DWT),
For each sub band,
Compute a threshold,
Apply the threshold on the wavelet coefficients of each band.
Compute the inverse DWT to reconstruct the despeckled image.

4. SPECKLE-REDUCING ANISOTROPIC DIFFUSION (SRAD) FILTERING

The essence of speckle-reducing anisotropic diffusion is the replacement of the gradient-based edge detector cd(|∇g|) in an original anisotropic diffusion PDE with the instantaneous coefficient of variation that is suitable for speckle filtering csrad(|∇g|) The speckle-reducing anisotropic diffusion filter uses two seemingly different methods, namely, the Lee [09] and Frost diffusion filters [13]. A more general updated function for the output image by extending the PDE versions of the despeckle filter is [15].

$$f_{i,j} = g_{i,j} + \frac{1}{n_s}\left(C_{srad}\left|\nabla_g\right| \nabla_{g_{i,j}}\right) \quad (4.14)$$

The diffusion coefficient for the speckle anisotropic diffusion csrad(|∇g|) is derived [15] as

$$C^2_{srad}\left(\left|\nabla_g\right|\right) = \frac{\frac{1}{2}\left|\nabla g_{i,j}\right|^2 + \frac{1}{16}\left(\nabla^2 g_{i,j}\right)^2}{\left[\nabla_{i,j} + \frac{1}{4}\nabla^2 g_{i,j}\right]^2} \quad (4.15)$$

It is required that csrad(|∇g|) > 0. The above instantaneous coefficient of variation combines a normalized gradient magnitude operator and a normalized Laplacian operator to act like an edge detector for speckle images. A high relative gradient magnitude and a low relative Laplacian indicate an edge. The filter utilizes speckle-reducing anisotropic diffusion after Eq. (3.12) with the diffusion coefficient csrad(|∇g|) in Eq. (4.15).

5. PROPOSED MOAL

The block diagram of proposed modal is shown in figure 5.1

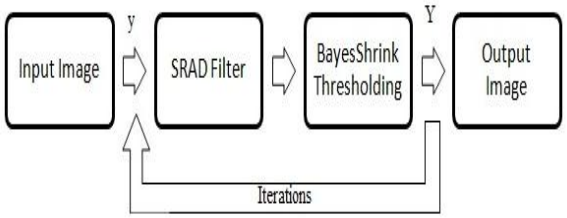

Figure 5.1 Block diagram of the proposed denoising algorithm.

In the proposed model the Bayesian Shrinkage of the non-linearly diffused signal is taken. The equation can be written as

$$I_n = B_s\left(I'_{n-1}\right) \quad (5.1)$$

Where Bs is the Bayesian shrink and In-1 is Speckle Reduction Anisotropic diffusion at (n-1)th time. Numerically can be written as

$$I_n = B_s\left(I_{n-1} + \Delta td_n\right) \quad (5.2)$$

Where Bs can be calculated by finding Tb as mentioned in e after taking wavelet transform of In-1

The intention to develop this method is to decrease the convergence time of the SRAD filter. It is understood that the convergence time for denoising is directionally proportional to the image noise level. In the case of SRAD filter, as iteration continues, the noise level in image decreases (till it reaches the convergence point), but in a slow manner. But in the case of Bayesian shrinkage, it just cut the frequencies above the threshold in a single step. An iterative Bayesian Shrinkage will not incur any change in the detail coefficients from the first one. Now consider the proposed algorithm, here the threshold for Bayesian shrinkage is recalculated each time after SRAD filter, and as a result of two successive noise reduction step, it approaches the convergence point much faster than SRAD filter.

The block diagram of proposed modal is shown in figure 5.1 the iteration process continues till the input signal y is converted to Y.As the convergence time decreases, image blurring can be restricted, and as a result image quality increases. The whole process is illustrated in Figure 5.2

Figure 5.2(a) shows the convergence of the image processed by SRAD filter. The convergence point is at P. Suppose at P we will get the better image, with the assumption that the input image is a noisy one. If this

convergence point P can be shifted towards y-axis, its movement will be as shown in Figure 5.2 (b). Now if we pull the point P towards y-axis, it will move in a left-top fashion. Here the Bayesian shrinkage is the catalyst, which pulls the convergence point P of the SRAD towards a better place.

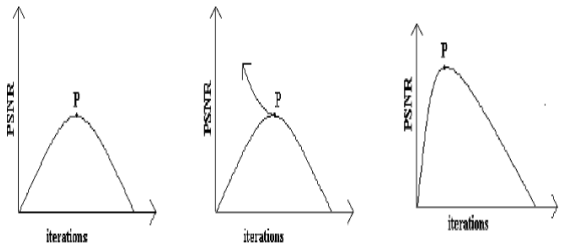

(A) (B) (C)

Figure 5.2 Working of Proposed modal

In figure 5.2 (a) shows the convergence of a noisy image (convergence at P). If this P can be shifted towards left, image quality can be increased and time complexity can be reduced as illustrated in (b). (c) Shows the signal is processed by Proposed modal. It can be seen that the convergence point is shifted to left and moved upwards.

6. RESULTS

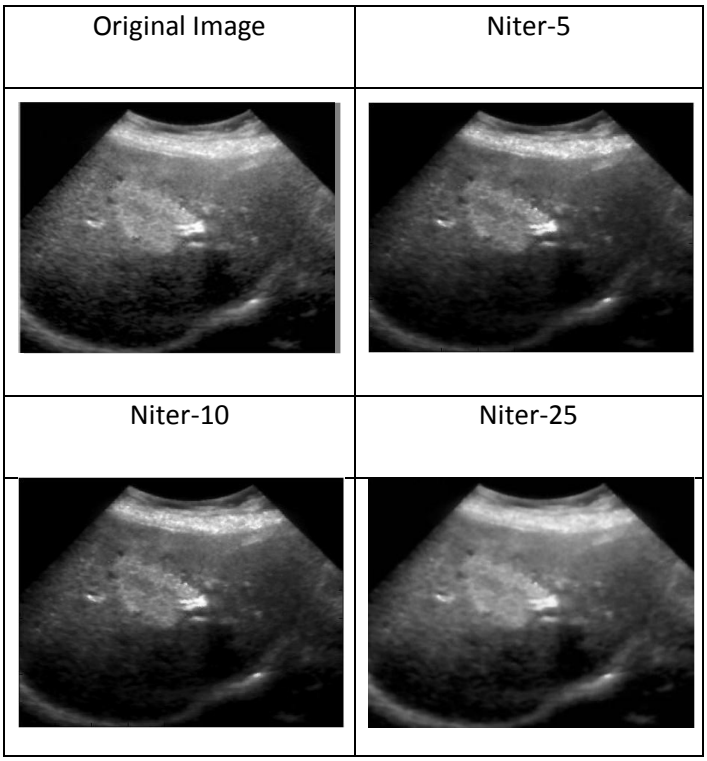

Figure 6.1 Proposed Method Outputs of Focal Hepatic Lesions

6.1.1 Results of Prostate Focal Hepatic Lesions

Table 6.1 Performance Parameter Of Focal Hepatic Lesions

Niter	MSE	SNR	PSNR	COC
Niter-4	18.90	78.60	35.33	0.9971

Niter-10	12.56	80.38	37.10	0.9981
Niter-25	22.76	77.96	34.52	0.9965

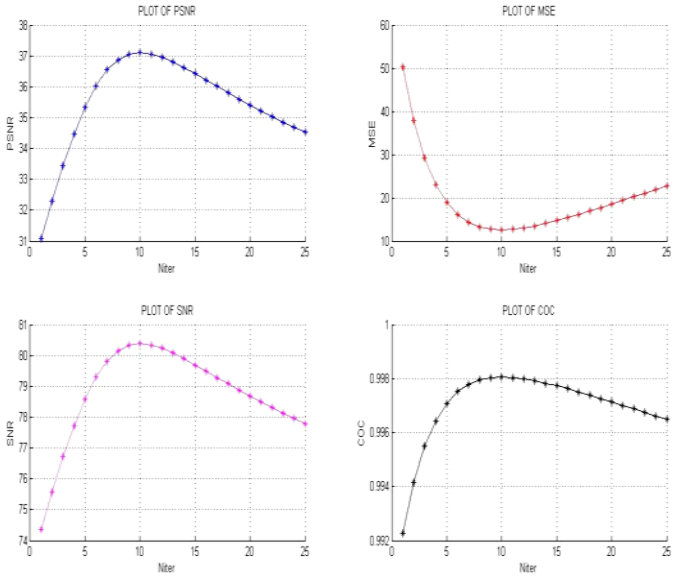

Figure 6.2 Results of PSNR, MSE, SNR, and COC of Focal Hepatic Lesions

7. CONCLUSION

In this paper for restoration of medical ultrasound imaging from the experimental and mathematical results on different techniques for restoration of medical ultrasound images is shown. it can be concluded that partial domain filtering methods such as mean filter, median filter, lee filter and frost filter remove noise but important diagnostic details are lost. Wavelet based bayesshrinkthresholding perform better then visushrinkthresholding and sureshrinkthresholding. Wavelet based threshold shrink techniques gives better results but they fail to perform well near edges. PDE based srad filter gives better denoising and with edge prevention but it require more iteration to reach convergence.

The proposed algorithm produces images which are cleaner and smoother and at the same time kept significant details, resulting in a clearer an appealing vision. Moreover, the proposed method is fast at reaching the convergence, which has a direct impact on noise reduction and preserve image edges. Experimental results on quality parameters psnr, snr, mse and coc prove that proposed method perform better form all other methods for removing speckle.

8. REFRENCES

CharuKhare, Kapil Kumar Nagwanshi, "Implementation and Analysis of Image Restoration Techniques", International Journal of Computer Trends and Technology- May to June Issue 2011.

S.Kalaivani Narayanan and R.S.D.Wahidabanu, "A View on Despeckling in Ultrasound Imaging", International Journal of Signal Processing, Vol. 2, No.3, September 2009.

Mark R. Banham and Aggelos K. Katsaggelos, "Spatially Adaptive Wavelet-Based Multiscale Image Restoration", IEEE TRANSACTIONS ON IMAGE: PROCESSING, VOL. 5, NO. 4, APRIL 1996.

AlirezaMallahzadeh, Hamid Dehghani, and ImanElyasi, "Multiscale Blind Image Restoration with a New Method", International Journal of Electrical and Electronics Engineering 2:8 2008

S.Sudha, G.R.Suresh and R.Sukanesh, "Speckle Noise Reduction in Ultrasound Images by Wavelet Thresholding based on Weighted Variance", International Journal of Computer Theory and Engineering, Vol. 1, No. 1, April 2009.

K. Karthikeyan, Dr. C. Chandrasekar " A Study on the Application of Wavelets for Despeckling Ultrasound Images" International Journal of Computer Information Systems, Vol. 1, No. 5, 2010

ImanElyasi, and SadeghZarmehi, "Elimination Noise by Adaptive Wavelet Threshold", World Academy of Science, Engineering and Technology 56 2009.

R. Sivakumar and D. Nedumaran "Comparative study of Speckle Noise Reduction of Ultrasound B-scan Images in Matrix Laboratory Environment" International Journal of Computer Applications (0975 – 8887), Volume 10– No.9, November 2010.

J.S. Lee, "Speckle analysis and smoothing of synthetic aperture radar images," Comp. Graphics Image Process., vol. 17, pp. 24-32, 1981

Tim Edwards, "Discrete Wavelet Transforms: Theory and Implementation," Discrete Wavelet Transforms, Stanford University, Draft #2, June 4, 1992

Donoho, D.L. (1992) De-noising by soft-thresholding, IEEE Transaction on Information Theory, Vol.41, No.3, Pp.613-627.

D.T. Kuan and A.A. Sawchuk, "Adaptive noise smoothing filter for images with signal dependent noise," IEEE Trans. Pattern Anal. Mach. Intell., vol. PAMI-7, no. 2, pp. 165-177, 1985.

V.S. Frost, J.A. Stiles, K.S. Shanmungan, and J.C. Holtzman, "A model for radar images and its application for adaptive digital filtering of multiplicative noise," IEEE Trans. Pattern Anal. Match. Intell., vol. 4, no. 2, pp. 157-165, 1982.

PIETRO PERONA AND JITENDRA MALIK. "Scale-Space and Edge Detection Using Anisotropic Diffusion", IEEE TRANSACTIONS ON PATTERN ANALYSIS AND MACHINE INTELLIGENCE, VOL. 12. NO. 7. JULY 1990

Yongjian Yu and Scott T. Acton "Speckle Reducing Anisotropic Diffusion" IEEE TRANSACTIONS ON IMAGE PROCESSING, VOL. 11, NO. 11, NOVEMBER 2002.

S.Kalaivani Narayanan and R.S.D.Wahidabanu, "A View on Despeckling in Ultrasound Imaging", International Journal of Signal Processing, Vol. 2, No.3, September 2009.

S. Grace Chang, Bin Yu and Martin Vetterli," Adaptive Wavelet Thresholding for Image Denoising and Compression", IEEE TRANSACTIONS ON IMAGE PROCESSING, VOL. 9, NO. 9, SEPTEMBER 2000.

Donoho, D.L. and Johnstone, I.M. (1995) Adapting to unknown smoothness via wavelet shrinkage. Journal of the American Statistical Association, Vol. 90, No. 432, Pp. 1200-1224.

M. Nikpour, H. Hassanpour, "Using diffusion equations for improving performance of wavelet-based image denoising techniques", Published in IET Image Processing.

JenyRajan , K. Kannan ,M.R. Kaimal"An Improved Hybrid Model for Molecular Image Denoising" J Math Imaging Vis, DOI 10.1007/s10851-008-0067-4.

Ultrasound [Online].Available: http://en.wikipedia.org/wiki/Ultrasound.

Wavelet [Online] Available: http://en.wikipedia.org/wiki/Wavelet

Noise in Image [Online] Available: http://www.mathworks.in/help/toolbox/images/ref/imnoise.html

General Ultrasound Imaging [Online] Available: http://www.radiologyinfo.org/en/info.cfm?pg=genus

Real- time Moving Object Detection and Tracking

Raj Hakani

raj.hakani1990@gmail.com

Assistant Professor, Electronics and Communication Engineering Department, Silver Oak College of Engineering & Technological, Gujarat Technological University, India

Abstract:-

In the presented paper Real time object is tracked from real time video. So, many algorithm are available to track an image but KLT tracker which is proposed by Kanade, Lucas and Tomasi is widely used for object tracking. To track an Object in a video that has been selected by the user in the first frame, the user may select a particular region or an object with a rectangular box in the first frame of the video and that object has to be used as reference object or image and algorithm will track the object or an image for rest of the video sequence.

Keywords: *Moving Object Detection and Tracking, KLT.*

1. Introduction

Real-time object detection and tracking is an important task within the field of computer vision. In the security monitoring like observation of people, vehicle or an objects in restricted environment, intelligent perception and object-based video compression and other areas like Robotics computer vision is widely used. There are three key steps in video analysis i.e. detection of interesting moving objects, tracking of such objects from frame to frame, and analysis of object tracks to recognize their behavior [1]. One of the most popular methods for feature point tracking is the KLT algorithm which was introduced by Lucas and Kanade [2] and later extended in the works of Tomasi and Kanade [3] and Shi and Tomasi [4]. The KLT algorithm detect a sparse set of feature points, these detected points now have the sufficient texture to track the image in the next frame and this points makes it reliable to track the object from the further frames with only this feature points. So when it gets the minimum set of feature points detected in the frame, then it will stick to the same object throughout the frames in the whole video and it will follow the objects so as and when in the frame, the object moves those feature points will also move thus one can track the object in the video with the help of those feature points.

2. OVERVIEW OF SYSTEM

In this paper, we design a Real time object detection and tracking system for single moving object using fixed webcam mounted in surveillance environment. Fig.1 Shows that Vision System included high resolution camera and camera is interface to laptop or PC. The Video (Sequence of Images) is captured by camera in maltab platform. For tracking of object in 'tracking algorithm' which runs in matlab[5] platform, the user has to select an object in the first frame.

Fig. 1 Vision System

3. METHODOLOGY

(i) Video sequence is given as input. A particular object is being detected by Viola - Jones detection algorithm. Now from the video particular object will be detected and sparse set of feature points will be designated on that object and thus object tracking is done by KLT algorithm.

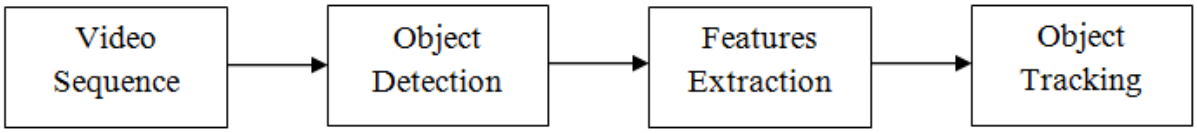

Fig. 2 Block Diagram of KLT Algorithm

(ii) Object detection

Detecting object from a video sequence is done by cascade object detector system, which uses the Viola - Jones detection algorithm along with the help of a trained classification model for the detection of the particular object .

Fig. 3 Object Selected by user in first frame

(iii) Point features identification

The KLT algorithm tracks a set of feature points across the video frames. once the feature points are detected in the object throughout the frame then it will identify the same points in the whole video.

Fig. 4 Features Selection

(iv) Object Tracking

To track the object over time, this example uses the Kanade-Lucas-Tomasi (KLT) algorithm. While it is possible to use the cascade object detector on every frame, it is computationally expensive. It may also fail to detect the object, when the subject turns or tilts the object quickly. This limitation comes from the type of trained classification model used for detection. The algorithm will compare or search the points of the object only once with one frame, if the points are not matched in that frame then it will not check again and eventually test fails.

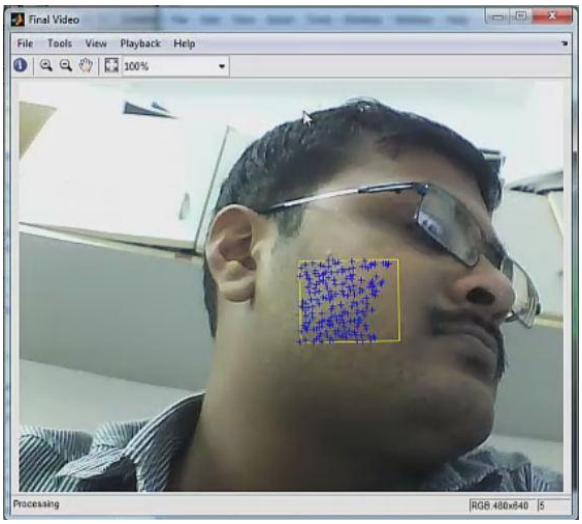

Fig 5. Real-time Moving Object Tracking

4. Experiment Results

In the presented paper the results obtained are as shown below:

A. Result of Object (Face) Tracking for Real Time Video


Fig. 6 Object Detection in the first frame of video


Fig. 7 Feature Selection

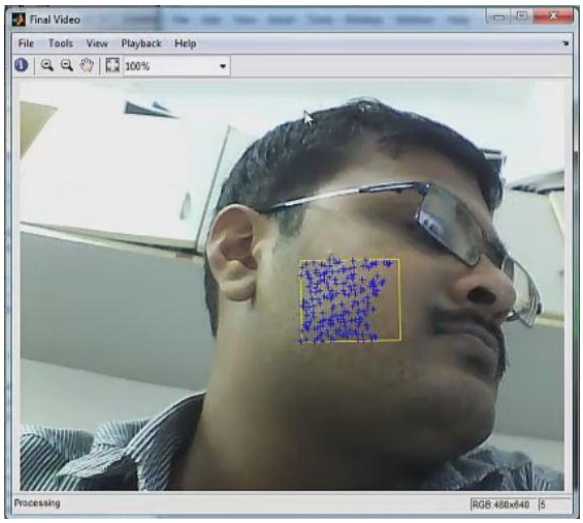

Fig. 8 Object Tracking Output at Frame 4

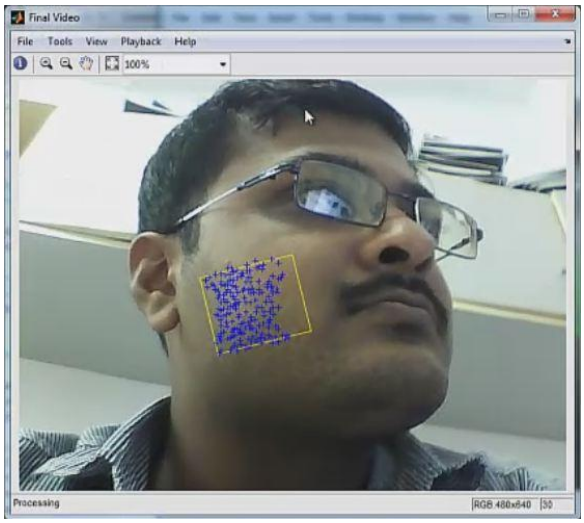

Fig.9 Object Tracking Output at Frame 30

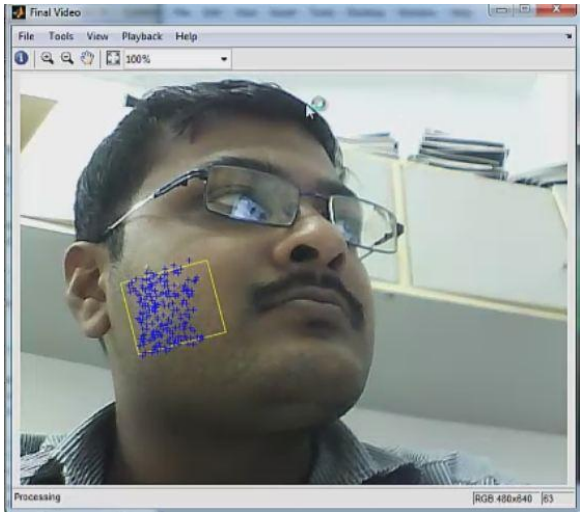

Fig.10 Object Tracking Output at Frame 63

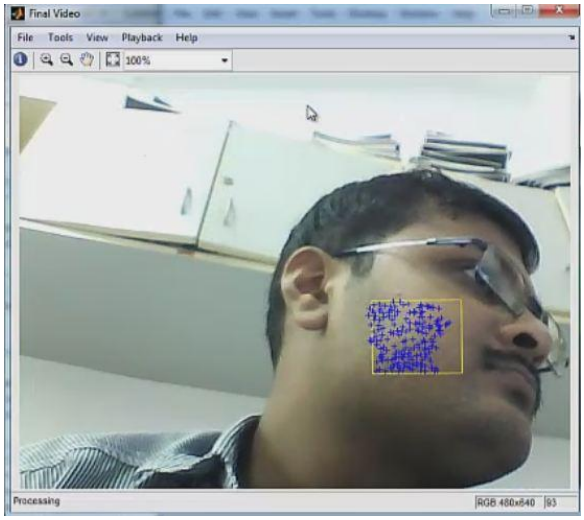

Fig.11 Object Tracking Output at Frame 93

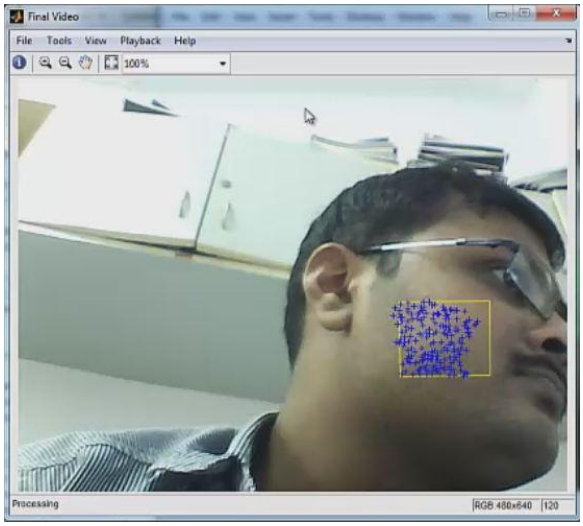

Fig.12 Object Tracking Output at Frame 120

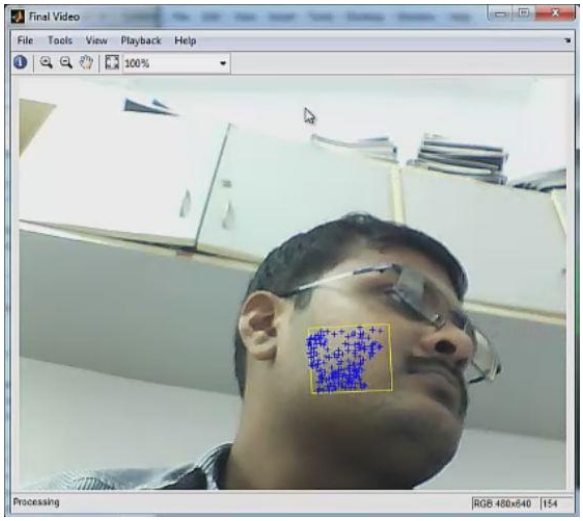

Fig.13 Object Tracking Output at Frame 154

B Result of Object (Latter) Tracking for Real Time Video

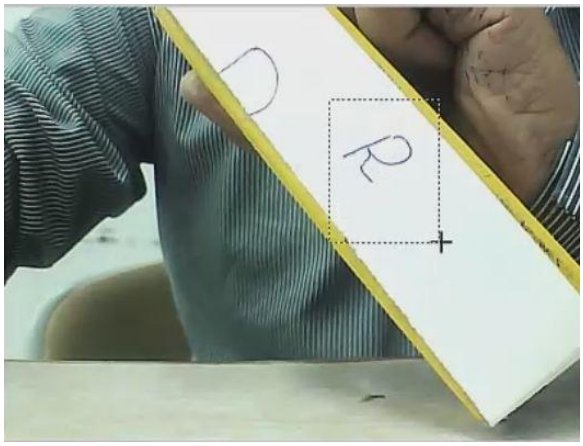

Fig.14 Object Detection in the first frame of video

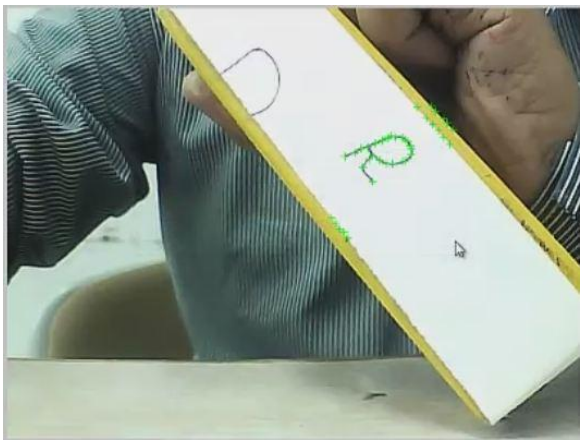

Fig.15 Feature Selection

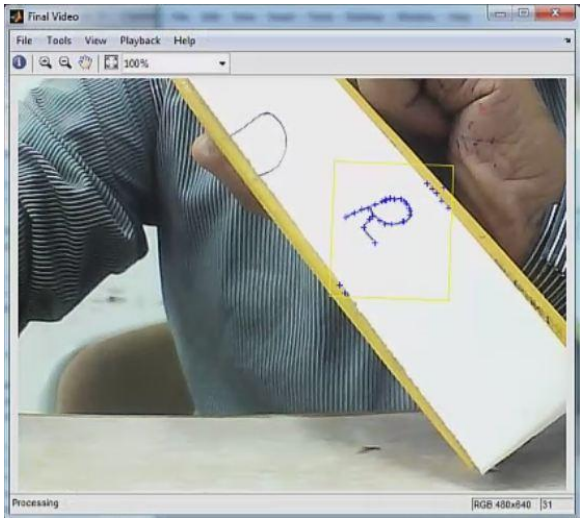

Fig. 16 Object Tracking Output at Frame 31

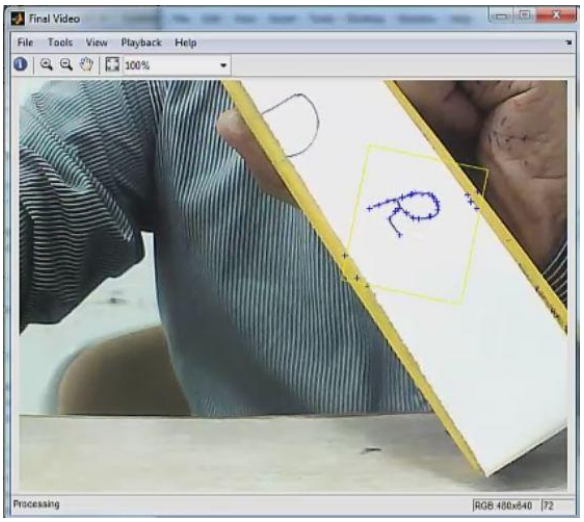

Fig.17 Object Tracking Output at Frame 72

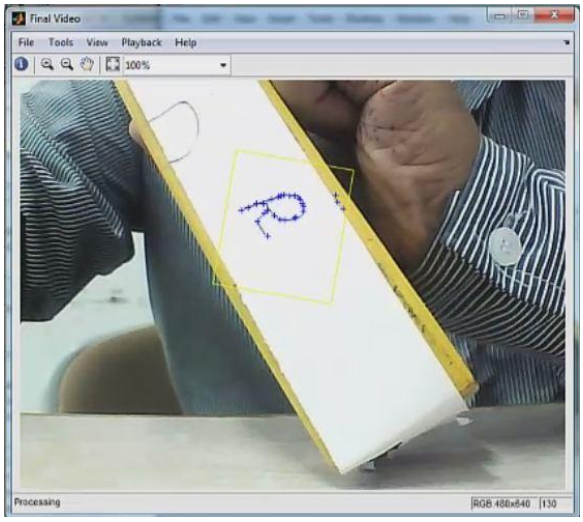

Fig.18 Object Tracking Output at Frame 130

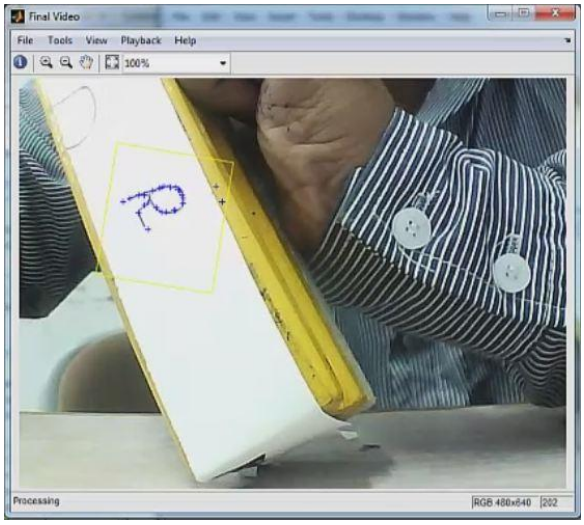

Fig.19 Object Tracking Output at Frame 202

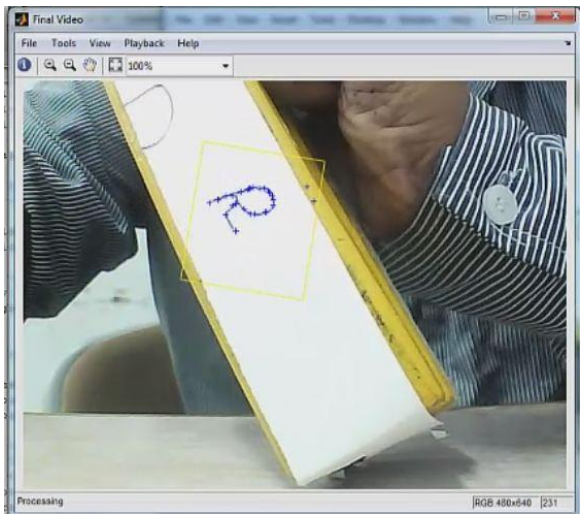

Fig.20 Object Tracking Output at Frame 231

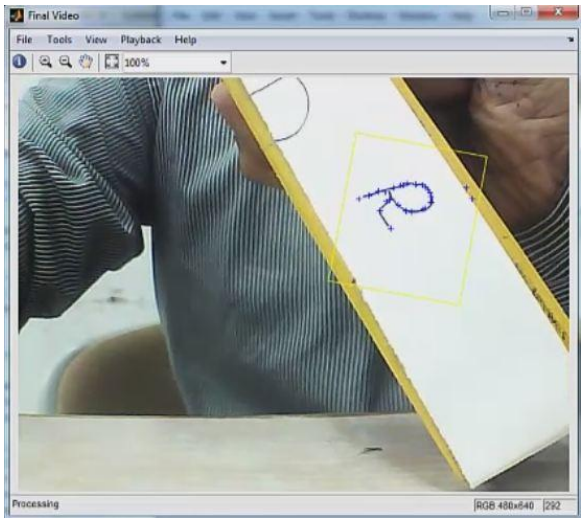

Fig.21 Object Tracking Output at Frame 292

C Result of Object (No. in Key) Tracking for Real Time Video

Fig.21 Object Detection in the first frame of video


Fig.22 Feature Selection

Fig.23 Object Tracking Output at Frame 16

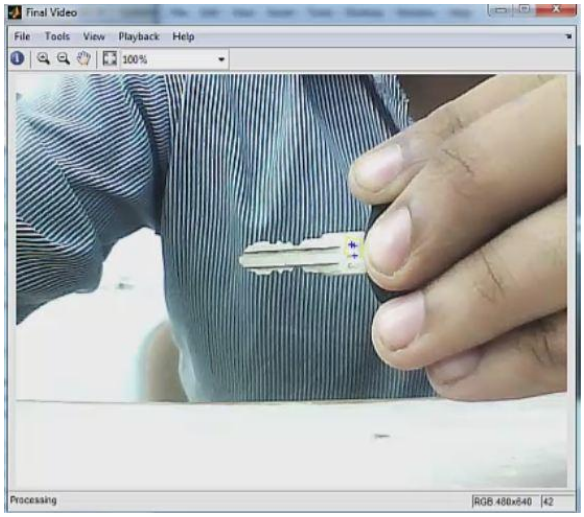

Fig.24 Object Tracking Output at Frame 42

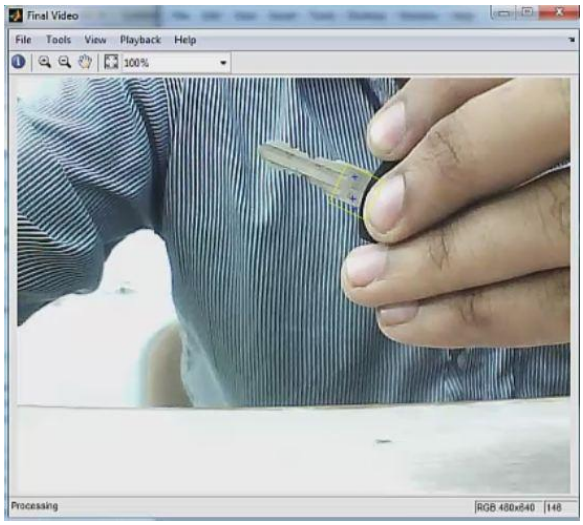

Fig.25 Object Tracking Output at Frame 146

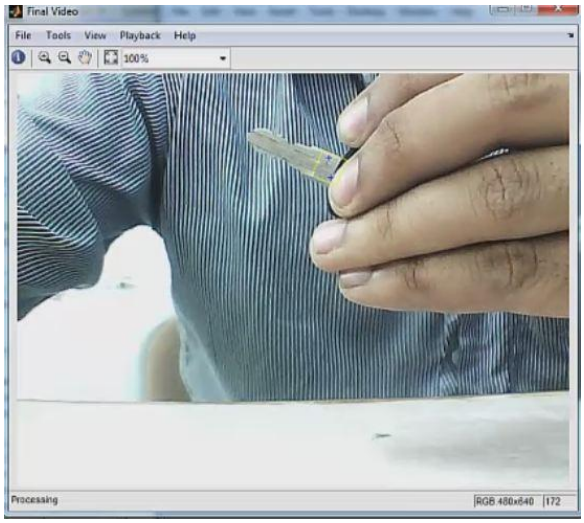

Fig.26 Object Tracking Output at Frame 292

Fig.27 Object Tracking Output at Frame 172

Fig.28 Object Tracking Output at Frame 211

D Result of Object (Pen) Tracking for Real Time Video

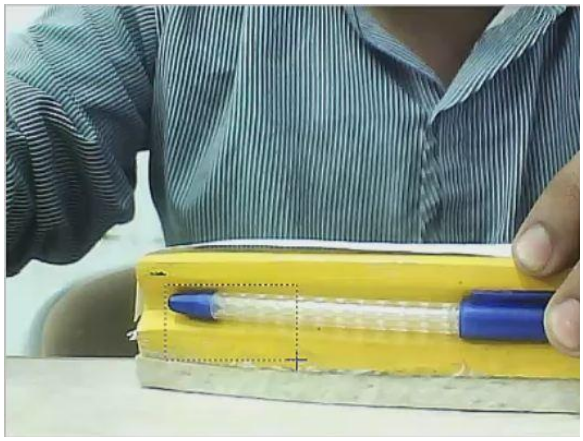

Fig.29 Object Detection in the first frame of video

Fig.30 Feature Selection

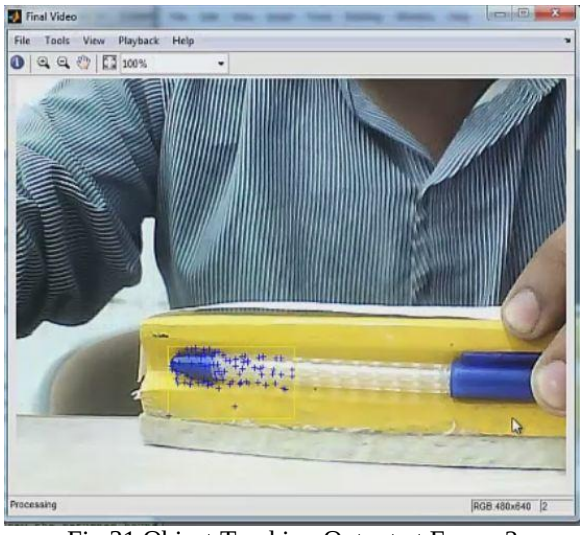

Fig.31 Object Tracking Output at Frame 2

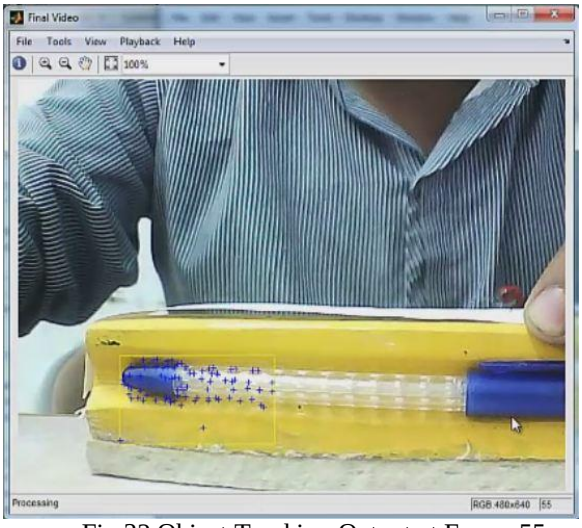

Fig.32 Object Tracking Output at Frame 55

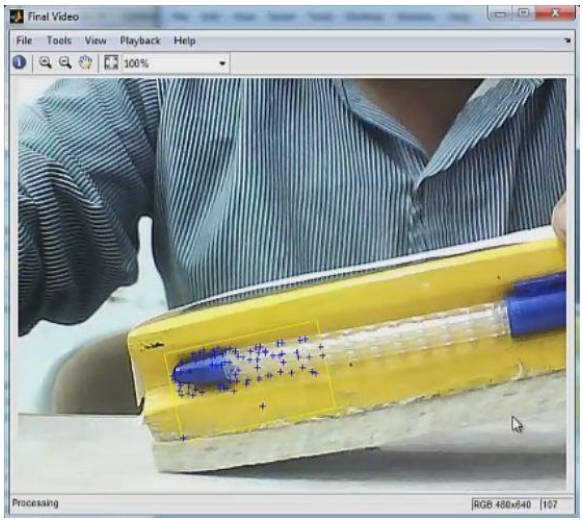

Fig.33 Object Tracking Output at Frame 107

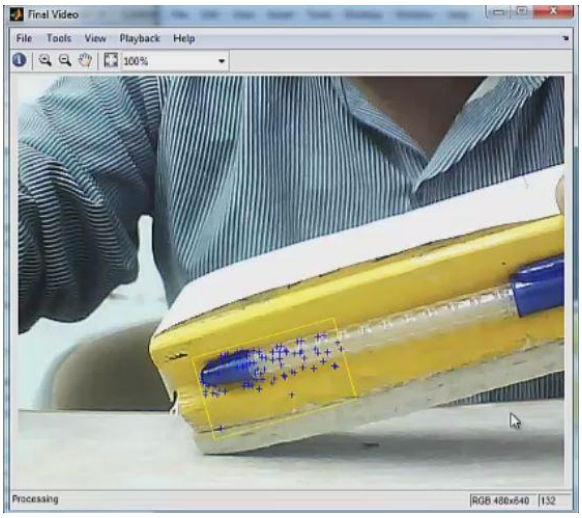

Fig.34 Object Tracking Output at Frame 132

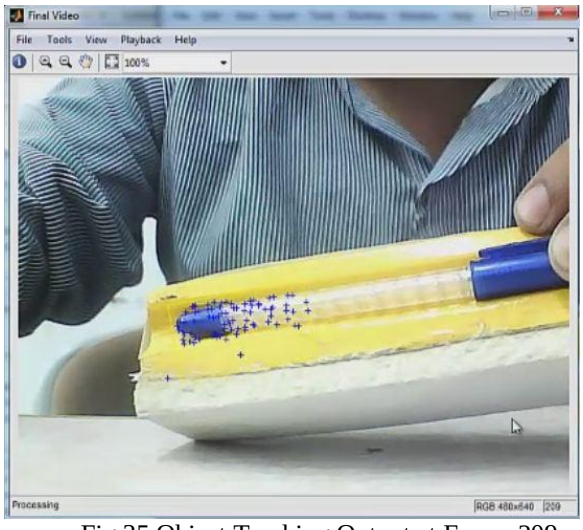

Fig.35 Object Tracking Output at Frame 209

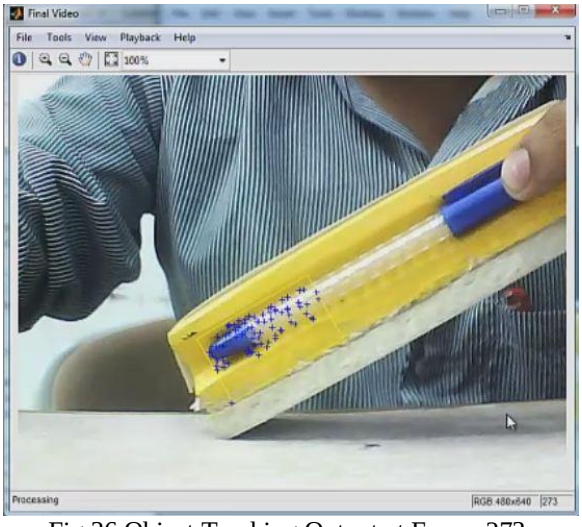

Fig.36 Object Tracking Output at Frame 273

5. Application

Security: In Historical Places, surveillance of antic item is an important task. To keep watch and track of antic item is done by real-time object tracking system.

Robot Vision: In robot navigation, the steering system needs to identify different obstacles in the path to avoid collision. If the obstacle are in moving conditions, then at this moment, real time object tracking algorithm will be used.

Traffic Monitoring: In some countries highway traffic is continuously monitored using cameras [6]. Any vehicle that breaks the traffic rules or is involved in other illegal act can be tracked down easily if the surveillance system is supported by an object tracking system.

6. Conclusion

In this paper, a Real-time Moving Object Detection and tracking system has been presented and implemented. Object selected on the first frame of a video sequence an KLT algorithm are used to extract feature of the object like (point, Edges, etc). Based on this feature object is track in the remain frame.

7. REFERENCES

[1]. Alok K. Watve, Indian Institute of Technology, Kharagpur, seminar on "Object tracking in video scenes", 2005

[2] B.D. Lucas, T. Kanade, An Iterative Image Registration Technique with an Application To Stereo Vision, Joint Conference on Artificial Intelligence, pp. 674-679, 1981

[3] C. Tomasi, T. Kanade, Detection and Tracking of Point Features, Technical Report CMU-CS-91-132, Carnegie Mellon University, 1991

[4] J. Shi, C. Tomasi, Good Features to Track, IEEE Conference on Computer Vision and Pattern Recognition, pp. 593-600, 1994

[5] http://www.mathworks.in/help/vision/examples/face-detection-and-tracking-using-the-klt-algorithm.html

[6] K. Wang, Z. Li, Q. Yao, W. Huang, and F. Wang, "An automated vehicle counting system for traffic surveillance," IEEE Int. Conf., on Vehicular Electronics and Safety, Japan, Dec 2007, pp. 1-6.

Calculation of fluid film Stiffness and Damping coefficients of A Five Pad Tilting Pad Hydrodynamic Journal Bearing

Asheesh Kumar

asheeshtech@gmail.com

Mechanical Engineering Department, Silver Oak College of Engineering & Technology, Gujarat Technical University, India

Abstract

In this paper,the fluid damping and stiffness coefficients of a tilting pad journal bearing which runat high journal speedare computed. The modeling for the analysis is done using Reynolds equation. The FEM model is prepared using Galerkin approach. The isoparametric quadrilateral element is taken for meshing of 5 pad of TPJB. The source code in Matlabis generated for computing the stiffness and damping coefficients for LBP type of loading in order to calculate the fluid film hydrodynamic pressure in the veering clearance space. The results are discussed for several loads.

Keywords: TPJB, FEM and Fluid film pressure.

1.Introduction

In this era of high speed and heavy load turbomachinery, the sliding contact bearings have achieved their significant importance. For the better stability of journal at its high speed, the Tilting Pad Journal Bearings are often used. In last three or four decades a substantial amount of work has been done on Tilting Pad Journal Bearing ignoring the turbulent effects. Manfrida and Martelli [1] proposed a new method, called the “force assembly method”, for the numerical calculation of the dynamic coefficients of tilting-pad bearings. Yang and Rodkiewiczt [4] analyzed the bearing performance of a centrally supported tilting square pad, subjected to harmonic vibration, numerically. Monmousseau and Fillon [3] studied the transient thermoelastohydrodynamic behavior of a tilting-pad journal bearing exposed to severe operating conditions.

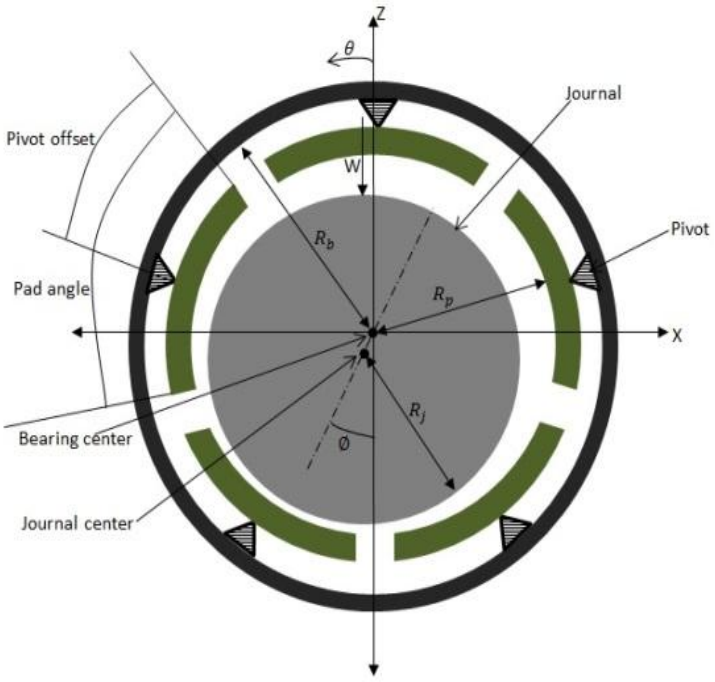

Fig.1 Schematic of Tilting Pad Journal Bearing

Chang *et al.* [5] presented thermo-elasto-hydrodynamic lubrication (TEHD) analysis to investigate the static performance of tilting-pad journal bearings. Yang et al. [8]studied the fluttering characteristics of the upper unloaded pads in a tilting pad journal bearing experimentally. Hargreaves and Fillon[6]described the investigation into the static and dynamic performance of a tilting pad lightly loaded journal bearing. Cha et al. [7] investigated the effect of pad compliance on the dynamic response of tilting pad journal bearings. But it is seen at high journal speed its behavior starts deviating from the experimental. Taniguchi et al.[11] described a thermo-hydrodynamic analysis of the 19 inch diameter tilting-pad journal bearing for steam turbine in comparison with experimental data. Bouard et al.[10] presented the influence of the flow regime on tilting-pad journal bearing performance. Three turbulent models were studied. Okabe and Cavalca [9]developedan analytical model of a tilting pad bearing based on the short bearing assumption with the turbulence effect included.

2. Analysis

The non-dimensional form of Reynolds equation for iso-viscous problem is given below

$$\frac{\partial}{\partial\alpha}\left(\frac{H^3}{12}\frac{\partial\bar{p}}{\partial\alpha}\right)+\frac{\partial}{\partial\beta}\left(\frac{H^3}{12}\frac{\partial\bar{p}}{\partial\beta}\right)=\frac{\Omega}{2}\frac{\partial\bar{h}}{\partial\alpha}+\frac{\partial\bar{h}}{\partial\bar{t}} \tag{1}$$

where, H = fluid film thickness;Ω = angular velocity; $\bar{p}$ = dimensionless hydrodynamic pressure

2.1 Fluid Film Thickness

The normalized form of the film thickness is:

$$H(\theta)=1-\zeta\cos(\theta-\varphi_i)-\frac{(R+d)}{c}\emptyset_i\sin(\theta-\varphi_i)+Xcos(\theta)+Ysin(\theta)+\overline{\delta_t}(\theta) \tag{2}$$where,

$\zeta=\frac{c-c_b}{c}$and$\delta_t(\theta)$ is the total internal surface displacement of the pad due to the combined distortion of load and thermal effects.

3. Results and Discussion

For the evaluation of results, the Reynolds equation is solved employing FEM for fluid film pressure. The source code generated in MATLAB is executed for the evaluation of stiffness and damping coefficients. TPJB of journal radius and length 0.05 m is taken for the performance analysis. The bearing preload factor and bearing pad clearance are 0.03 mm and 0.1 mm respectively. Lubricant viscosity and density are 0.027[Pa-s] and 845[kg/m^3] respectively. The results obtained are shown in figure 2 and figure 3.The value of fluid film stiffness coefficient Kxx is maximum for the four pad arrangement as compare to five pad arrangement when the offset is 50% and also when offset is 60%.The value of fluid film damping coefficient Cxx is found to be maximum for the offset of 50% as compare to 60% offset for the four pad arrangement and also for the five pad arrangement.

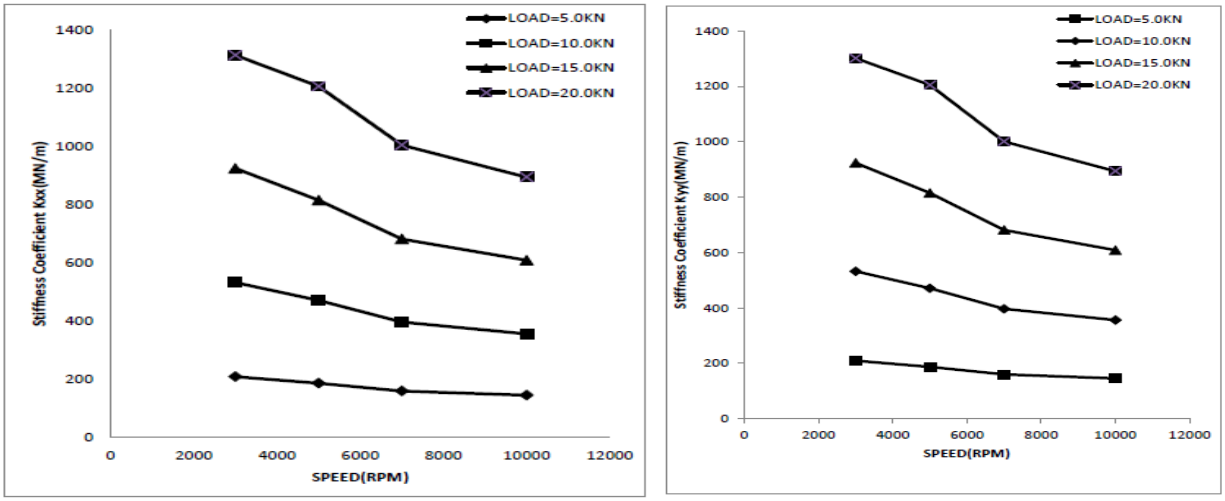

Fig.2 Variation of stiffness coefficients along with speed

This is due to high stability at 50% offset compare to 60% offset. The value of fluid film damping coefficient Cyy is found to be maximum for the offset of 50% as compare to 60% offset for the five pad arrangement and not for the four pad arrangement.

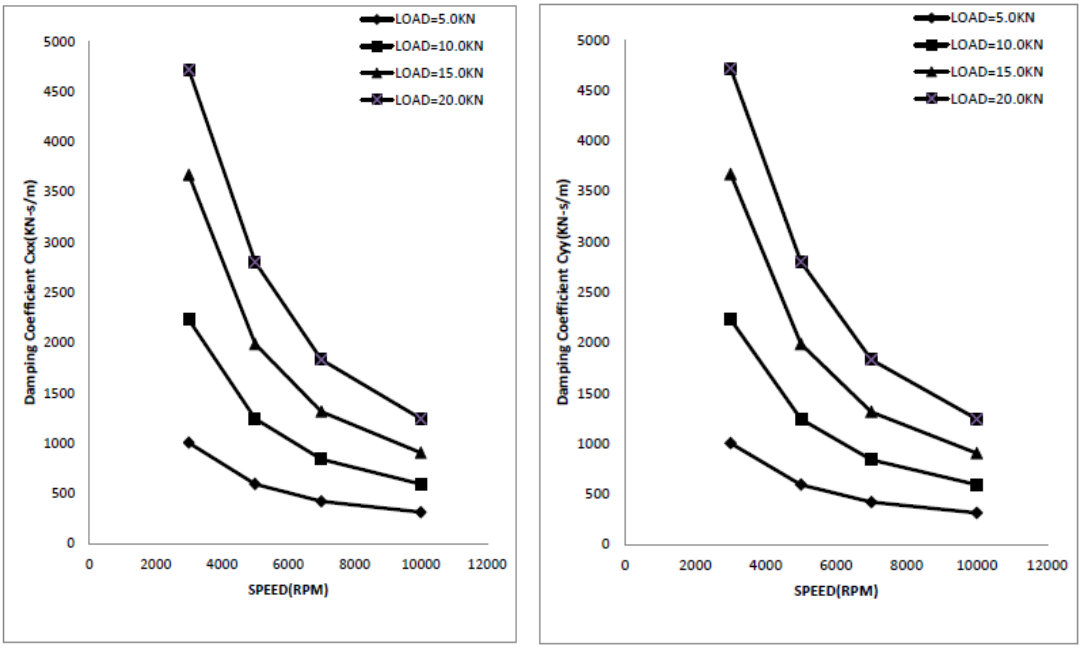

Fig. 3 Variation of Damping along with Speed

4. Conclusion

On the basis of numerically simulated results, the following conclusions may be drawn

- The stiffness increases with the increase in load for the same speed. The increase in value is large at lower speeds compared to higher speeds or very negligible at higher speed.
- The damping increases with the increase in load for the same speed. The increase in value is large at lower speeds compared to higher speeds.

References

[1] G. Manfrida and F. Martelli. (1981). A new approach to the theoretical calculation of the dynamic coefficients of Tilting-Pad Bearings. *Wear*, 249-258.

[2] A.M. El-Butch and N.M. Ashour. (1999). Analysis of heavy duty tilting-pad journal bearing taking into account pad distortion and possible adoption of rubber pad segments. *Tribology International*, 285-293.

[3] P. Monmousseau and M. Fillon. (2000). Transient thermoelastohydrodynamic analysis for safe operating conditions of a tilting-pad journal bearing during start-up. *Tribology International*, 225-231.

[4] Peiran Yang and C. M. Rodkiewiczt . (1996). Time-dependent TEHL solution to centrally supported tilting pad bearings subjected to harmonic vibration. *Tribology International*, 433-443.

[5] Qiuying Chang, Peiran Yang, Yonggang Meng and Shizhu Wen. (2002). Thermoelastohydrodynamic analysis of the static performance of tilting-pad journal bearings with the Newton–Raphson method. *Tribology International*, 225-234.

[6] D.J. Hargreaves and M Fillon. (2007). Analysis of a tilting pad journal bearing to avoid pad fluttering. *Tribology International*, 607-612

[7] Matthew Cha, Patrik Isaksson and Sergei Glavatskih. (2013). Influence of pad compliance on nonlinear dynamic characteristics of tilting pad journal bearings. *Tribology International*, 46-53.

[8] Seong Heon Yang, Chaesil Kim and Yong-Bok Lee. (2006). Experimental study on the characteristics of pad fluttering in a tilting pad journal bearing. *Tribology International*, 686-694.

[9] Eduardo Paiva Okabe and Katia Lucchesi Cavalca. (2009). Rotordynamic analysis of systems with a non-linear model of tilting pad bearings including turbulence effects. *Nonlinear Dyn*, 481-495.

[10] L. Bouard, M. Fillon and J. Frene. (1996). Comparison between three turbulent models- application to thermohydrodynamic analysis of tilting pad journal bearings. *Tribology International*, 11-18.

[11] S. Taniguchi, T. Manko, K. Takeshita and T. Ichimura. (1990). A thermohydrodynamic analysis of large Tilting-Pad Journal Bearing in laminar and turbulent flow regimes with mixing. *Journal of Tribology*, 542-550.

Edge Based Image Steganography Techniques

Satvik Khara [1], RikinThakkar [2]

satvik.it@socet.edu.in[1], rikinthakkar.it@socet.edu.in[2]

Information Technology Department, Silver oak college of Engineering & Technological Gujarat Technological University, India

Abstract:-

Steganography is used to provide security and it aims at hiding sensitive information. This aim is achieved by hiding the actual information into other information in such a way that no one can detect it. A variety of cover or carrier file formats can be used to carry out steganography e.g. text, images, audios, videos, etc. In this paper, images are used as cover carrier because of their high frequency on internet. Many steganography techniques have been introduced which have some advantages and disadvantages. The purpose of this paper is to provide the report on edge based image steganography techniques.

Keywords: *Steganography, Image steganography, Edge Based Image Steganography, canny edge detector, LSB substitution*

.

1. Introduction

The use of internet is increasing day by day and transfers of important information like data and images are also increasing. As important information is transferred; security of such information is also necessary. Security can be provided using encrypting such information. In encryption information is changed in such a way that no one can read this information. Sometimes during encryption; messages can be changed and attacker can get confidential information. Steganography is another way of securing the secret information. Steganography is a branch of information security that hides the important information in to an innocent media in such a way that no one except recipient can extract the information [1]. Different steganographic techniques have been introduced since ancient times. Ancient techniques make use of invisible ink; microdots character arrangement and many more [2]. Due to digitization in modern times, digital media has become the source of steganography e.g. images, text, audio and video files [3, 29].

Firstly both cover image and message bits are given as an input to the embedding algorithm. An Embedding algorithm is a steganography technique that will embed the message bits into the cover image such that no one can detect it. This algorithm will generate stego-image as an output. Stego-image is the cover image containing message bits inside it. This image is transferred over the media between sender and receiver. At the receiver end, an extraction algorithm will work on the stego-image and extracts the hidden message bits from the stego-image [29]. There are three basic parameters for evaluation of different steganography techniques.

1. Imperceptibility: It is the ability of steganography method to avoid detection of hidden message through human visual system (HVS) and statistical analysis. It can be measured through peak signal to noise ratio (PSNR) [5].
2. Capacity: It is number of bits of message that are hidden into a stego-image [29].

3. Robustness: It is ability of the steganography technique to retain the hidden message after many image related operations. These operations are compression, cropping, rotation and filtering etc. Many steganography techniques have been introduced so far to achieve higher imperceptibility, capacity and robustness [23].

The easiest way to hide information within the image is least significant bit substitution (LSB) technique. In this technique least significant bits of each pixel are replaced with the binary data (i.e. information) [6]. However this is not a secure technique as the stego-image contains flecks at the place where the message bits are hidden and hidden message bits can be easily recovered through repetition of the same process. Many attacks like sample pair analysis [7], difference image-histogram [8], blind detection algorithm [9] has been performed on this method [23, 29].

In order to overcome the problem of LSB substitution a new tool named "Hide and Seek for Windows 95" has been introduced sometimes ago. This tool distributes the information to be hidden randomly across the image pixels [10]. Its drawback is that the information, hide using both these methods can be easily detected by the attackers [29, 23, 11].

2. Related Work

In 2006, a new algorithm named as first filter algorithm has been introduced to overcome the problems of above mentioned techniques. The main idea of this algorithm is that variation in features of image is less noticeable. First filter algorithm uses edge detection filters like Laplace formula and sobel filter. Also another algorithm named battlesteg has been purposed through the combination of first filter algorithm and hide seek method [29].

Battlesteg stands for battleship steganography. In this algorithm two main terms ships and shots are used [12]. Main drawback of this method is that further processing cannot be done on the steg-image [23].

Comparison of these two algorithms is done with the traditional methods (i.e. LSB replacement and hideseek) using machine learning rather than evaluating the steganalysis information manually. Result of comparison is presented in[12]. It is concluded that first filter algorithm is better than other three methods until embedding rate is less than 7% and LSB replacement lies between first filter algorithm and battlesteg algorithm [23, 12].

In 2006, an adaptive filtering based image steganography technique has been introduced. In Adaptive steganography, statistical properties are taken under consideration to avoid steg analysis. The challenging issue in existing adaptive steganography methods is that they don't specify any method to control the number of bits hidden in carrier medium [13] [14] [15] [16] . In this technique, data bits hidden into the high intensity components and low intensity components are not used for hiding data. This method firstly passes the image to the filter to separate low and high intensity component. Then inverse transformation of both the images is performed after that data bits are embedded into high frequency spatial image (HFSI). Then combination of both HFSI and low frequency spatial image LFSI results into stego-image. During embedding magnitude of the pixel is also considered. Higher the value of magnitude higher the number of bits embedded in that pixel [29, 17].

Magnitude in HFSI is always considered to be greater than 128 so embedding rate of 1bpp is achieved in this technique. Instead of using high pass filter, multi band filter can also be used. The main advantage of this technique is that it limits the quantity of hidden information by adjusting cut off frequency [29].High embedding rate and high confidentiality is achieved through this method. Disadvantage is that if there is a small variation in the cutoff frequency and order of filter at receiver and sender end, the decoded message will not be same as that of original message [29, 17].

In 2007, Random edge LSB (RELSB) technique has been introduced. This approach randomly hides the message bits into the regions that have least similarity with their neighborhood. These regions contain edges, thin lines, end of lines etc. Robert cross gradient operator is used to extract such regions. Then random locations in these regions are selected using random number generator algorithms like PRNG. The simplified data encryption standard is used to encrypt the message bits. Encryption is done to provide more security. Data is hidden in such a way that same edges and line pixels are detected before and after data embedding. This approach has been better than LSB substitution [6], random LSB Embedding [10], edge LSB embedding [12]as gradient energy technique can detect number of hidden bits in all these three technique but not in RELSB[29,18].

In 2008, another edge based LSB steganography technique has been introduced. This is based on pixel value differencing (PVD) and LSB replacement [19] with some modification and provides more capacity and imperceptibility. The difference of a given pixel with its neighbor pixel is used to decide the embedding rate for that pixel. In this approach, firstly image is divided into non overlapping two consecutive blocks of size two. Then difference of two pixels into the blocks is calculated to categorize blocks into levels i.e. lower level, middle level and higher level. Blocks with higher difference value will fall in higher level and will be embedded with more number of bits than blocks under other two levels. This implements the idea that more bits of edge pixels can be used to embed data than other pixels. After embedding, if level of a block is changed then value of pixel is modified in such a way that level remains same. This provides high fidelity stego-image. Main drawback of this method is that range used at sender end is also needed to send to receiver for extraction [29, 20].

In order to overcome the main drawback of edge adaptive steganography [20], a new method has been introduced in 2009 named as variable rate steganography using neighbor pixel relationship. This technique also overcomes the drawback PVD technique [21] which also uses range table. The pixel's relationship with its neighborhood is used to decide whether it is an edge pixel or smooth area pixel. On the basis of neighborhood relationship three methods "four neighbors method", "diagonal neighbor method", "eight neighbor method" were given. All these methods have better Peak signal to noise ratio (PSNR). But main drawback is that only half numbers of the pixels are used for embedding rather than using almost all pixels [29, 22].

In 2010, to increase the embedding capacity with higher PSNR rate a new technique has been introduced. Hybrid edge detector is combination of canny edge detector [23] and fuzzy edge detector [24]. Combination of both these detectors provides more number of edge pixels than that of their individual results. In this method, after getting edge pixels using hybrid detector image is divided into non overlapping block of size say n. LSBs of first pixel in each block is used to describe the status of other pixels in the block i.e. edge pixels or a non-edge pixels. Edge pixels are embedded with the more number of bits than the non-edge pixels. This method resists statistical analysis based attack as data is not hidden in all the pixels. Beyond providing high embedding capacity higher PSNR is also ensured by this method [29, 23].

In 2011, a new edge embedding technique has been introduced, which targets on higher PSNR rather than higher embedding rate. This method provides better PSNR Than [20] [22] [23]. Edges of the image are obtained using sobel canny edge detector. Only horizontal edges of a particular edge length are used further. These edge pixels are used to calculate the difference of edge pixels with upper edge boundary. If this difference is greater than some predefined difference then these upper boundary pixels are used for embedding data bits accordingly. In this way, the stego-image with least perceptual transparency is obtained. The strong point of this method is high PSNR value but having a drawback of least embedding capacity [29].Another drawback is that it uses horizontal direction edge pixel boundary only [29, 25].

In 2012, a new parameterized canny edge detection based embedding approach has been introduced. Parameterized canny edge detector uses three parameters i.e. higher threshold value, Gaussian filter and lower threshold value. The value of all these three parameters are user defined. This property makes the stego-image more robust as different values of these parameters yields different outputs. In this approach, three LSBs of all three channels of edge pixels are replaced with the secret data bits. The advantages of this approach are imperceptibility and irrecoverability [29, 26].

In 2013, to improve the capacity and PSNR, new LSB based edge embedding technique using hybrid edge detection filter is introduced. Rather than applying Canny with fuzzy edge detector, combination of the Canny and enhanced Hough edge detector is used to get edge pixels. Message to be embedded is encrypted with AES [27] to provide another level of security [29]. The encrypted message bits are hidden in the smooth area pixels and edge area pixels. For hiding the message bits in smooth area adaptive LSB Substitution technique has been used. Whereas for hiding message bits in the edge area two components-based LSB Substitution techniques has been used. This method ensures the higher PSNR value and high embedding capacity. Also this method provides security against various attacks e.g. visual analysis, histogram analysis, chi-square and RS analysis [29, 28].

3. Conclusion

Steganography is an important field of digital image processing and information security. Various steganography techniques introduced to provide very high Imperceptibility, robustness and capacity. In this paper, many methods are explained one by one. Out of all these techniques, Edge embedding technique using hybrid edge detection filter is giving PSNR value as well as high embedding capacity. AES is used for encryption, so higher security is also provided. So Edge embedding technique using hybrid edge detection filter is better option when high PSNR, high embedding capacity and high security is required.

4. REFERENCES

[1] Artz, D., "Digital Steganography: Hiding Data within Data," IEEE Internet Computing Journal, vol. 5, no. 3, pp. 75-80, June 2001.

[2] Anderson R. J., "Stretching the Limits of Steganography," Springer Lecture Notes in Computer Science, vol.1174, pp. 39–48, 1996 .

[3] Westfeld A, J. Camenisch et al., "Steganography for Radio Amateurs— A DSSS Based Approach for Slow Scan Television", Springer-Verlag Berlin Heidelberg, pp. 201-215, 2007.

[4] M. Hossain, S. A. Haque and F. Sharmin, "Variable Rate Steganography in Gray Scale Digital Images Using Neighborhood Pixel Information", The International Arab Journal of Information Technology, vol. 7, no. 1, pp. 34-38, 2010.

[5] A. Shaddad, J. Condell, K. Curran, and P. Mckevtt., "Biometric inspired digital image steganography," Proceedings of 2008 15th Annual IEEE International Conference and Workshop on the Engineering of Computer Based Systems, pp. 159-168, 2008.

[6] Thien, C. C., Lin, J. C., "A Simple and High-Hiding Capacity Method for Hiding Digit-By-Digit Data in Images Based On Modulus Function," Pattern Recognition, vol. 36, no. 12, pp. 2875-2881, June 2003.

[7] S. Dumitrescu, X. Wu, and Z. Wang, "Detection of LSB Steganography via Sample Pair Analysis", Proceedings of 2003 IEEE Transaction on Signal, vol.51, no. 7, pp. 1995-2007, 2003.

[8] T. Zhang and X. Ping, "Reliable detection of LSB steganography based on the difference histogram", IEEE International Conference on Acoustics, Speech, and Signal Processing, vol. 3, pp. 545-548, April 2003.

[9] L. Zhi, S. A. Fen and Y. Y. Xian,"A LSB steganography detection algorithm", Proc. of IEEE Symposium on Personal Indoor and Mobile Radio Communication, pp. 2780-2783, September 2003.

[10] Maroney, C. Hide and Seek 5 for Windows 95, computer software and documentation, originally released in Finland and the UK.

[11] Katzenbeisser. S,Fabien, Petitcolas. A.P., "Information hiding techniques for steganography and digital watermarking",Artech House, Norwood, MA 02062, USA, 1999.

[12] Kathryn Hempstalk, "Hiding Behind Corners: Using Edges in Images for Better Steganography", Proceedings of the Computing Women's Congress, 2006.

[13] R. Chandramouli, N.D. Memon and G. Li, "Adaptive Steganography," Proceedings on Security and Watermarking of Multimedia Contents III, Special session on Steganalysis, SPIE Photonics West, vol. 4675, pp. 69-78, April 2002.

[14] Karen Bailey, Kevin Curran and Joan Condell, "An Evaluation of Pixel based Steganography and Stego detection Methods," The Imaging Science Journal, vol. 52, no. 3, pp. 131 - 150, Sept 2004.

[15] Elke Franz and Antje Schneidewind, "Adaptive Steganography Based on Dithering," Proceedings Of the 2004 workshop on multimedia and security, ACM, pp. 56-62, 2004.

[16] M. M. Amin, M. Salleh, S. Ibrahim, M. R. K.Atmin and M. Z. I. Shamsuddin, "Information Hiding using Steganography," 4th national Conference on Telecommunication Technology, NCTT 2003, IEEE, pp. 21 – 25, Jan 2003

[17] Santosh Arjun, N. and Atul Negi, "A Filtering Based Approach to Adaptive Steganography," 10th Conference, TENCON 2006, IEEE, pp. 1-4, Nov 2006.

[18] Manglem Singh, Birendra Singh and Shyam Sundar Singh, "Hiding Encrypted Message in the Features of Images," IJCSNS, vol. 7, no. 4, April 2007.

[19] H. C. Wu, N. I. Wu, C. S. Tsai, and M. S. Hwang, "Image steganographic scheme based on pixel-value differencing and LSB replacement methods," Proceedings of 2005 Instrument Electric Engineering, Vis. Images Signal Process, vol. 152, no. 5 pp. 611–615, 2005.

[20] Cheng-Hsing Yang, Chi-Yao Weng, Shiuh-Jeng Wang, Hung- Min Sun, "Adaptive Data Hiding in Edge Areas of Images with Spatial LSB Domain Systems," IEEE Transactions on Information Forensics and Security, vol. 3, no. 3, pp. 488-497, 2008.
[21] D. C. Wu and W. H. Tsai, "A Steganographic method for images using pixel value differencing," Pattern Recognition Letters, vol. 24, pp. 1613-1626, 2003.
[22] Hossain, M. Al Haque and S. Sharmin, F., "Variable rate Steganography in gray scale digital images using neighborhood pixel," 12th International Conference Dhaka, Information Computers and Information Technology, ICCIT '09, pp. 267-272, Dec 2009.
[23] Wen-Jan Chen a, Chin-Chen Chang, T. Hoang Ngan Le, "High payload steganography mechanism using hybrid edge detector," Expert Systems with Applications, vol. 37, pp. 3292–3301, 2010.
[24] Sonka, M., Hlavac, V. and Boyle, Image processing, analysis, and machine vision, Thomson Brooks/ Cole, 1999.
[25] Hussain, M. and Hussain, "Embedding data in edge boundaries with high PSNR," Proceedings of 7th International Conference on Emerging Technologies (ICET 2011), pp.1-6, Sept 2011.
[26] Youssef Bassil, "Image Steganography Based on a Parameterized Canny Edge Detection Algorithm," InternationalJournal of Computer Applications (0975 – 8887), vol. 60, no. 42012.
[27] Specification for the Advanced Encryption Standard (AES),Federal Information Processing Standards Publication 197,2001.
[28] Mamta Juneja and Parvinder S. Sandhu, "A New Approach forInformation Security using an Improved SteganographyTechnique," J Inf Process Syst, vol. 9, no. 4, 2013.
[29] Deepali Singla, Mamta Juneja, "An Analysis of Edge Based Image Steganography Techniques in Spatial Domain" IEEE, 06 – 08 March, 2014

Comparative Analysis of Clustering Algorithms on Graphics Processor

Dharmesh Bhalodia[1], Richard Sonaliya[2]

dharmeshbhalodia33@gmail.com[1], richardsonaliya.ce@socet.edu.in[2]

Computer Engineering Department, Silver oak college of Engineering & Technological, Gujarat Technological University, India

Abstract:-

Cluster analysis plays a critical role in a wide variety of applications, but it is now facing the computational challenge due to the continuously increasing data volume. Parallel computing is one of the most promising solutions to overcoming the computational challenge. In this paper an effort has been made to conduct detail survey of three different types of clustering algorithms implementation on graphics processor, these types are k-means, Hierarchical Agglomerative Clustering (HAC) and Clustering Affinity Search Technique (CAST). Graphics Processing Units (GPU) have recently been the subject of attention in research as an efficient coprocessor for implementing many classes of highly parallel applications. The GPUs design is engineered for graphics applications, where many independent SIMD workloads are simultaneously dispatched to processing elements. While parallelism has been explored in the context of traditional CPU threads and SIMD processing elements, the principals involved in dividing the steps of a parallel algorithm for execution on GPU architectures remains a significant challenge.

Keywords:*Clustering Algorithm, K-means, HAC, CAST, Graphics Processorand CUDA.*

1. Introduction

Clustering is a learning method that is kind of unsupervised type. That partitions a set of data objects into group, is called cluster, such that intra-cluster similar to each cluster and inter-cluster dissimilar [1, 2]. The k-Means algorithm is popular clustering algorithms and is widely used in a wide variety of fields like pattern recognition, image analysis, statistical data analysis, and bioinformatics [3, 4]. It has been selected as one of top 10 data mining algorithms [5]. The time complexity of k-Means algorithm increase with the size and also the dimensionality of the data set. Hence clustering large-scale data sets is time consuming task. Parallelizing k-Means is a promising approach to overcoming the challenge of the huge computational power requirement [6-8]. In [6], P-CLUSTER has been designed for a cluster of computers with a client-server model in which a server process partitions data into blocks and sends the initial centroid list and blocks to each client. It has been further enhanced by pruning as much computation as possible while preserving the clustering quality [7]. And also the k-Means clustering algorithm has been parallelized by exploiting the inherent data-parallelism and utilizing message passing in [8].

Recently, as a general-purpose and high performance parallel hardware, Graphics Processing Units (GPUs) developing continuously and provide another promising platform for parallelizing k-Means. GPUs are dedicated hardware for manipulating computer graphics. Due to the huge computing demand for real-time and high-definition 3D graphics, the GPUs have evolved into massively parallel many-core processors. The advances of computing power and memory bandwidth in GPUs have driven the development of general-purpose computing on GPUs (GPGPU).

At the start of multicore CPUs and GPUs the processor chips have become parallel systems. But Speed of the program will be increased if software exploits parallelism provided by the underlying Multiprocessor architecture [9]. Hence there is a big need to design and develop the software so that it uses Multithreading, each thread running concurrently on a processor, potentially increasing the speed of the Program dramatically. To develop such a scalable parallel applications, a parallel programming model is required that supports parallel multicore programming environment. NVIDIA's graphics processing units (GPUs) are very powerful and highly parallel. GPUs have hundreds of processor cores and thousands of threads running concurrently on these cores, thus because of intensive computing power they are much faster than the CPU.

CUDA stands for Compute Unified Device Architecture. It is a parallel programming paradigm released in 2007 by NVIDIA. It is used to develop software for graphics processors and is used to develop a variety of general purpose applications for GPUs that are highly parallel in nature and run on hundreds of GPU's processor cores. CUDA uses a language that is very similar to C language and has a high learning curve. It has some extensions to that language to use the GPU-specific features that include new API calls, and some new type qualifiers that apply to functions and variables. CUDA has some specific functions, called kernels. A kernel can be a function or a full program invoked by the CPU. It is executed N number of times in parallel on GPU by using N number of threads. CUDA also provides shared memory and synchronization among threads.

2. Related Work

2.1 k-Means Algorithm

UV_k-Means[10], in order to avoid the long time latency of global memory access, it copies all the data to the texture memory, which uses a cache mechanism. Then, it uses constant memory to store k centroids, which is also more efficient than using global memory. Each thread is responsible for one data point, finding the nearest centroid; each block has 256 threads, and the grid has n/256 blocks. The work flow of UV_k-Means is straight forward. The first step, each thread calculates the distance from one corresponding data point to every centroid and finds the minimum distance and corresponding centroid. And the second step, each block calculates a temporary centroid set based on a subset of data points, and each thread calculates one dimension of the temp centroid. And finally the temporal centroid sets are copied from GPU to CPU, and then the final new centroid set is calculated on CPU. UV_k-Means has achieved a speedup of 20X to 40X over the single-thread CPU-based k-Means. This speedup is mainly achieved by assigning each data point to one thread and utilizing the cache mechanism to get a higher data fetching efficiency. However, the efficiency could be further improved by other memory access mechanisms such as registers and shared memory.

HP_k-Means [11].is efficient implementation compare to UV_K-Means algorithm on GPUs. In general, HP_k-Means considers the GPU memory hierarchy: firstly, it arranges the data to make the best use of the

memory bandwidth; secondly, it uses constant and texture memory to utilize the cache mechanism; thirdly, because of multiple reading it uses shared memory.

GPUMiner [12], stores all input data in the global memory, and loads k centroids to the shared memory. Each block has 128 threads, and the grid has n/128 blocks. The main characteristic of GPUMiner is the design of a bitmap. The workflow of GPUMiner is as follows. First, each thread calculates the distance from one data point to every centroid, and changes the suitable bit into true in the bit array, which stores the nearest centroid for each data point. Second, each thread is responsible for one centroid, finds all the corresponding data points from the bitmap and takes the mean of those data points as the new centroids. The main problem of GPUMiner is the poor utilization of memory in GPU, since GPUMiner accesses most of the data (input data point) from global memory. As pointed out in [11], bitmap approach is elegant in expressing the problem, but it is not a good method for high performance, since bitmap takes more space when k is large and requires more shared memory.

You Li et al [13] implemented and demonstrated new algorithm and achieves speed up compare to UV_k-means, HP_K-means and GPUMiner. They implemented for high and low dimensional data. Low dimensional data utilizes the GPU on-chip register and high dimensional data utilizes shared memory.

2.2 Hierarchical Agglomerative Clustering

Earlier, Arul Shalom et al [14] deals with the implementation of the pair-wise distance computation, which is one of the fundamental operations in HAC. The GPU NVIDIA 8800 GTX is employed and it uses CUDA programs to speed up the computations. Gene expression data are used and the traditional HAC algorithm is implemented using half matrix for pair-wise distance computation. The shared memory of the GPU is used and the threads are synchronized at block level. The experimental analysis shows that speedup of 20 to 44 times is achieved in the GPU compared to the CPU implementation. It is important to note that this speedup is achieved for the pair-wise distance computations alone and not for the complete HAC algorithm.

An efficient implementation of the traditional implementation of HAC algorithm [15] using CUDA parallel processing architecture, the large global memory, and the programmable GPU are exploited. A relatively cheaper graphics card, NVIDIA GPU 8800 GTS which has lower specifications than the GTX version is employed. The global memory is utilized rather than the shared memory in the GPU, which is relatively simple to be programmed, though the access speed is slower. Results in the order of 30 to 65 times speedup are achieved based on certain test conditions and CUDA programming parameters. In traditional HAC, computing the half distance matrix is the arithmetically intense computational step which in this implementation still has high time complexity and memory complexity.

Later, Arul Shalom et al [16] accelerated traditional HAC and Partially Overlapping Partitioning HAC[14] algorithm on GPU, the identification of minimum distances in each cell is done in parallel. The distance computations and the minimum distance pair identification are data independent and are realized in parallel. In the PoP HAC implementation, the task of computing distance matrix is accomplished by employing several blocks whereas only one block is used in the traditional HAC on GPU. The PoP cells are created in the CPU. Each cell data is then transferred to the global memory of the GPU and are located via cell index and pointers to each cluster it contains. Each PoP cell is assigned to a block. Experimental results shows that it achieves 443 time faster than traditional PoP CPU implementation.

2.3 Clustering Affinity Search Technique

Kawuu W. Lin et al implemented very famous clustering Affinity Search Technique (CAST) on GPU [17]. The sequential CPU version of CAST proposed by Ben-Dor et al. [18] , which is widely used in clustering the biological data like microar-ray data and gene expression. In Tseng and Kao [19], the authors proposed an algorithm that can achieve high clustering accuracy and automation that was extended from CAST by integrating validation techniques. However, a complete clustering process when using CAST to cluster data requires a lot of floating point computing. CAST needs to pre-calculate a similarity matrix for storing the similarity values of objects.

The algorithm flow begins by randomly selecting a node as a new cluster. Then the ADD phase and REMOVE phase are used to form the cluster. In the ADD phase, the node with the maximum affinity value is added to the cluster, and the algorithm updates the affinity values in parallel by using GPU. In the REMOVE phase, it removes the node whose affinity value is the minimum. After the removing, the affinity values are updated in parallel in GPU. The clustering is repeated until there is no change to the current cluster. The algorithm recursively performs the clustering if there exists un-clustered node; the algorithm ends after all of the nodes are clustered and

outputs the clusters. This algorithm requires only 30% time of traditional CAST algorithm. Experimental results also prove that it is can apply for very large database where main memory is in limited size

3. Conclusion

The present paper covers the detailed study of selected implementation of clustering algorithms on massively parallel Graphics Processor. We describe three types of clustering algorithms that accelerates their traditional version on GPU and also describe to achieve the speedup ratio from 2X to 40X. Through all the mentioned algorithms it can be said thatGPUs can compute very large dataset in least time compare to CPU. Moreover Graphics Processer computing with CUDA Architecture can utilize for general purpose applications.

4. References

[1] P.-N. Tan, M. Steinbach, and V. Kumar, Introduction to Data Mining, Addison-Wesley Companion Book Site 2006.

[2] A. K. Jain and R. C. Dubes, Algorithms for Clustering Data, Prentice-Hall, 1988.

[3] X. Wang and M. Leeser, "K-means Clustering for Multispectral Images Using Floating-Point Divide," in Proceedings of the 15th Annual IEEE Symposium on Field-Programmable Custom Computing Machines, 2007.

[4] H. Zhou and Y. Liu, "Accurate Integration of Multi-view Range Images Using K-means Clustering," Pattern Recogn., vol. 41, pp. 152-175, 2008.

[5] X. Wu, V. Kumar, J. R. Quinlan, J. Ghosh, Q. Yang, H. Motoda, G. J. McLachlan, A. Ng, B. Liu, P. S. Yu, Z.-H. Zhou, M. Steinbach, D. J. Hand, and D. Steinberg, "Top 10 Algorithms in Data Mining," Knowledge Information Systems, vol. 14, pp. 1-37, 2008.

[6] D. Judd, P. K. McKinley, and A. K. Jain, "Large-Scale Parallel Data Clustering," in Proceedings of the International Conference on Pattern Recognition (ICPR'96) Volume IV, 1996.

[7] D. Judd, P. K. McKinley, and A. K. Jain, "Large-Scale Parallel Data Clustering," IEEE Trans. Pattern Anal. Mach. Intell., vol. 20, pp. 871-876, 1998.

[8] I. S. Dhillon and D. S. Modha, "A Data-Clustering Algorithm on Distributed Memory Multiprocessors," in Revised Papers from Large-Scale Parallel Data Mining, Workshop on Large-Scale Parallel KDD Systems, SIGKDD: Springer-Verlag, 2000.

[9] NVIDIA CORPORATION, CUDA Programming Guide, http://developer.nvidia.com/cuda

[10] S. Che, M. Boyer, J. Meng, D. Tarjan, J. W. Sheaffer, and K. Skadron, "A Performance Study of General-Purpose Applications on Graphics Processors Using CUDA," Journal of Parallel and Distributed Computing, 2008.

[11] R. Wu, B. Zhang, and M. Hsu, "Clustering billions of data points using GPUs," in UCHPC-MAW'09: Proceedings of the combined workshops on UnConventional high performance computing workshop plus memory access workshop, Ischia, Italy, 2009, pp. 1-6.

[12] W. Fang, K. K. Lau, M. Lu, X. Xiao, C. K. Lam, P. Y. Yang, B. He, Q. Luo, P. V. Sande, and K. Yang, "Parallel Data Mining on [13] Graphics Processors," Technical Report HKUSTCS08, 2008.

[13] You Li, Kaiyong Zhao, Xiaowen Chu, and Jiming Liu "Speeding up K-Means Algorithm by GPUs" 10th IEEE International Conference on Computer and Information Technology (CIT 2010)
DOI 10.1109/CIT.2010.60

[14] S.A.A. Shalom, Manoranjan Dash, "Hierarchical Agglomerative Clustering Using Graphics Processor with Compute Unified Device rchitecture", IEEE Computer Society, 2009, pp. 556-561.

[15] N. Corporation, "Cuda programming guide 2.0," Book Cuda programming guide 2.0, Series Cuda programming guide 2.0, ed., 2008.

[16] S. A. Arul Shalom, Manoranjan Dash, "Efficient Hierarchical Agglomerative Clustering Algorithms on GPU Using Data Partitioning", 12th International Conference on Parallel and Distributed Computing, Applications and Technologies,134, DOI 10.1109/PDCAT.2011.38

[17] Kawuu W. Lin , Chun-Hung Lin and Chun-Yuan Hsiao, "A parallel and scalable CAST-based clustering algorithm on GPU", Soft Comput (2014), DOI 10.1007/s00500-013-1074-y

[18] Ben-Dor A, Shamir R, Yakhini Z ," Clustering gene expression patterns". J Comput Biol 6(3/4):281–297 1999

[19] Tseng S, Kao C-P ,"Mining and validation gene expression patterns": an integrated approach and applications. Informatica 27:21–27, 2003

Optimum Design of Impeller for Improving Head of a Submersible Pump

Reepen Shah[1], Parth Patel[2]

ripen.me@socet.edu.in[1], parthpatel.me@socet.edu.in[2]

[1,2]*Assistant Professor, Department of Mechanical Engineering, Silver oak college of Engineering & Technology, Gujarat Technological University, India*

Abstract:-

The present paper describes an improvement in the head of mixed flow pump impeller. Computational Fluid Dynamics(CFD) analysis is one of the advanced CAE tools used in the pump industry. From the results of CFD analysis, the velocity and pressure in the outlet of the impeller is predicted. The optimum inlet and outlet vane angles are calculated for the existing impeller by using the empirical relations. The CAD models of the mixed flow impeller with optimum inlet and outlet angles are modelled using CAD modelling software Solid Works 2009. By changing the outlet angle and the Number of blades of impeller, the head of the impeller is improved. From this analysis, it is understood that the changes in the inlet blade angle and Number of blade change the head of the impeller. From the optimization, the head of the impeller is 12.156 m, with optimum blade angle 59^o& keeping number of blades equal to 7.

Keywords: *Mixed Flow Pump, Computational Fluid Dynamics (CFD) Analysis, Impeller Design, Submersible Pump.*

1. Introduction

The increasing performance levels and operating conditions requirements make the task of designing a pump impeller very challenging. The role of internal flows and the viscous effects in submersible impellers are fundamental and must be taken properly into account in the design process in order to obtain optimum performance. Formerly it was sufficient for a designer to analyze the steady state operation of a pumping system but nowadays with the increasing complexity of pumping systems, a wide variety of Submersible pump types have been constructed and used in many different applications in industry and other technical sectors. However, their design and performance prediction process is still a difficult task, mainly due to the great number of free geometric parameters, the effect of which cannot be directly evaluated. For this reason CFD analysis is currently being used in the design and construction stage of various pump types. WORLD PUMPS [1] has presented that the head obtained by mixed flow pump is higher than radial & axial flow pump. Efficiency of mixed flow pump was between radial and axial flow pump. Mixed flow pump used where the high delivery rates are required against moderate heads. The different factors used in design of mixed flow pump like selection of casing (tubular casing, volute casing), effect of backflow, cavitations, pre-rotation of water are discussed in design aspects. Vasilios et al [2] describes the flow domain is discredited with a polar, unstructured, Cartesian mesh that covers a periodically symmetric section of the impeller. The numerical results are compared to the measurements, showing good agreement and encouraging the extension of the developed computation methodology for performance prediction and for design optimization of such impeller geometries. J.Manikandan et al [3] shows the study of mixed flow pumps. The leakage according to S. C. Chaudhari, C. O. Yadav and A. B. Damor, loss contributes about 7 percent of the total flow. From the Computational Fluid Dynamics analysis the internal flow pattern, Pressure and Velocity contour are predicted which will be useful for further enhancement of the pump. S.Rajendran1 et al [4] describes the simulation of the flow in the impeller of a centrifugal pump. The numerical solution of the discredited three-dimensional, incompressible Navier-Stokes equations over an unstructured grid is accomplished with an ANSYS-CFX. The flow pattern, pressure distribution in the blade passage, blade loading and pressure plots are discussed in this paper. Gundale et al [5] presents the purpose of the analysis is to verify the performance at duty point or BEP (Best Efficiency Point). Nataraj et al [6] studied the Taguchi's parametric design concept for performance enhancement of centrifugal pump. For the experiment eight virtual model of impeller was selected by varying four parameters. After doing the

simultaneous optimization the optimum condition of four operating parameter was found. Miner et al [7] presents the Non dimensional impeller results and Non-dimensional stator results were compared to get the final result show that the shapes and magnitudes of the velocity & static pressure profiles were correctly predicted. The largest error found in predictions of the total pressure and differences in the tangential velocity profile. Karanth et al [8] shows an optimum radial gap which could help providing maximum energy transfer by the impeller blades as well as maximum energy conversion by diffuser vanes. The static pressure recovery and total pressure loss for the diffusing components of the fan change with the radial gap. The larger is the radial gap, the smaller are the pressure fluctuations at the exit flange of the fan.
Manivannan et al [9] described the efficiency of the existing impeller is calculated by the empirical relations. The calculation of head, power rating & efficiency of existing impeller was found to be 19.24 m, 9.46 KW, & 55% respectively.

2. Pump specifications

2.1 Impeller Geometry

In this work, the mixed flow pump detailed geometric feature of the impeller was studied and parameterization of impeller geometry was done. Parameterization was done by reducing number of controlling geometric variables, facilitating the investigation of their individual or combined effects on the flow and the impeller performance. A typical submersible pump consists of impeller, diffuser, riser, discharge adapter, intermediate bowl and shaft. The performance of a pump depends on active pump components. The active pump components of a mixed flow pump are mixed flow impeller and guide vanes. These parts are important while analysing a pump because mechanical energy (rotation) is transferred into fluid energy (pressure, velocity) by the active pump components.

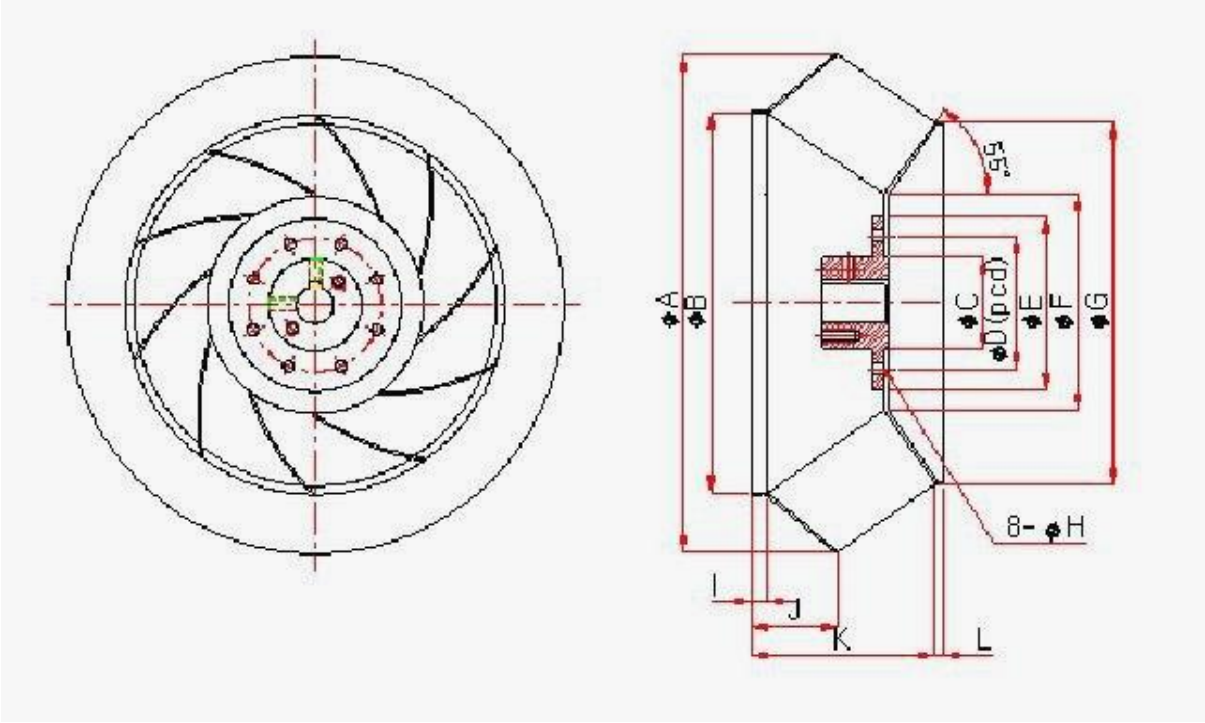

Figure 1: *Mix flow type impeller*

The geometry of a mixed flow pump impeller is highly complex in nature. The mixed flow geometry consists of several features among those following geometric features are important as they have direct effect on overall pump performance.
Some of the important parameters of impeller from above geometry are:
A – Outer hub diameter
B – Outlet diameter

G – Inner hub diameter
F – Inlet diameter
Other parameters are related to Blade geometry.

Table 1: Existing Mixed Flow Impeller Dimensions

Parameter	Size
Impeller inlet diameter(D_1)	345mm
Impeller outlet diameter(D_2)	606.5mm
Number of blades(N_b)	5
Number of stages	Three
Shaft Diameter(D_s)	78mm
Blade Inlet Height(B_1)	64mm
Blade Outlet Height(B_2)	53mm
Rotation(N)	2860rpm
Inlet Blade Angle	56

Parameterization was done by reducing number of controlling geometric variables (inlet angle, outlet angle), to investigate their individual or combined effects on the flow and the impeller performance. After parameterization, mixed flow impeller can be represented using a relatively small number of parameters some of them are shown in Figure 1.and their values are given in Table 1. The rotation speed and the main impeller dimensions, namely the exit diameter D2 as well as the blade inlet and exit angles, β1 and β2, respectively, determines the nominal head.

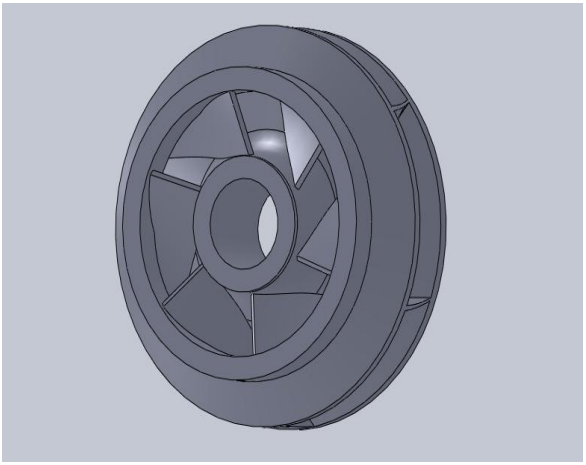

Figure 2: 3D Model of Mixed Flow Impeller

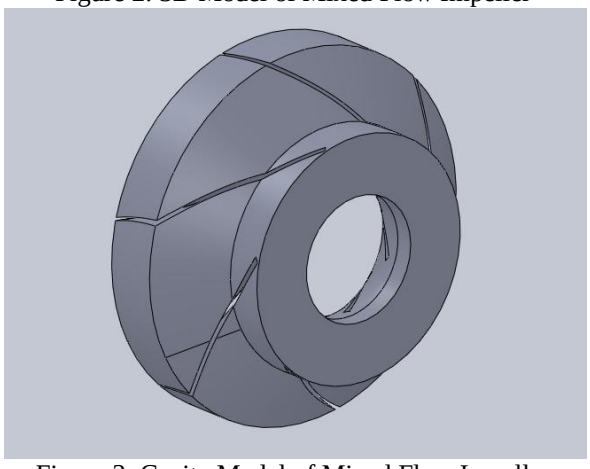

Figure 3: Cavity Model of Mixed Flow Impeller

The above cavity model is required for the further analysis in ANSYS software. Now Stress analysis (Pressure and Velocity variation) would be studied.

3. Analysis of mixed flow impeller

The analysis of the volume of impeller is further carried out by making the use of ANSYS, In which we have make the use of Finite Element Analysis method by generating the mesh. The resulting model generated by the mesh in the system is shown in the figure below.

3.1 Meshing of Impeller

Meshing Type : 3D
Type of Element : Tetrahedral
No. of Nodes : 11637
No. of Elements : 49456

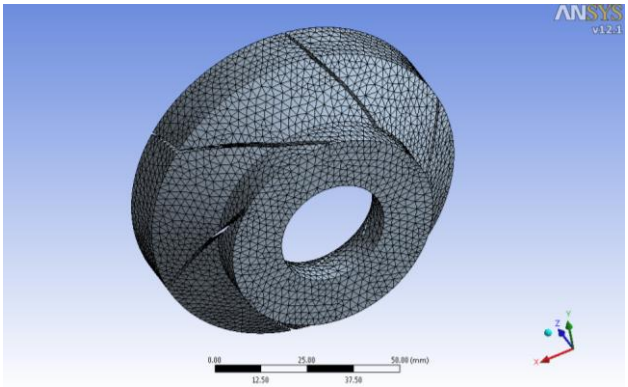

Figure 4: Meshed Model of Impeller Cavity

By generating the mesh model of the impeller we will make the variation of pressure at inlet and outlet portion of it by naming them as shroud and hub. Then the process will follow the analysis by making use of the various tools of the ANSYS software, which will in turn help us for the discharge evaluation with variation in the various designing values.

4. Results

4.1 Velocity Stream Contour

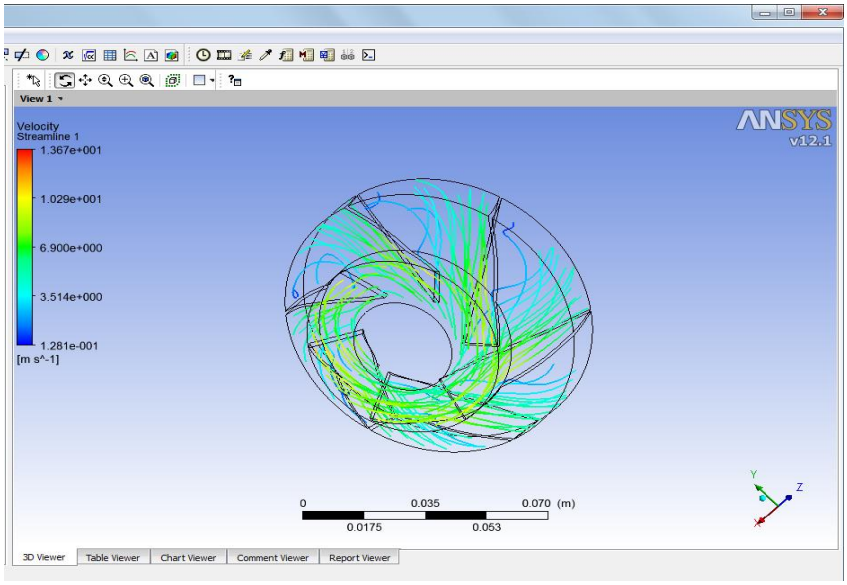

Figure 5: Velocity Contours

- Velocity of fluid is initially high but as it flows up, it loses some energy due to which velocity decreases.

4.2 Pressure Contour

4.2.1 Inlet

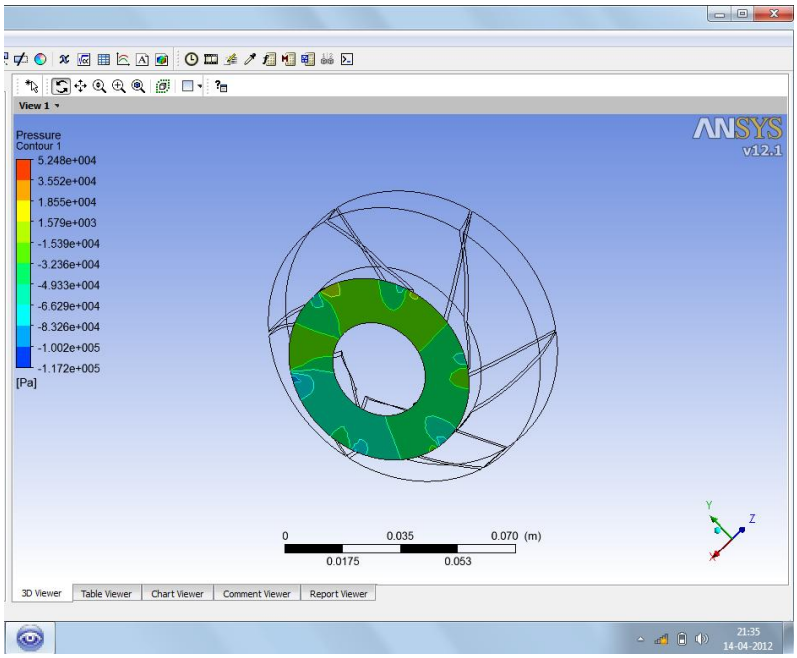

Figure 6: Inlet Pressure Contours

- Inlet pressure does not have effect on the performance of impeller.

4.2.2 Outlet

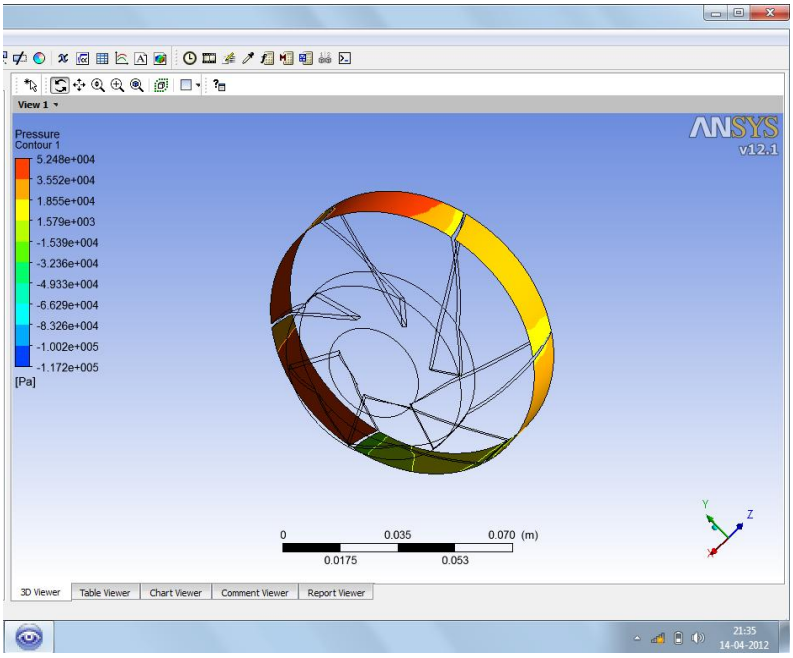

Figure 7: Outlet Pressure Contours

- Outlet pressure effects more than inlet pressure, on the performance of impeller as the flow is going to the outer side.

4.2.3 Pressure variation at Outlet

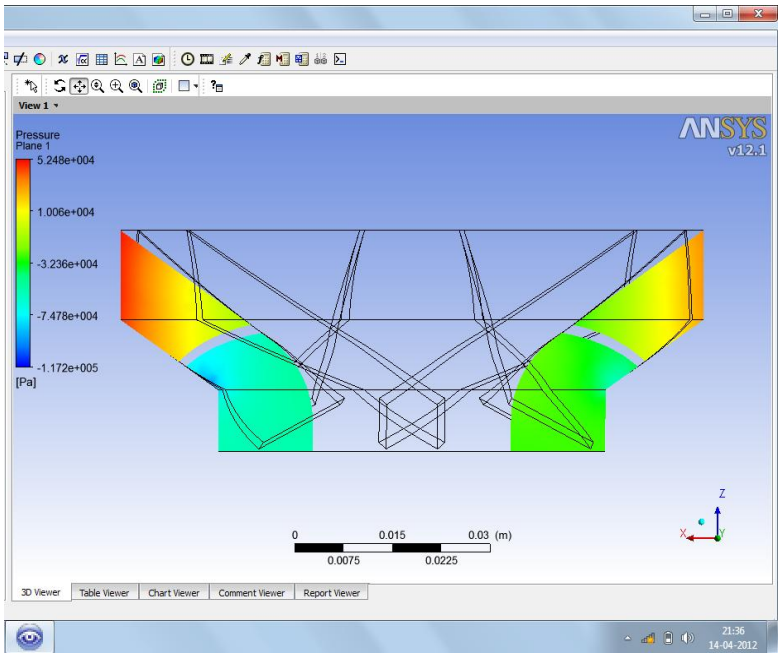

Figure 8: Pressure Variation at Outlet of the Impeller

- Pressure variation at the outlet gives more effect on impeller as shown in figure.

4.3 Optimization of results

4.3.1 Optimization for Inlet Blade Angle

Table 2: Effect of inlet angle on head (m):

Sr No.	Inlet Angle	Head (m)
1	56	10.5
2	56.67	11.6336
3	59	12.156
4	65	11.598

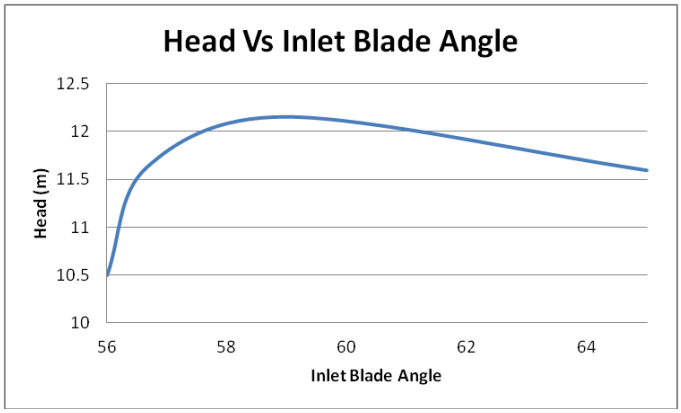

Figure 9: Head Vs Inlet Blade angle

Table 3: Effect of number of Blade:

Sr No.	Number of Blade	Head (m)
1	5	10.215
2	6	11.6336
3	7	12.546

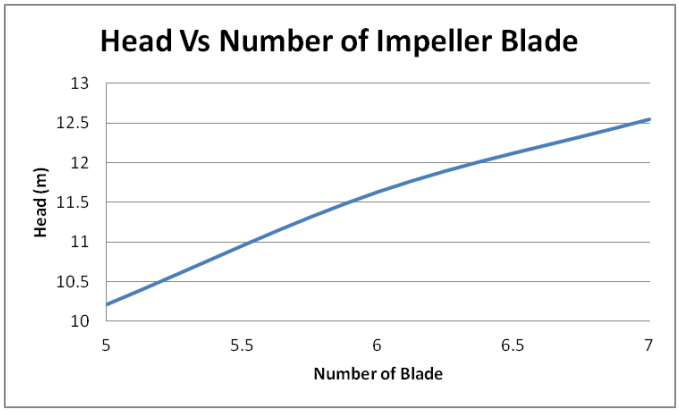

Figure 10: Head Vs Number of Impeller Blades

5. Conclusion & Result Discussion

By selecting the optimum inlet blade angle & number of blades improves the performance of pump that is simulated in this study

- Optimum inlet angle is 59^{o} and number of blades is 7 which increase the performance of pump.
- Outlet pressure also increases.
- Number of blade can also increase the efficiency.
- Performance of the pump impeller also increases.
- Optimum head found is12.156 m in our case.

Thus selecting suitable blade angles and number of blades are important from the manufacturing point of view.

6. REFERENCES

[1] "World pump", Elsevier Science Ltd, October 1995, 0262 1762/95/$7.0

[2] Vasilios a.Grapsas, john s. Anagnostopoulos and dimitrios e. Papantonis, "Experimental and numerical study of a radial flow pump impeller with 2d-curved blades", ICFM&E Athens, Greece, august 25-27, 2007.

[3] J. Manikanandan, V.Senthil and Nagrajan "performance evaluations of mixed flow pump using CFD" Euro Journals Publishing, Inc. 2012

[4] S.Rajendran1 & Dr.K.Purushothaman 2"Analysis of a centrifugal pump impeller using ANSYS-CFX"

[5] Virajit A. Gundale, S.A. PATIL 'Improvement in the Design of Radial type Vertical type Submersible open well pumps impeller using CFD'

[6] M Nataraj and V P Arunachalam, "Optimizing impeller geometry for performance enhancement of a centrifugal pump using the Taguchi quality concept", Part A: Journal of Power and Energy, May 2006, 220: 765.

[7] Steven M.Miner, "CFD Analysis of the First-Stage Rotor and Stator in a Two-Stage Mixed Flow Pump", International Journal of Rotating Machinery, March 2004, 2005:1, 23–29.

[8] K. Vasudeva Karanth and N. Yagnesh Sharma, "CFD Analysis on the Effect of Radial Gapon Impeller-Diffuser Flow Interaction as well as on the Flow Characteristics of a Centrifugal Fan", Hindawi Publishing Corporation, IJRM,February 2009, Article ID 293508.

[9] A. Manivannan "Computational fluid dynamics analysis of a mixed flow pump impeller, IJES Vol. 2, No. 6, 2010, pp 20

[10] S. C. Chaudhari, C. O. Yadav & A. B. Damor "A comparative study of mix flow pump impeller CFD analysis and Experimental data of submersible pump, IJRET, Vol. 1, Issue 3, Aug 2013, 57-64